O.V. FOMIN, A.O. LOVSKA

TEMPERATURE EFFECTS ON RAILWAY ROLLING STOCK COMPONENTS

MONOGRAPH

Part 1

Primedia eLaunch
in collaboration with European Scientific Platform

O.V. FOMIN, A.O. LOVSKA

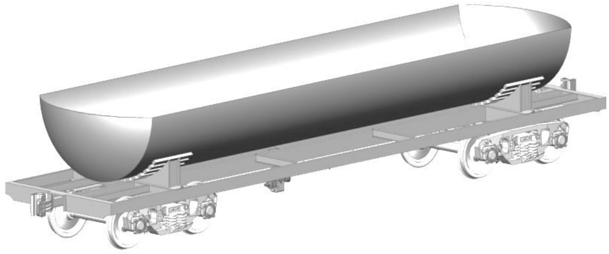

TEMPERATURE EFFECTS ON RAILWAY ROLLING STOCK COMPONENTS

MONOGRAPH

Part 1

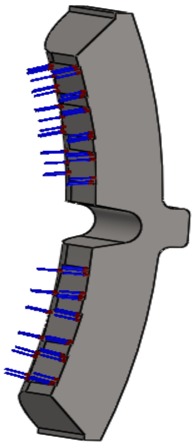

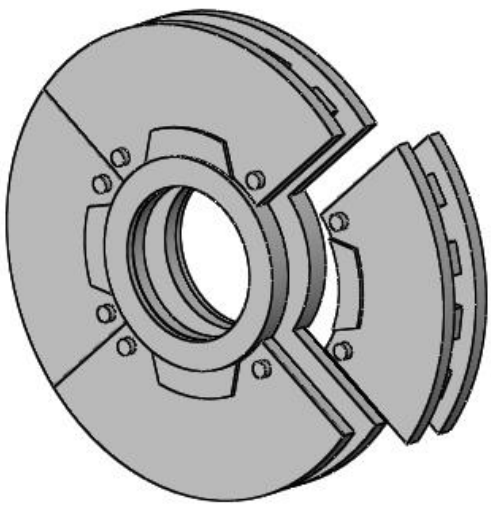

Dallas, USA
Primedia e-Launch LLC
2022

UDC 629.463
F 71

Reviewers:

MASLIYEV Vyacheslav	Doctor of Technical Sciences, Professor Department of Electric Transport and Heat Engineering National Technical University «Kharkiv Polytechnic Institute», Ukraine
SAPRONOVA Svitlana	Professor, Doctor of Technical Sciences Department of cars and carriage facilities State University of Infrastructure and Technologies, Ukraine
USTENKO Oleksander	Doctor of Technical Sciences, Professor Dean of the Faculty of Mechanics and Energy Ukrainian State University of Railway Transport, Ukraine

F 71 Fomin, O., and A. Lovska. *Temperature effects on railway rolling stock components (Part 1).* Dallas, USA: Primedia eLaunch LLC, 2022. 144 p.

ISBN 979-8-88831-318-3
DOI 10.36074/teorrsc-monograph.2022

The purpose of the book is to highlight the features of temperature effects on the components of railway rolling stock and to create measures to improve the efficiency of its operation. Theoretical provisions, methodological bases and practical decisions on determination of temperature influence on components of rolling stock of railways at operational modes of loading are provided.

The monograph is intended for scientific and technical specialists whose activities are related to the design and study of mechanics of rolling stock structures, including scientists, designers, designers, researchers, doctoral students and graduate students.

The monograph can be used as a textbook for undergraduates and bachelors in relevant specialties.

UDC 629.463

ISBN 979-8-88831-318-3

CONTENTS

INTRODUCTION

Ensuring the efficient operation of railway rolling stock as a leading branch of the transport network requires the introduction of its modern structures. At the same time, ensuring the competitiveness of the railway industry leads to increased requirements for technical, economic and operational indicators of rolling stock.

During operation, rolling stock experiences loads due to many factors, one of the most decisive of which is the temperature load. It has a significant impact on the strength, reliability and safety of rolling stock, as it can change the structure of materials. However, the existing regulatory framework used in the design of rolling stock does not take into account the temperature effects on its components. This causes damage to its components, the need for additional maintenance costs, poses a threat to traffic safety and so on. Therefore, there is a need to study and determine the temperature impact on the components of rolling stock, as well as to create recommendations for improving its operating conditions.

The purpose of the monograph is to highlight the features of temperature effects on the components of railway rolling stock and to create measures to improve the efficiency of its operation. To achieve this goal, the following tasks are defined:

- to investigate the design features and main characteristics of hopper cars for the transportation of hot steel pellets and sinter;

- to determine the load of the load-bearing structure of the hopper car and propose measures to increase the efficiency of transportation of high-temperature cargoes;

- to propose measures for improving the elements of tribotechnic pairs of rolling stock brakes.

The object of the study is the processes of occurrence and distribution of temperature effects in the components of rolling stock.

The subject of the study is the regularities of the distribution of temperature influence on the components of rolling stock, as well as modeling of their load at temperature conditions.

The monograph is intended for scientific and technical specialists, whose activities are related to the design and study of mechanics of rolling stock structures, including scientists, designers, engineers, researchers, doctoral students and graduate students.

The monograph can be used as a textbook for undergraduates and bachelors in relevant specialties.

SECTION 1
DESIGN FEATURES AND MAIN CHARACTERISTICS OF HOPPER CARS FOR TRANSPORTATION OF HOT RELEASES AND SINTER

1.1 Analysis of structures and main characteristics of hopper cars for transportation of hot pellets and sinter of the operated fleet

One of the most common types of vehicles used to transport high-temperature cargoes by railway is hopper cars.

Currently, there are a large number of designs of hopper cars for the transportation of pellets and hot sinter. Let us consider the design features of this type of car on the example of the model 20-471.

Specialized hopper gondola car model 20-471 (Figures 1.1 [1]) is designed for the transportation of hot pellets and sinter with a cargo temperature of up to 700°C from production sites to the receiving hoppers of the blast furnace [2].

Fig. 1.1. **Specialized hopper gondola car model 20-471**

The body of the hopper gondola car has the frame 4, two vertical sides 2, two end walls 1 with an angle of 41 ° to the plane of the frame and two hoppers with two unloading hatches 3 size 3500x400x560 mm (Figure 1.2). The body frame consists of a ridge beam, two end, pivot and transverse beams.

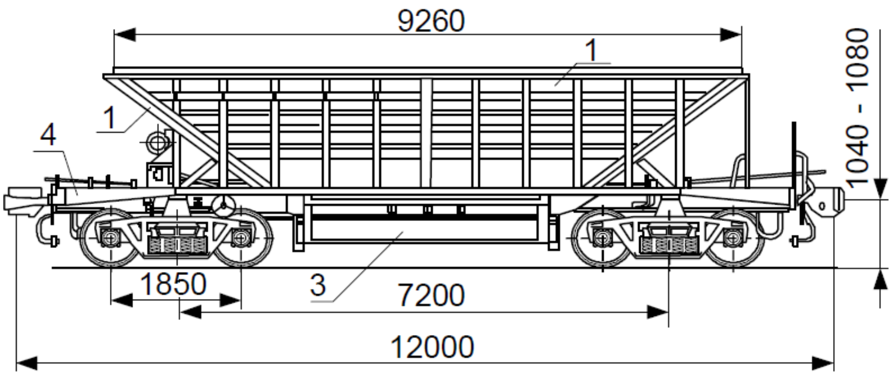

Fig. 1.2 **Specialized gondola car for transportation of hot pellets and sinter**

The main technical characteristics of the car are given in table 1.1 [8].

Table 1.1

The main technical characteristics of the hopper model 20-471

Name of parameter	Value
Load capacity, not more than, t	65.0
Body volume, m^3	42.0
Car weight, t	23.7
Estimated load from the wheelset on the rails, kN (ts)	215.6
Care base, mm	7200
Length of the car on axes of autocouplings, mm	12000
Dimensions by the GOST	1-BM
Height to the coupling axis from the level of the rail heads, mm	1040 – 1080
Number of hatches: - for loading - for unloading	- 1
Design speed, km / h	120
Inter-repair mealage, km	210000
Service life, years	15

The ridge beam is made of two I-beams No 45, covered with sheets at the top and bottom. End, pivot and cross beams are welded respectively trough-shaped, box and I-beam sections.

The frame of the side wall is made of rolled and bent profiles: the upper belt of box section is made of channel No 14 and bent element, the lower belt and pivot rack - of closed rectangular profile of 160x80x7 mm box section. The lower and upper belts are inerconnected with twelve racks. Intermediate racks are made of the channel No14. The end wall frame is welded using the channels

No 10 and No 14. The wall cladding is a set of bent profile panels that do not have a rigid connection with the frame, which ensures their mobility during thermal expansions to prevent warping of the load-bearing elements of the body.

The covers of the hopper unloading hatches are opened and closed by means of a special unloading mechanism (Figure 1.3), which is located under the hoppers and is a system of levers actuated by pneumatic cylinders with remote control. The hatch cover has a frame design which is sheathed with goffer sheets.

A visor is welded to the lower belt, which in the closed position is under the lower strapping of the body, thus creating a reliable seal against spills of pellets. From the ends of the cover seal is created by protruding sheets, which are placed in the grooves of the hatches in closed position. The unloading mechanism has a system of levers 2, 5, 6 connecting the hatch covers 1 with the shaft 7, which by means of a gear pair 3 under the action of two pneumatic cylinders 4 rotates to a certain angle, opening or closing the unloading hatch covers. The covers are closed due to the passage of the levers connecting them through the "dead point".

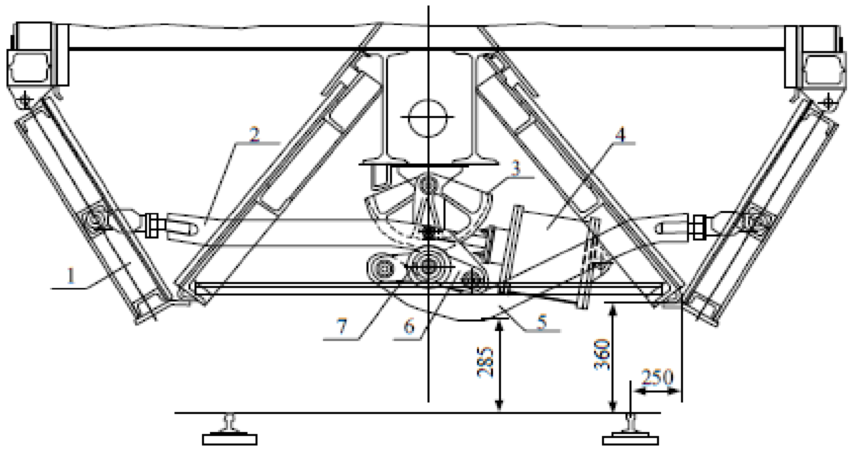

Fig. 1.3 **The car unloading mechanism**

The size of the opening of the hatch covers can be adjusted from 300 to 570 mm by setting the sector to different heights. All bearing elements of a body are made of low-alloy steel 09G2D.

Hopper car model 20-7032 (Figure 1.4) is designed for transportation of 1520 mm hot pellets and sinter by railway with a temperature not exceeding 700°C, as well as for their mechanical unloading. Unloading is carried out on both sides of the railway gauge through unloading hatches in special unloading devices. Brake is the automatic pneumatic, manual brake. Chassis is two two-axle carts model 18-7055 type 2 (GOST 9246-2013 / DSTU 7530-2014). Autocoupling CA - 3. The car is equipped with an absorber of high energy consumption class T1 [3].

Fig. 1.4 **Hopper car model 20-7032**

The main technical characteristics of the car are given in the table 1.2.

Table 1.2

The main technical characteristics of the hopper car model 20-7032

Name of parameter	Value
Load capacity, not more than, t	70.5
Body volume, m^3	45.0
Car weight, t	-
Estimated load from the wheelset on the rails, kN (ts)	23.5
Care base, mm	230.3 (23.5)
Length of the car on axes of autocouplings, mm	7 780
Dimensions by the GOST	12 000
Height to the coupling axis from the level of the rail heads, mm	1-BM
Number of hatches: - for loading - for unloading	1060±20
Design speed, km / h	- 2
Inter-repair mealage, km	120
Life time, years	210 000
Load capacity, not more than, t	15

The hopper car model 20-480 was serially launched since 1982 till 1986 by the PJSC “Dniprovagonmash” (Figure 1.5). It is designed to transport hot pellets and sinter, as well as other cargoes that do not require protection from precipitation.

Fig. 1.5 **Hopper car model 20-480**

The main technical characteristics of the car are given in the table 1.3 [4].

Table 1.3

The main technical characteristics of the hopper model 20-480

Name of parameter	Value
Load capacity, not more than, t	71.0
Body volume, m^3	42.0
Car weight, t	22.0
Estimated load from the wheelset on the rails, kN (ts)	228.0
Care base, mm	5870
Length of the car on axes of autocouplings, mm	10000
Dimensions by the GOST	1-BM
Height to the coupling axis from the level of the rail heads, mm	1040 – 1080
Number of hatches: - for loading - for unloading	 - 2
Design speed, km / h	120
Inter-repair mealage, km	210 000
Service life, years	15

Hopper car model 20-4015 is designed for transportation of pellets and sinter by main railway gauges of 1520 mm and gauges of industrial enterprises [5]. The car was built by the PJSC "Dniprovagonmash" (Figure 1.6).

Fig. 1.6 **Hopper car model 20-4015**

The design of the car provides mechanized loading through an open body and automated unloading on receiving devices (into the hoppers, on trestles). Non-rigid (floating) fastening of body panels allows to do loading of cargoes with a temperature of up to 700°C. The car is equipped with an unloading mechanism with pneumatic drive and automatic locking, which provides a reliable closure of the hatch covers, full unloading and automation of the unloading process. Angles of inclination of end walls provide effective dumping of the unloaded cargo. The car can be used to transport goods that do not require protection from the weather.

The main technical characteristics of the car are given in table 1.4.

Table 1.4

The main technical characteristics of the hopper car model 20-4015

Name of parameter	Value
Load capacity, not more than, t	70.0
Body volume, m^3	45.0
Car weight, t	24.0
Estimated load from the wheelset on the rails, kN (ts)	230.5
Care base, mm	7780
Length of the car on axes of autocouplings, mm	12000
Dimensions by the GOST	1-BM
Height to the coupling axis from the level of the rail heads, mm	1040 – 1080
Number of hatches: - for loading - for unloading	 - 2
Design speed, km / h	120
Inter-repair mealage, km	210 000
Service life, years	15

Hopper car model 20-4015-01 is a modification of model 20-4015-01 (Figure 1.7) [6].

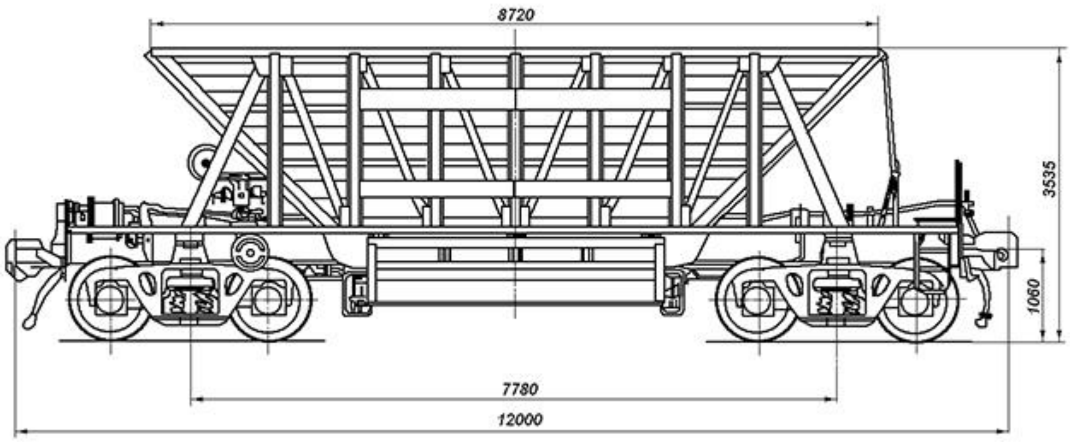

Fig. 1.7 **Hopper car model 20-4015-01**

The main technical characteristics of the car are given in the table 1.5.

Table 1.5

The main technical characteristics of the hopper car model 20-4015-01.

Name of parameter	Value
Load capacity, not more than, t	71.0
Body volume, m^3	44.0
Car weight, t	23.0
Estimated load from the wheelset on the rails, kN (ts)	230.5
Care base, mm	7780
Length of the car on axes of autocouplings, mm	12000
Dimensions by the GOST	1-BM
Height to the coupling axis from the level of the rail heads, mm	1060
Number of hatches: - for loading - for unloading	 - 2
Design speed, km / h	120

The branch of Panyutyn Car Repair Plant of the JSC Ukrzaliznytsia has produced the hopper car model 20-9749 (Figure 1.8). The car has four unloading hatches with unloading on both sides [7].

Fig. 1.8 **Hopper car model 20-9749**

The main technical characteristics of the car are given in the table 1.6.

Table 1.6

The main technical characteristics of the hopper car model 20-9749

Name of parameter	Value
Load capacity, not more than, t	69.0
Body volume, m^3	45.0
Car weight, t	25.0
Estimated load from the wheelset on the rails, kN (ts)	235.0
Care base, mm	7780
Length of the car on axes of autocouplings, mm	12000
Dimensions by the GOST	1-BM
Height to the coupling axis from the level of the rail heads, mm	1040 – 1080
Number of hatches: - for loading - for unloading	 - 4
Design speed, km / h	120
Inter-repair mealage, km	210 000
Service life, years	15

Hopper car model 19-9982, manufactured by the State Machinery Plant "Karpaty", designed for reliable transportation of pellets or sinters with a temperature not exceeding 700°C, and other bulk and small loads that do not require protection from precipitation on public roads and industrial enterprises (Figure 1.9) [9].

Production of hopper cars meets the requirements of the TU U30.2-37958251-005-2013, certified in the system UkrSEPRO UA 1.098.0011424-13 and meets the requirements of the DSTU ISO 9001: 2009.

Fig. 1.9 **Hopper car model 19-9982**

The main technical characteristics of the car are given in the table 1.7.

Table 1.7

The main technical characteristics of the hopper model 19-9982

Name of parameter	Value
Load capacity, not more than, t	71.0
Body volume, m³	45.0
Car weight, t	23.0
Estimated load from the wheelset on the rails, kN (ts)	230.5
Care base, mm	7800
Length of the car on axes of autocouplings, mm	12000
Dimensions by the GOST	1-BM
Height to the coupling axis from the level of the rail heads, mm	1060
Number of hatches: - for loading - for unloading	 - 4
Design speed, km / h	120

Hopper car model 20-793 is designed for transportation and mechanized unloading of hot pellets and sinter on main and industrial railway gauges with a width of 1520 mm (Figure 1.10) [10].

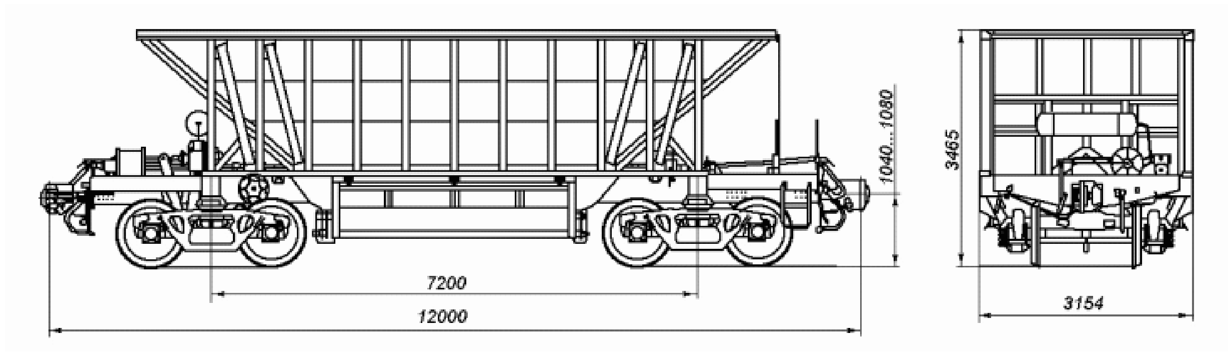

Fig. 1.10 **Hopper car model 20-793**

The main technical characteristics of the car are given in the table 1.8.

Table 1.8

The main technical characteristics of the hopper car model 20-793

Name of parameter	Value
Load capacity, not more than, t	70.0
Body volume, m^3	42.0
Car weight, t	23±3%
Estimated load from the wheelset on the rails, kN (ts)	228.0
Care base, mm	7200
Length of the car on axes of autocouplings, mm	12000
Dimensions by the GOST	1-BM
Height to the coupling axis from the level of the rail heads, mm	1040 – 1080
Number of hatches: - for loading - for unloading	 - 2
Design speed, km / h	120

Four-axle gondola car model 20-9839 (Figure 1.11), designed for transportation bulk cargoes on main railway gauges with a rail gauge width of 1520 mm that requires shelter from precipitation, including hot pellets [19].

The gondola has an all-metal body with a volume of 45 m^3, capable of withstanding loads up to 71 tons. The car is equipped with two carts model 18-1750 type 2, the size of the car is according to the GOST 9238 - 1-VM. The car for cargo unloading is equipped with two unloading hatches each of which has the size 562x1596 mm.

Fig. 1.11 **Hopper car model 20-9839**

The main technical characteristics of the car are given in the table 1.9.

Table 1.9

The main technical characteristics of the hopper car model 20-9839

Name of parameter	Value
Load capacity, not more than, t	71
Body volume, m^3	45
Car weight, t	23
Estimated load from the wheelset on the rails, kN (ts)	230,5
Care base, mm	7780±5
Length of the car on axes of autocouplings, mm	12000±20
Dimensions by the GOST	1-BM
Height to the coupling axis from the level of the rail heads, mm	1060±20
Number of hatches: - for loading - for unloading	 - 2
Design speed, km / h	120

Hopper car model 20-5197 with heat-resistant body cladding is designed for transportation pellets and sinter by railway with a temperature of up to + 400°C and their mechanized unloading (Figure 1.12). The car cladding is movable, which allows to compensate for thermal expansion. Compared to similar cars, the pellet truck of Ural designers has a larger body volume (48 m^3) and load capacity (75.5 tons).

Fig. 1.12 **Hopper car model 20-5197**

The hopper car is installed on innovative carts of the 18-194-1 model with the increased axial loading of 245 kN. The service life of the car has been increased from 15 to 24 years [31].

The main technical characteristics of the car are given in the table 1.10.

Table 1.10

The main technical characteristics of the hopper model 20-5197

Name of parameter	Value
Load capacity, not more than, t	75.5
Body volume, m^3	48.0
Car weight, t	24.0
Estimated load from the wheelset on the rails, kN (ts)	245.0
Care base, mm	6780
Length of the car on axes of autocouplings, mm	11000
Dimensions by the GOST	1-BM
Height to the coupling axis from the level of the rail heads, mm	1040 – 1080
Number of hatches: - for loading - for unloading	 - 2

The design of the hopper model 20-9916 provides mechanized loading through an open body and automated unloading on receiving devices (in hoppers, on trestles) [32].

Non-rigid (floating) fastening of body panels allows to do loading of freights with the temperature of up to 700°C. The car is equipped with an unloading mechanism with pneumatic drive and automatic locking, which provides a reliable closure of the hatch covers, full unloading and automation of the unloading process. Angles of inclination of end walls provide effective unloading of the cargo. The car can be used to transport cargoes that do not require protection from the weather.

The main technical characteristics of the car are given in the table 1.11.

Table 1.11

The main technical characteristics of the hopper model 20-9916

Name of parameter	Value
Load capacity, not more than, t	71.0
Body volume, m³	45.0
Car weight, t	23.0
Estimated load from the wheelset on the rails, kN (ts)	235
Care base, mm	7780
Length of the car on axes of autocouplings, mm	12000
Dimensions by the GOST	1-BM
Height to the coupling axis from the level of the rail heads, mm	1040 – 1080
Inter-repair mealage, km	210 000
Service life, years	15

The hopper is roduced according to the TU U 30.2-05749336-004: 2012 "Cars for pellets model 20-9916 and model 20-9916-01", developer and manufacturer is the PJSC "Verhniodniprovsk Machinery Construction Plant".

The hopper car model 20-9916-01 (Figure 1.13) is a modification of the hopper car 20-9916 [33].

Fig. 1.13 **Hopper car model 20-9916-01**

The main technical characteristics of the car are given in the table 1.12.

Table 1.12

The main technical characteristics of the hopper model 20-5197

Name of parameter	Value
Load capacity, not more than, t	72.0
Body volume, m^3	45.0
Car weight, t	22.0
Estimated load from the wheelset on the rails, kN (ts)	235.0
Length of the car on axes of autocouplings, mm	10000
Dimensions by the GOST	1-BM
Height to the coupling axis from the level of the rail heads, mm	1040 – 1080
Inter-repair mealage, km	210000
Service life, years	15

The hopper model 19-9809 is designed for transportation of pellets and sinter by main railway gauges with a width of 1520 mm and railway gauges of industrial enterprises (Figure 1.14).

Fig. 1.14 **Hopper car model 19-9809**

The main technical characteristics of the car are given in the table 1.13 [34].

Table 1.13

The main technical characteristics of the hopper model 19-9809

Name of parameter	Value
Load capacity, not more than, t	70.0
Body volume, m^3	45.0
Car weight, t	24.0
Estimated load from the wheelset on the rails, kN (ts)	235.0

Table 1.13 (continuation)

Name of parameter	Value
Care base, mm	7800
Length of the car on axes of autocouplings, mm	12020
Dimensions by the GOST	1-BM
Height to the coupling axis from the level of the rail heads, mm	120
Inter-repair mealage, km	210000
Service life, years	15

The car-hopper of model 19-1241 allows to transport practically all bulk types of cargoes (sinter, pellets, ores of ferrous and nonferrous metals, crushed stone, etc.), on the car small-sized brake elements are used that is much more compact, than on available analogs, it is applied a separate brake system and a reliable unloading system, reinforced visor and armor plates of the frame as the most burning parts of the body.

The main technical characteristics of the car are given in the table 1.14 [35].

Table 1.14

The main technical characteristics of the hopper model 19-9809

Name of parameter	Value
Load capacity, not more than, t	69.0
Body volume, m^3	45.0
Car weight, t	24.0
Estimated load from the wheelset on the rails, kN (ts)	230.5
Care base, mm	7200
Length of the car on axes of autocouplings, mm	12000
Dimensions by the GOST	1-BM
Number of hatches: - for loading - for unloading	 - 2
Design speed, km / h	120
Inter-repair mealage, km	210000
Service life, years	15

It is important to say that the designs of hopper cars are constantly being improved and updated. Therefore, the analysis of the designs of hopper cars is applied to the existing car fleet.

1.2 Patent analysis of load-bearing structures of hopper cars for transportation of pellets and hot sinter

To determine promising areas for improvement of the load-bearing structures of hopper cars, an analysis of Ukrainian patents was conducted.

Thus, the patent [11] considered the railway gondola car for hot pellets and sinter, the construction of which consists of a module of the crew part, autocoupling module, module of brake equipment, frame module, body module. The frame, side walls and end walls are made of articulated bearing shells, which in configuration repeat the axes of the bearing elements of a typical structure, and are connected by methods of hanging and welding.

Patent [12] describes the design of a railway gondola car for hot pellets and sinter, which consists of a module of the crew part, containing two double-axle carts, auto-coupling module, module of brake equipment, frame module with spine and pivot beams, unloading module shaft, a body module comprising two vertical side walls having the cladding and the frame consisting of upper and lower strapping, struts, connecting beams connecting the lower strapping and end beams of the frame module, and two sloping end walls with cladding and a frame consisting of upper and lower strappings and horizontal belts. The spine beam of the frame module is made of I-beams No 45, each of which has a welding structure. The upper sheet of the pivot beam is made of steel sheet with a thickness of 10 mm. The unloading shaft of the unloading equipment module is made of a round pipe. The bearing units of the unloading equipment module are made with inserts of composite materials. The cladding of the side and end walls of the body module is made of steel sheets 5 mm thick. Upper, lower strapping, side wall slants, upper, lower strapping, horizontal end wall belts are made of profiles in the form of a square pipe. The connecting beams connecting the lower strapping and the end beams of the frame module are made of one channel. The technical result is a reduction in material consumption and a corresponding increase in load capacity while ensuring conditions of strength and operational reliability.

The patent [13] presents a hopper car, the design of which consists of a crew module, containing two double-axle carts, autocoupling module, brake equipment module, frame module, which includes spine, end, pivot and intermediate beams, unloading equipment module, body module, which contains two vertical side walls, including upper and lower straps, vertical and inclined racks, and two inclined end walls, which include upper and lower straps, while the elements of the load-bearing structure of the car are made of round pipes and filled with viscous material with damping and anti-corrosion properties, and the functions of absorbing energy arising from the action of operating loads, transferred to the spine beam of modified design, namely, which includes an intermediate adapter consisting of a thrust part, which houses the base plate of a typical design, while the thrust part of the adapter is connected to the piston through the rod, which has two cables valves – inlet and outlet, viscous damping and anti-corrosion material is placed on the left and right side of the piston, and to create a pressure of viscous damping anti-corrosion material when moving the piston during the perception of shock load in the spine beam a bottom is provided, the limiter is provided to limit the movement of the adapter at "jerk-stretching", and also the top and bottom binding of lateral walls are provided. The load-bearing structure consists of two sections, which base on three carts and interact with each other by means of a joint assembly, while the pivot beam is replaced by a round beam on the side of supporting the sections on the middle cart (Figure 1.15).

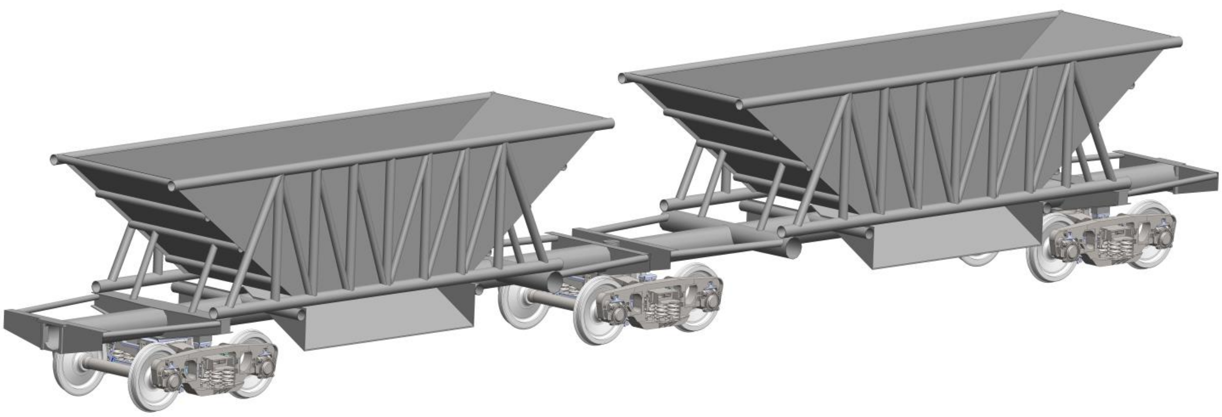

Fig. 1.15 **Articulated hopper car for transporting pellets and hot sinter**

In the patent [14] describes a hopper car, which consists of a module of the crew part, containing two double-axle carts, autocoupling module, brake equipment module, frame module, consisting of a spine, end, pivot and intermediate beams, unloading equipment module and body module, which consists of two side vertical walls, which include the upper and lower strapping, vertical and inclined racks, two end sloping walls, which include the upper and lower strapping, and two hoppers with two unloading hatches. The spine beam is made of a U-shaped profile, behind which between the rear stops of the autocouplings there are elastic elements covered with a horizontal sheet on top. To limit the movement of horizontal sheets in the vertical plane on the U-shaped profile, brackets are provided (Figure 1.16).

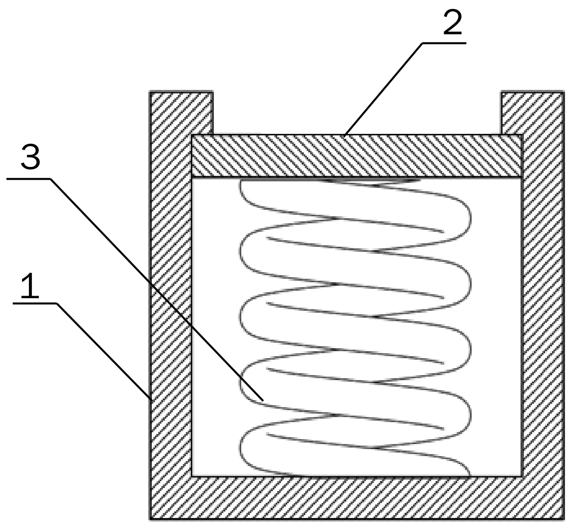

1 - U-shaped profile; 2 - horizontal sheet; 3 - elastic element

Fig. 1.16 **The back beam of a hopper car for transporting pellets and hot sinter**

Patent [15] covers the construction of an open type hopper railway car, which consists of a crew unit comprising two double-axle carts, an auto-coupling module with standard harness devices, a brake equipment module, a frame module consisting of a spine, end, pivot and intermediate beams, an unloading equipment module and a body module consisting of two side vertical walls which include upper and lower strapping, vertical and inclined racks, two end inclined walls which include upper and lower strapping, and two hoppers with two unloading hatches, thus the module of the autocoupling equipment does not contain harness devices, and their functions on absorption the energy arising from the action of operating loads transferred to the spine beam of the modified structure, namely, which includes an intermediate adapter consisting of a thrust part on which a base plate of a typical structure is placed, while the thrust part of the adapter connects to the piston through the rod which contains two throttle valves – intake and exhaust, viscous damping and anti-corrosion material is placed on the left and right sides of the piston, and a bottom is provided to create a pressure of viscous damping anti-corrosion material when moving the piston during the perception of shock load in the spine, the limiter is provided for restriction movements of the adapter at "jerk-stretching", and also the top and bottom bindings of lateral walls, which are proposed to be made of round pipes and filled with viscous material with damping and anti-corrosion properties, as well as the end, pivot and intermediate beams of the frame module of the upper and lower straps, vertical and inclined racks of end side, top and bottom wall straps of the body modules made of round pipes, which are filled with a viscous material with damping and anti-corrosion properties (Figure 1.17).

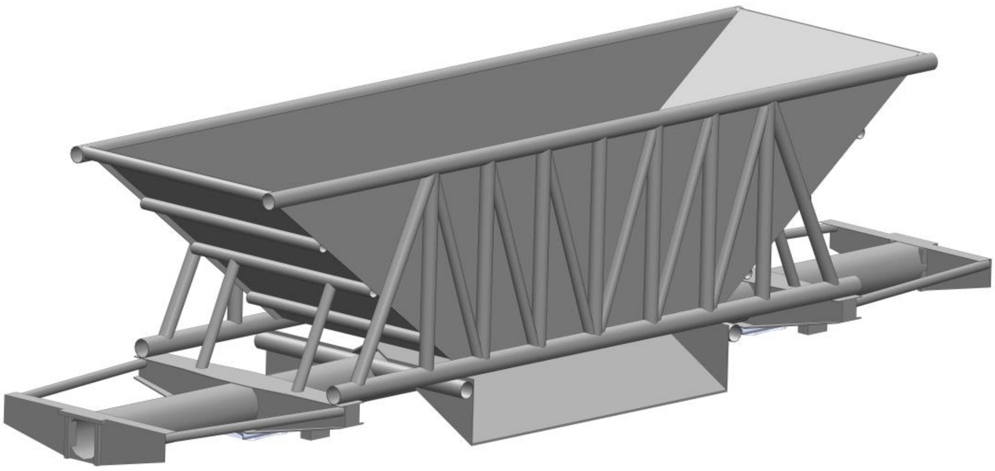

Fig. 1.17 **Load-bearing structure of a hopper car for transportation of pellets and hot sinter**

Patent [16] describes the design of a railway hopper car, comprising a frame mounted on the running gear, on which is rigidly fixed body with internal and external unloading hatches, a mechanism for moving the covers of internal and external hatches, which contains drive shafts connected to the respective power cylinders and connected to the hatch covers by lever systems, and a hinged dispenser with rigidly fixed stops for fixing the hatch covers in the transport position, while the drive shafts are rigidly fixed two-arm levers, the ends of which are connected to the hatch covers by folded rods, parts of which are connected with the possibility of mutual rotation.

The design of a hopper railway car containing a body with vertical longitudinal walls, a frame with placed brake, clutch and unloading devices mounted on carts is given in the patent [17]. The body is made of three sections. The cantilever sections are movable relative to the fixed middle, hinged to it with the location of the axes of rotation perpendicular to the longitudinal axis of the body and the outer width of each cantilever body is less than the inner width of the fixed part.

The proposed design solutions for the improvement of hopper cars help to reduce the dynamic load of their load-bearing structures under operating conditions, increase the service life of cars and reduce the cost of their maintenance. However, maintenance and repair of such car structures are difficult. In addition, the implementation of the proposed solutions does not always reduce the packaging of cars, and accordingly increases their sprung mass. Therefore, the creation of highly efficient designs of cars for the transportation of high-temperature goods with improved strength and dynamic performance is a very important issue.

1.3 Analysis of literature sources to determine the temperature effect on the components of the rolling stock

The question of determining the temperature effect on the components of rolling stock during operation is quite relevant. Components of rolling stock that have a frictional interaction are subjected to temperature loading.

For example, the work [42] highlights the results of determining the influence of the design of brake pads on the temperature and stress fields of the disk. A method for improving the heat flux distribution of the brake disc by optimizing the position of the friction brake unit is proposed.

The thermal behavior of the cast iron brake unit during braking was modeled in the work [43]. The research was conducted in the ANSYS software package. The research results are confirmed experimentally.

At the same time in the considered works the researches of influence of temperature loading on components of tribotechnical pairs at braking are not carried out.

Significant temperature effects are also experienced by wheelsets under interaction with the railway gauge.

The influence of heat load on the contact of the wheel with the rail is considered in the work [44]. The main factors influencing the temperature load of the wheel are determined. The need to adjust existing standards for its calculations is noted.

The paper [45] investigated the influence of the heat load on the service life of a railway wheel. The obtained results confirm the important influence of thermal loads on the service life of the fatigue wheel under operating load modes.

However, these articles do not specify the requirements and recommendations for ensuring the safety of operation of railway wheels, taking into account the temperature effects on them.

The occurrence of thermal processes also takes place during the operation of energy-absorbing devices of rolling stock (spring suspension, absorbers, etc.).

Determination of the effect of preload on the absorber of the car is carried out in the work [46]. The fatigue strength of the body of the absorber is determined. The requirements for ensuring the reliability of its operation are given.

Simulation of the elastic-friction absorber is carried out in the work [47]. A computational model of the elastic-friction absorber using the NX Motion software package has been developed. A comparative analysis of the results obtained analytically and using NX Motion.

It is important to say that when calculating the absorbers are not taken into account the temperature effect on their strength.

The study of the dynamics of cars on the promising designs of carts is carried out in the publication [48]. The results of the calculation proved the feasibility of using these models of carts under freight cars. However, the paper does not determine the effect of temperature load on the operation of these models of carts.

The load-bearing structures of wagons during the defrosting of goods in greenhouses, also test the temperature load. However, so far these issues have not been adequately covered in scientific publications.

Improving the load-bearing structure of the gondola to ensure strength in operating conditions is carried out in the work [49]. The peculiarities of the calculation of the strength of the advanced load-bearing structure of the car with the help of computer simulation are highlighted.

The publication [84] investigated the process of thawing iron-containing raw materials in cars. The results of an experimental study of the thawing process are presented. The temperature at which the cargo is thawed with the possibility of further unloading from the car is determined.

However, the question of the effect of temperature load on the load-bearing structure of the gondola car during thawing in the greenhouse is not taken into account.

The features of topological optimization of the car body are given in the work [50]. It uses computer simulation using the finite element method. The research results confirmed the effectiveness of the proposed methodology for car bodies. As an example, the calculation was performed for the body of a passenger car. With regard to the load-bearing structure of the pellet car, as the most loaded type of car in operation, this technique was not used.

Issues of optimization of bodies of open type freight cars with a bearing floor are covered in the work [51]. An algorithm for compatible structural and parametric optimization of the side wall and the frame of the gondola car with a load-bearing floor for an axial load of 25 t / axle has been developed.

The optimization of the load-bearing structure of a hopper car for transportation of pellets and hot sinter is covered in the work [52]. The purpose of optimization was to reduce the material consumption of the load-bearing structure of the hopper car. The dynamic load and strength of the load-bearing structure of the hopper car are determined. However, when calculating the strength of the authors did not take into account the temperature load on the load-bearing structure of the car.

A unified concept of impact strength is considered in the work [53] in order to optimize the body of rolling stock. The body is presented in the form of a rigid frame structure. The task of optimization was to minimize body weight, taking into account stress limits.

However, the effect of temperature influence on the load-bearing structure of the car when thawing the cargo in it is not taken into account during the research.

During the repair of vehicles, including wagons, thermal editing has recently become widespread.

Thus, the results of determining the effect of thermal correction on the mechanical properties of steel are presented in the world [54]. Features of application of thermal correction in practice are given. The properties of materials that can be changed during this process are determined.

Features of the welding process of aluminum and steel for car bodies are highlighted in the work [55]. The requirements to the welding process, as well as the prospects of its development in relation to car bodies are determined. However, such studies require further consideration and development for wagon structures.

Currently, a large number of cars with improved technical, economic and operational characteristics are being designed. However, their design does not take into account the possible temperature effects on load-bearing structures.

Thus, the analysis of the design of the freight car BCNHL is carried out in the work [56]. Possible options for improving the technical and economic performance of cars are given. However, the authors do not indicate the possibility of using universal cars for the transportation of high-temperature goods.

The results of determining the load of the load-bearing structure of a car with composite walls are highlighted in the the work [57]. The authors limited themselves to the normative values of loads acting on the car in operation. The authors also do not pay attention to determining the temperature load of the load-bearing structure of the car, which is also of scientific interest, because its walls are made of composite material.

The study of the strength of the load-bearing structure of the car made of composite material reinforced with fiber is carried out in [58]. Conclusions on the obtained stress state of the load-bearing structure of the car under shock loads are given. However, the determination of the temperature load of the load-bearing structure of the car with composite components was not performed.

Analysis of the possibility of modernization of the freight car by using composite panels in its components is carried out in the work [59]. The expediency of the proposed introduction into the load-bearing structure of the car is substantiated. Along with this issue, the attention in this work is not paid to the feasibility of using composite materials in order to be able to transport high-temperature cargoes in cars.

The publication [60] provides the feasibility for the use of composite panels in the modernization of freight car bodies. The advantages of the proposed modernization and prospects of its further development on narrow gauge cars are noted. However, the analysis of the stress state of the load-bearing structure of a freight car with composite components is not performed.

The peculiarities of introduction of new polymer composite materials in transport engineering are highlighted in the work [61]. The research was carried out on the example of flooring of railway cars. Prospects for the use of this material in passenger car construction are presented. At the same time there is an interest in the use of this material in freight car construction.

Analysis of physical and mechanical and insulating properties of composite materials that are reinforced with carbon fiber for the floor of cars was carried out in the work [62]. The expediency of using this material in car construction is substantiated. However, this publication does not pay attention to the issues of determining the main indicators of strength of load-bearing structures of cars with composite components.

Improving the method of calculating the components of the load-bearing structure of the gondola car for strength is covered in the work [63]. The load of the bearing structure of the car at operating modes is determined. Adjustment of normative documents regulating requirements for design and calculations of wagons is proposed. However, the attention is not paid to the question of determining the temperature load of the load-bearing structure of the car.

The work [64] covers the features of the automated car for increase of efficiency of railway transportations. The car is oriented to work in the conditions of internal terminals, ports and the industrial railway enterprises. The results of experimental tests of the car structure are given. However, the design of this car does not allow the transportation of high-temperature cargoes by rail.

The design of the Zans type car for bulk cargo transportation is considered in the work [65]. Prospects for the operation of this car are determined. The results of calculations on the strength of its load-bearing structure are given.

Analysis of the static strength of the load-bearing structure of the Zans series car is performed in the work [66]. For this purpose, the authors constructed a refined finite-element model of the load-bearing structure of the car and determined the fields of dislocation of the maximum stresses in it.

It is important to say that this type of car is not intended for transportation of high-temperature cargo, which limits the possibilities of its operation.

Optimization of the load-bearing structure of a freight car is carried out in the work [67]. The gondola car was chosen as a prototype. The results of strength calculations confirmed the feasibility of structural improvements to the gondola car.

The peculiarities of modernization of a freight car of Sgnss type on the basis of dynamic tests are considered in the [68]. The results of numerical and experimental modeling of car load are given.

Determination of the strength of the load-bearing structure of the car taking into account its modernization is carried out in the work [69]. The main indicators of strength, as well as fatigue strength of the load-bearing structure of the car are calculated. Requirements for its re-equipment are specified.

The substantiation of modernization of freight cars is covered in the [70]. At the same time, it is proposed to carry out modernization during periodic types of car repairs. The purpose of this modernization is to improve the operating conditions of cars. At the same time, these upgrades do not provide the possibility of transporting high-temperature cargo in cars.

The authors in their work [71] proposed a method for extending the service life of cars in order to further re-equipment of them for transportation of the specified range of cargoes. The results of the calculations confirmed the feasibility of the proposed measures. However, the authors did not consider the possibility of creating or upgrading cars with heat-resistant properties.

Justification of the extension of the service life of a covered car, which has exhausted its rated service life, is published in the work [72]. It is noted that the service life of a covered car can be extended. In addition, this design of the car can be upgraded to meet the needs of cargoes.

Prediction of the residual life of the hopper-dispenser car after long operation, taking into account the actual physical and mechanical characteristics of the material of load-bearing structures is carried out in the work [73]. The results of virtual and experimental studies of the strength of the load-bearing structure of the car are presented.

Features of improving the design of the hopper car for grain transportation are highlighted in the publication [74]. The possibility of optimizing the elements of the car body was carried out based on the analysis of the most characteristic nodes and structural features of specialized hopper cars for the transportation of bulk cargo. That is, the experience of operating individual components of the body with subsequent integration into a new structure is taken into account. However, in the reviewed works, the temperature effect on their components was not taken into account when calculating the strength of the load-bearing structures of the cars.

The work [75] provides justification for extending the service life of a hopper car for the transportation of pellets and hot sinter, which has exhausted its resource. The results of the calculation of the dynamic load and strength of the load-bearing structure of the hopper car are presented. The conducted studies proved the possibility of its further exploitation. Along with this, the authors did not take into account the effect of temperature on the load-bearing structure of the hopper car when determining its operational load.

The issue of the introduction of promising materials in mechanical engineering, including heat-resistant ones, is quite urgent, which is confirmed by a large number of publications in world periodicals.

Studies of the impact resistance of a railway tank car made of fiber-reinforced composite materials are given in the publication [76]. The influence of the initial tension on the strength of the boiler is considered. It was established that the effect of the initial tension is more significant in the case when the load acts parallel to the direction of the main fiber. However, the work does not determine the influence of the use of composite materials on the load of cars, including temperature.

The work [77] provides the substantiation of the use of polymer composite materials in railcar construction is provided. These materials are proposed to be used in the manufacture of the car floor. The results of experimental studies on the method of pressing the composite in the form are highlighted. It is important to say that the authors have not considered the possibility of using this material in the manufacture of supporting body elements.

Features of the calculation of a freight car with laminated composite walls are highlighted in the work [78]. The calculation was implemented using the finite element method in the Ansys 14.5 software package. The results of determining the optimal thickness of the walls of the car body, provided that its strength is ensured, are presented. At the same time, when determining the stress state of the supporting structure of the car, the authors did not take into account the temperature effect on its components.

The work [79] gives the features of the use of environmentally friendly composites for the manufacture of vehicles for the automotive industry. The results of calculations on the strength of transport means made of this material are highlighted. It has been established that the use of composites on a natural basis is more rational from the economic and technical point of view in comparison with the standard ones.

An analysis of the properties of composite materials and the possibility of their application in the construction of vehicles is given in the work [80]. The research was carried out in relation to the body of the bus. It was established that the use of composites contributes to the reduction of body weight almost by 20% while ensuring the conditions of strength and operational reliability. However, the expediency of using these materials in the manufacture of load-bearing structures of railway vehicles is aslo of interest from the point of view of temperature resistance.

Features of the production and use of modern polymer composite materials in the manufacture of railway cars are presented in the [81]. The research is focused on the development of nanocomposites from recycled polypropylene reinforced with natural fiber. It should be noted that the issue of determining the strength of the load-bearing structure of the car with the use of this material and temperature effects was not paid attention to in the work.

Features of the use of composite materials with improved mechanical properties in the manufacture of aerospace vehicles are highlighted in works [82, 83]. The expediency of using composite materials in this field and the prospects for the further development of these issues are substantiated. At the same time, the question of the effectiveness of the use of composite heat-resistant materials in the railway industry requires an additional study.

The conducted literature review shows that the issue of determining the temperature effect in mechanical engineering, including car structures, is quite promising and relevant, but their development in relation to the application in car structures requires further study. Such a situation makes it necessary to carry out additional studies and create relevant reseraches in this direction.

1.4 The main measures of labor protection and features of repair of load-bearing structures of hopper cars for transportation of hot pellets and sinter

Repair of supporting structures of hopper cars for transportation of hot pellets and sineter is carried out in the car assembly section of the depot.

One of the necessary conditions for production work is to ensure normal conditions in terms of temperature and air purity in the operation area [87]. Optimal microclimatic conditions in this area in accordance with the DSN 3.3.6042-99 "Sanitary norms of the microclimate of industrial premises": temperature not lower than 18°C, relative air humidity 40-60%, air movement speed not more than 0.25 m/s. It is advisable to use collective and individual means of labor protection. Collective protection – heating, ventilation, local suction devices (in electric welding booths), individual protection – overalls, shoes, hand and face protection.

To ensure safe levels of noise and vibration in accordance with the GOST 12.1.003 - 83 SSBT "Noise. General safety requirements" sound insulation – partitions, cabins, casings are applied.

Locksmith-assembly and mechanical tools, which are used in the repair of load-bearing structures of carss, must be serviceable. It should be checked at least once a month.

According to the DSN 3.3.6042-99, work in the wagon assembly station can be classified as the medium difficulty work.

Before starting work with a hand-held electric tool, its completeness and reliability of fastening parts should be checked, the serviceability of the cable should be determined, the operation of the tool at idle speed should be checked.

When working, cleaning, pouring flux into the hopper, the electric welder must wear a respirator and gloves. Sifting flux in open sieves is prohibited.

The total illumination of the departments of the car assembly area should be from 100 lux to 300 lux, depending on the degree of visual work; the area of work on metalworking machines should have a total illumination of 500 lux to 750 lux, in accordance with the NAOP 5.1.11-3.02-91 "Norms for artificial lighting of railway transport facilities" with combined lighting.

For the purpose of complete safety when working on the equipment, the following is prohibited:

- to allow people who have not been instructed in labor protection to work;

- work on the equipment if there is a malfunction in any assembly unit or control system;

- perform maintenance during work;

- perform measurements and inspection during work.

At the end of the work, the equipment is turned off.

The requirements for cargo-lifting mechanisms must meet the requirements of the “Rules of Safety and Industrial Sanitation for the Maintenance and Repair of Wagons” TsV/64-92 dated July 4, 1992.

To ensure electrical safety in accordance with the GOST 12. 1. 030 - 81 “Electrical safety. Protective grounding, zeroing” closed types of shields, circuit breakers, lamps, and electric motors are used.

Electric motors, generators and other electrical equipment are maintained in strict accordance with the requirements of the “Rules for the Technical Operation of Consumer Electrical Appliances” and the “Safety Rules for the Operation of Consumer Electrical Appliances”.

The main protective insulating means against electric shock are assembly tools with insulated handles, as well as gloves, galoshes and mats made of dielectric rubber (NPAOP 40.1-1.07-01 “Rules for the use of electrical protective equipment”).

Control periodic tests of electrical strength of gloves are carried out at least once every 6 months, galoshes – at least once a year, and rugs – at least once every two years.

Electrical equipment, as well as mechanisms powered by electric current, must be grounded.

When repairing the components of the supporting structure of the hopper car, the following operations are carried out [18]:

- the body is cleaned, inspected, corrosion wear of the body cladding is measured with an ultrasonic thickness gauge. On the basis of the conducted comprehensive control, the scope of repair is determined. If the cladding wear is more than 0.5 of the sheet thickness on the area of more than a half of the sheet, the sheet is replaced with a new one.

- deformed and damaged racks of the car are repaired, and those with cracks and breaks are repaired with further strengthening of the joint with a pad or replaced with new ones of a similar design.

- deflections of the upper and lower body harnesses of more than 15 mm inside the car and 15 mm outside the car are rebent. Bends of the upper and lower straps in the vertical plane between the racks that are more than 15 mm are rebent.

It is allowed to leave unrepaired local smooth dents on bindings with a depth of 10 mm on a length of up to 200 mm. The total deflection of the straps over the entire length of more than 25 mm is not allowed.

- damaged metal body cladding is repaired by welding. Cracks with a length of up to 100 mm are welded without the installation of reinforcing overlays, with a longer length – with the installation of reinforcing overlays.

It is not allowed to install more than two overlays with an area of 0.3 m^2 on one part of the cladding. In case of corrosive damage or burning of metal with a thickness of more than 2 mm on the area of more than a half of the sheet, the cladding sheet is replaced with a new one.

- when placing the cladding on the side wall, the sheets, pressure bars and overlays are fastened with bolts to the racks, the gap between the cladding and the frame of the side and end walls should not exceed 2 mm.

- the details of fastening the cladder to the body frame (carrying bars, overlays, pressure bars) are checked, those that are missing are re-installed. Missing or defective overlays and bolts with countersunk heads for fastening the cladding of the end walls are replaced with new ones.

- repaired or new hoppers of the car frame are installed at an angle of inclination to the horizontal in accordance with the requirements specified in the drawings of the manufacturing plant.

- the fastening of the body components to the backbone beam inside the body must be done in accordance with the drawings of the manufacturing plant. The walls of the formwork, which protect the backbone beam from high temperatures and provide the necessary angle of inclination of the unloading plane, must have a thickness of at least 8 mm. When the thickness of the formwork sheet is worn by more than 1/3, it is replaced with a new one.

- the fastening of the hopers' cladding, which are subject to the greatest wear during operation, must be performed in accordance with the drawings of the manufacturering plant.

- manhole covers are removed from the car to check the technical condition and repair. Deformed covers are repaired, those with cracks or local damage are repaired.

It is allowed to repair manhole covers by placing no more than two overlays on an area of no more than 1/3 of the manhole area by welding on the inside. The thickness of the overlays should be from 6 to 8 mm. It is not allowed to place reinforcing overlays in places where hatch covers adjoin the hopper. The welding of the holes in the hatch cover should be carried out by placing overlays.

- hatch covers damaged by corrosion more than 1/3 in thickness, and more than a half of the surface of the hatch cover, are replaced with new ones.

- hatch covers must rotate on the hinges without jawing and ensure a tight fit around the entire perimeter. No more than 1 mm gap between the holes and the rollers in the hinges is allowed. Local gaps between the manhole cover and its abutment plane are allowed to be no more than 2 mm.

- the total expansion or contraction of the side walls in the middle part of the car should be no more than 30 mm from the limit dimensions, and one side wall – no more than 15 mm. A gap of more than 3 mm between the formwork and the end inclined part of the body is not allowed.

CONCLUSIONS TO THE SECTION 1

1. The design and main characteristics of the hopper cars for the transportation of hot pellets and sinter of the operated park were analyzed. The design of the hopper car is considered on the example of the model 20-471. The main technical characteristics of the hopper cars produced in Ukrainian and Russia are given.

2. A patent analysis of the supporting structures of hopper cars for the transportation of pellets and hot sinter was carried out. At the same time, the analysis was carried out in relation to Ukrainian inventions and utility models. Prospective directions for improving the load-bearing structures of hopper cars for the transportation of pellets and hot sinter have been determined.

3. An analysis of literary sources on the determination of the temperature effect on the components of the rolling stock was carried out. The main

operational situations of the occurrence and effect of temperature load on the components of rolling stock structures have been determined. Measures regarding the improvement of components of the rolling stock to ensure their heat resistance during operational modes are considered.

4. The main labor protection measures and features of repairing the supporting structures of hopper cars for transportation of hot pellets and sinter are considered. The main requirements for the component of the load-bearing structures of the hopper cars and the permissible values of their geometric parameters are indicated, as well as the measures that are taken to eliminate damage to the load-bearing structures of hopper cars.

SECTION 2
DETERMINING THE LOAD OF THE LOAD-BEARING STRUCTURE OF THE HOPPER CAR AND CREATING MEASURES TO INCREASE THE EFFICIENCY OF TRANSPORTATION OF HIGH-TEMPERATURE CARGOES

2.1 Determining the load of the load-bearing structure of the hopper car due to temperature effects

To determine the temperature load of the supporting structure of the hopper car, a calculation was made using the finite element method [39, 40]. For this, its spatial model was built in the SolidWorks software complex. The model 20-9749 hopper car, built by SE "Ukrspetsvagon" (Ukraine), was chosen as the prototype car.

The spatial geometric model of the supporting structure of the hopper car is shown in the Figure 2.1.

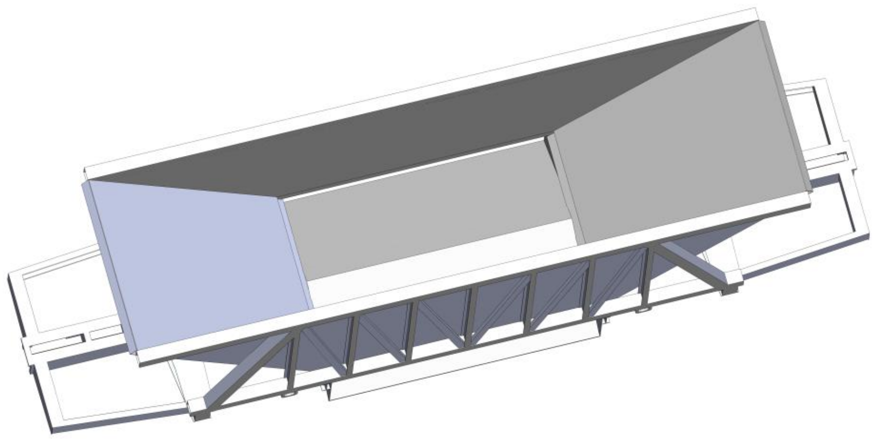

Fig. 2.1 **Spatial model of the supporting structure of the hopper car**

The calculation is implemented in the CosmosWorks software environment.

Isoparametric tetrahedra are taken into account when compiling the finite element model. The optimal number of model elements is determined by the graphic-analytical method. The number of model nodes was 126.221 and number of elements – 376.670.

The maximum size of the element was 60 mm, and the minimum - 12 mm. The percentage of elements with an aspect ratio of less than three is 7.43. The percentage of elements with an aspect ratio greater than ten is 32.5. The minimum number of elements in a circle was 9, the ratio of the increase in the size of the elements was 1.6.

The calculation diagram of the supporting structure of the hopper car in the most unfavorable operating mode – shunting co-impact, is shown in Figure 2.2.

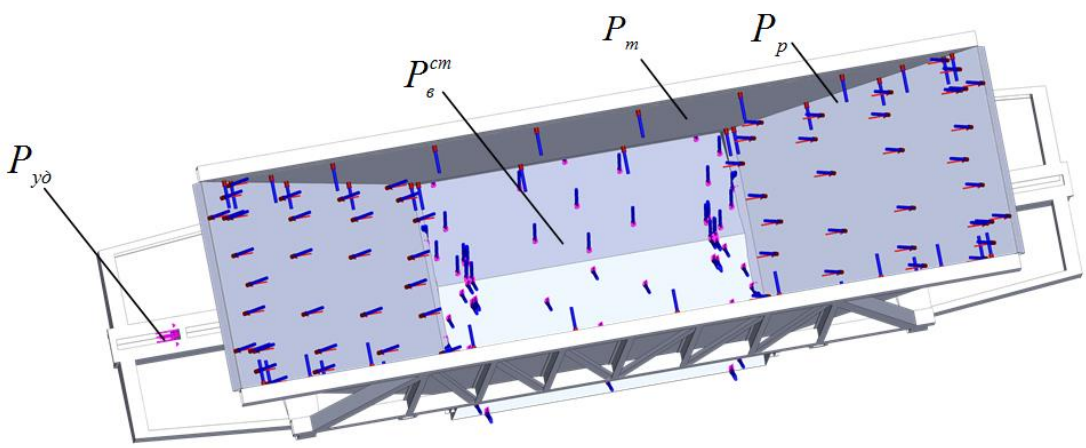

Fig. 2.2 **Calculation diagram of the supporting structure of the hopper car**

It is taken into account that the supporting structure of the car is subjected to a vertical static load P_v^{st}. The structure of the body is also affected by the pressure of the spacer from the bulk cargo P_s, the numerical value of which is found by the formula (1). The vertical surface of the rear stop is subjected to the P_{sh} shock load, the numerical value of which, according to regulatory documents, is 3.5 MN [20, 21]. A temperature load P_t, equal to 700°C, was applied to the internal surfaces of the body.

The active pressure of the spacer of the bulk cargo was determined by the formula:

$$P_a = \gamma \cdot g \cdot H \cdot tg^2\left(\frac{\pi}{4} - \frac{\varphi}{2}\right), \tag{2.1}$$

where γ *– density of bulk cargo, t/m³;*

H – height of the side wall, m;

φ – the angle of the natural slope of the load, degrees;

g – free fall acceleration, m/s².

Fixing of the model was carried out in the areas where the body rests on the running parts. The construction material is 09G2S steel. The calculation results are given below (Figures 2.3, 2.4).

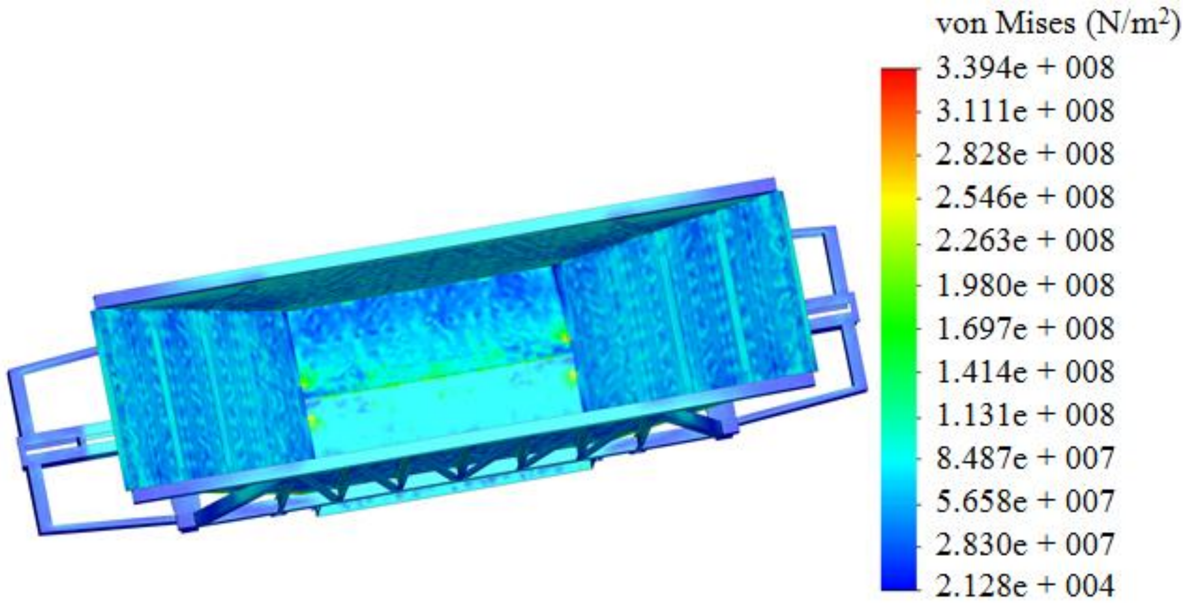

Fig. 2.3 **Stressed state of the supporting structure of the hopper car**

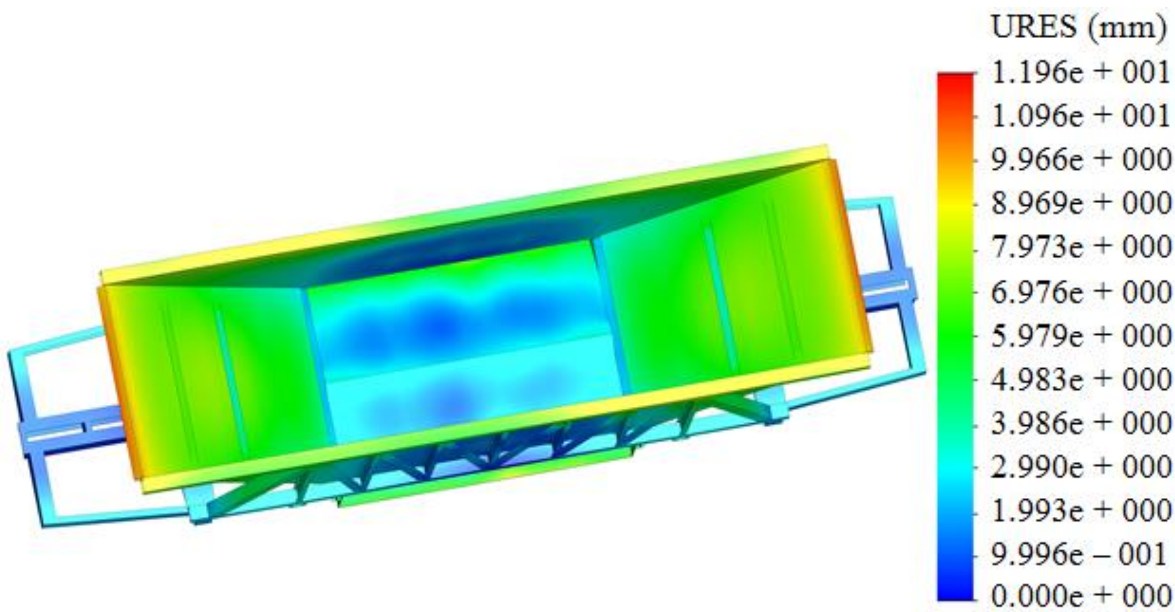

Fig. 2.4 **Movement in nodes of the supporting structure of the hopper car**

The maximum equivalent stresses in the supporting structure of the hopper car are about 340 MPa and are concentrated in the zone of interaction of the backbone beam with the pivot beam. The maximum displacements occur in the unloading hoppers, as well as the upper binding and amount to about 12.0 mm. The maximum stresses in the load-bearing structure of the hopper car, which are caused by the temperature load, occur in the vertical racks and hump.

According to the calculation scheme shown in the Figure 2.2, the distribution of the maximum equivalent stresses along the height of the rack is constructed. The calculation results are shown in the Figure 2.5.

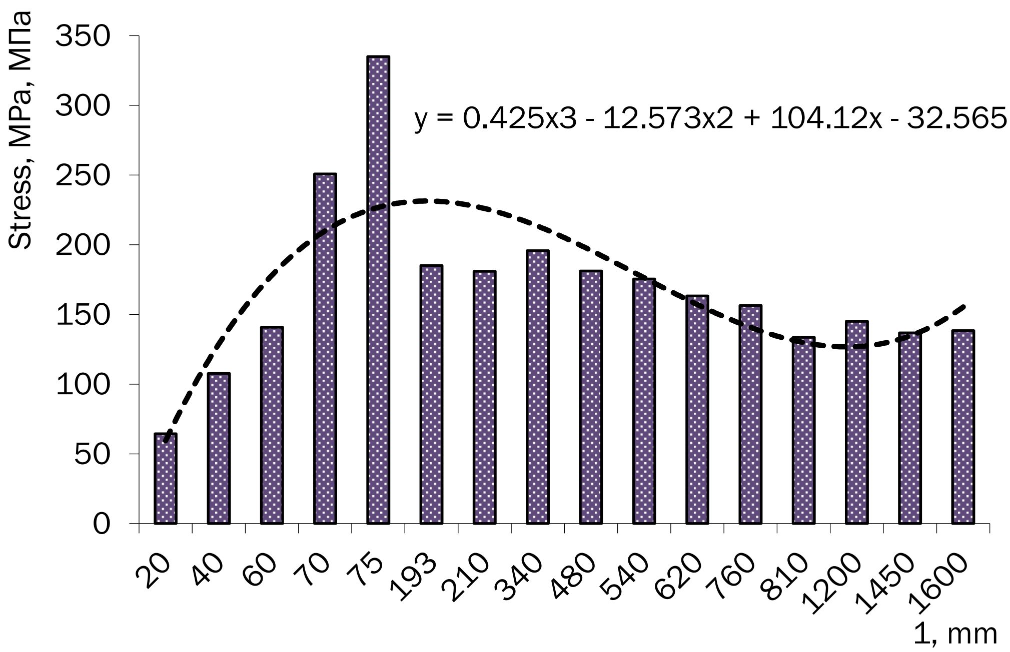

Fig. 2.5 **Distribution of the maximum equivalent stresses by the height of the hopper car rack**

At the same time, the maximum equivalent stress occurs closer to the lower part of the rack and is 335 MPa, which is 3% lower than the turnover stress of the construction material [20, 21].

Figure 2.6 shows the dependence of the maximum equivalent stresses in the vertical rack of the hopper car on temperature influence.

Figure 2.6 shows that this dependence is linear. At the same time, stresses were removed from the most loaded zone of the vertical rack.

The maximum equivalent stresses at the temperature of the transported cargo of 700°C are almost equal to the yield point of the construction material. With a slight increase in the temperature effect on the supporting structure, its

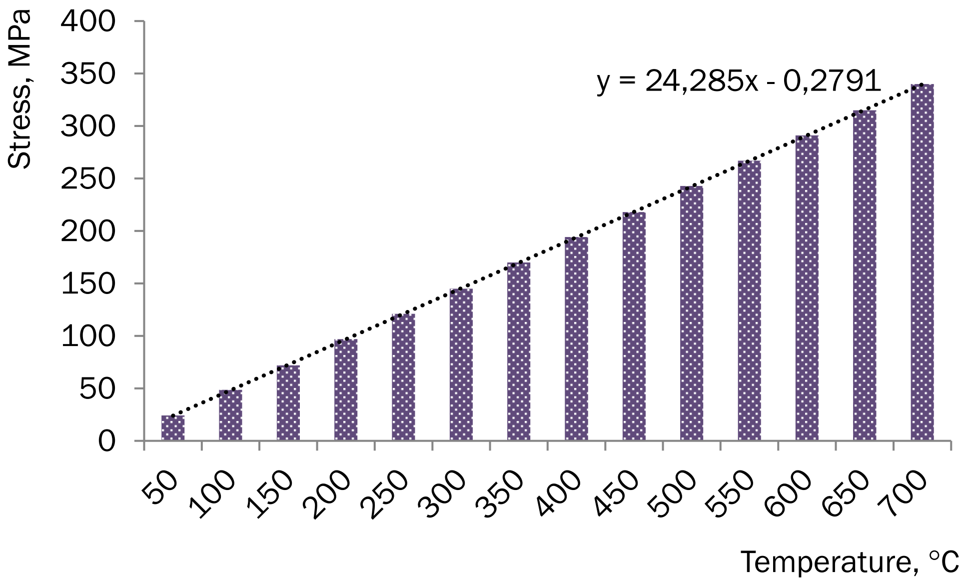

Fig. 2.6 **Dependence of the maximum equivalent stresses in the vertical rack of the hopper car on temperature influence**

---

strength indicators will not be ensured. This makes it necessary to create measures to ensure the strength of the components of the supporting structure of the hopper car. For example, improving the load-bearing structure of the hopper car by making the most heavily loaded components from heat-resistant material.

2.2 Improvement of the supporting structure of the hopper car to ensure its durability in operation

To ensure the strength of the load-bearing structure of the hopper car under operating loads, measures are proposed to improve it. Preliminary strength calculations carried out by the authors showed that one of the most heavily loaded components of the supporting structure of the hopper car is the backbone beam, hump and upper strapping. In order to improve their strength, it is proposed to manufacture the spinal beam from two rectangular tubes, of closed cross-section (Figure 2.7), but the hump and upper binding – of a composite heat-resistant material (Appendix A). The research was carried out in relation to the hopper car for the transportation of pellets and hot sinter model 20-9749, built by SE "Ukrspetsvagon".

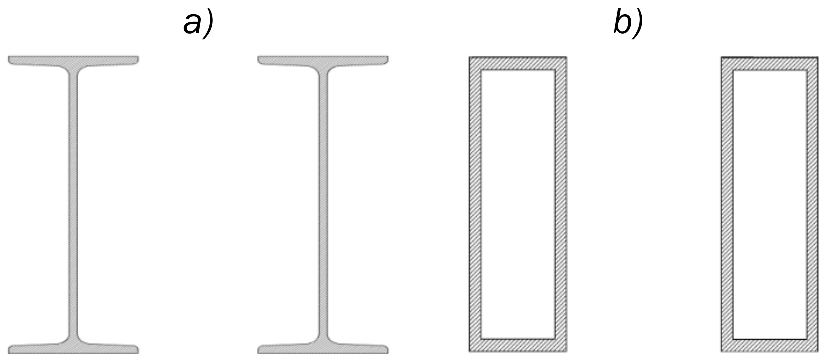

Fig. 2.7 **Section of the backbone beam of a hopper car**
a) typical design; b) improved design

The geometric parameters of the spinal beam are determined by the optimization method based on strength reserves. The proposed improvement helps to reduce the tare of the supporting structure of the hopper car by 2.7% compared to the typical design. The spatial model of the improved design of the hopper car frame is shown in the Figure 2.8.

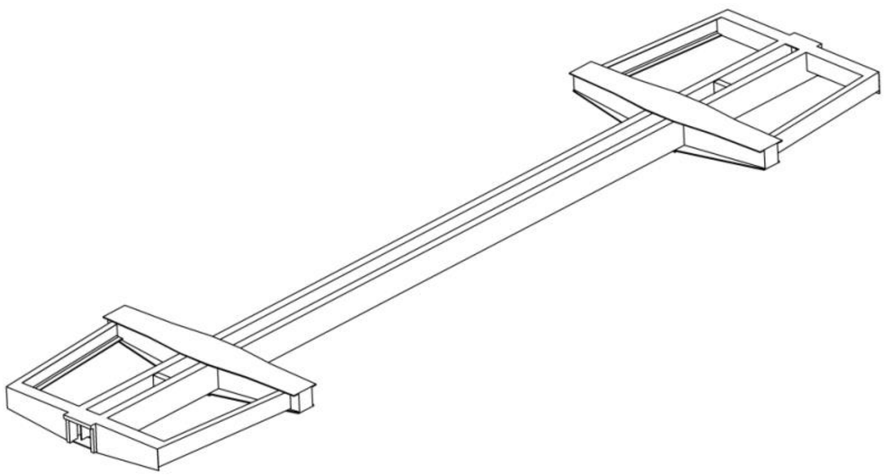

Fig. 2.8 **Improved design of the hopper wagon frame**

In order to determine the dynamic load of the hopper car, taking into account the proposed solutions, mathematical modeling was carried out. At the same time, the mathematical model developed by prof. Bogomazom G. I. [23]. Within this study, the model was adapted to determine the dynamic loading of a hopper car. The model also takes into account the frictional forces that arise between the heels of the body pivot bearing and the pivot bearings of the carts.

The calculation scheme of the hopper car is shown in Figure 2.9.

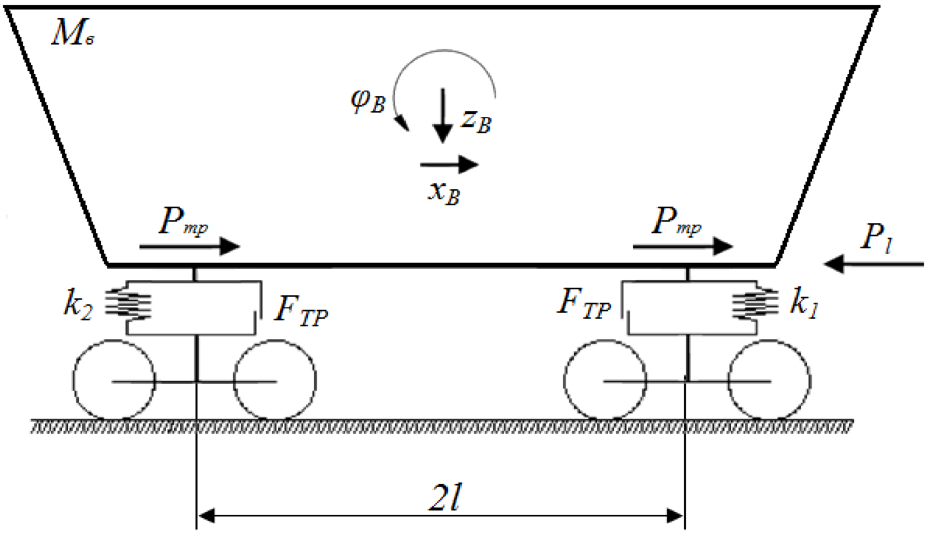

Fig. 2.9 **Calculation diagram of a hopper car**

The equations of motion of the calculation model have the form:

$$\begin{cases} M_{бр}\cdot x''+\left(M_B\cdot h\right)\cdot\varphi''=P_n-2P_{тр}, \\ I_B\cdot\varphi''+\left(M_B\cdot h\right)\cdot x''-g\cdot\varphi\cdot\left(M_B\cdot h\right)=l\cdot F_{TP}\left(sign\left(z-l\cdot\varphi\right)'-sign\left(z+l\cdot\varphi\right)'\right)+ \\ +l\left(k_1\cdot\left(z-l\cdot\varphi\right)-k_2\cdot\left(z+l\cdot\varphi\right)'\right), \\ M_B\cdot z''=k_1\cdot\left(z-l\cdot\varphi\right)+k_2\cdot\left(z+l\cdot\varphi\right)-F_{TP}\left(sign\left(z-l\cdot\varphi\right)'-sign\left(z+l\cdot\varphi\right)'\right), \end{cases} \tag{2.2}$$

where M_{gr} *– gross weight of the hopper car;*

M_c *– weight of the supporting structure of the hopper car;*

I_c *– the moment of inertia of the hopper car;*

P_l *– the value of the longitudinal force on the rear stop of the auto coupling, which is taken to be equal to 3.5 MN [20, 21];*

P_{fr} *– frictional forces that occur between the frame pivot bearings and the cart pivot bearings;*

l *– half of the base of the hopper car;*

F_{FR} *– the value of the dry friction force in the spring set;*

k_1, k_2 *– stiffness of the springs of the spring suspension of the hopper wagon carts;*

x, φ, z – coordinates corresponding, respectively, to the longitudinal, angular around the transverse axis and vertical movement of the hopper car.

The system of differential equations of motion (2.2) was solved using the Runge-Kutta method in the MathCad software package. The initial displacements and velocities are assumed to be zero.

The results of the calculations showed that the maximum accelerations acting on the supporting structure of the hopper car are equal to 37.6 m/s^2 (0.37g). The obtained acceleration value is taken into account when calculating the strength of the supporting structure of the hopper car. At the same time, the finite element method was used, which was implemented in the SolidWorks Simulation software package.

The optimal number of elements of the finite-element model of the supporting structure of the hopper car was determined using the graphic-analytical method. Isoparametric tetrahedra are used as finite elements. The number of grid nodes was 57746, and the number of elements was 169187. At the same time, the maximum element size is 100 mm, the minimum is 20 mm. The number of elements in the circle is 9. The ratio of the increase in the size of the element was 1.7.

When drawing up the calculation scheme, the following loads are taken into account: vertical static load P_V^{st}, pressure of bulk load spacer P_{sp}, as well as longitudinal load P_l acting on the frame from the self-coupling device (Figure 2.10). A temperature load was also applied to the internal surfaces of the body, which was assumed to be equal to 700°C.

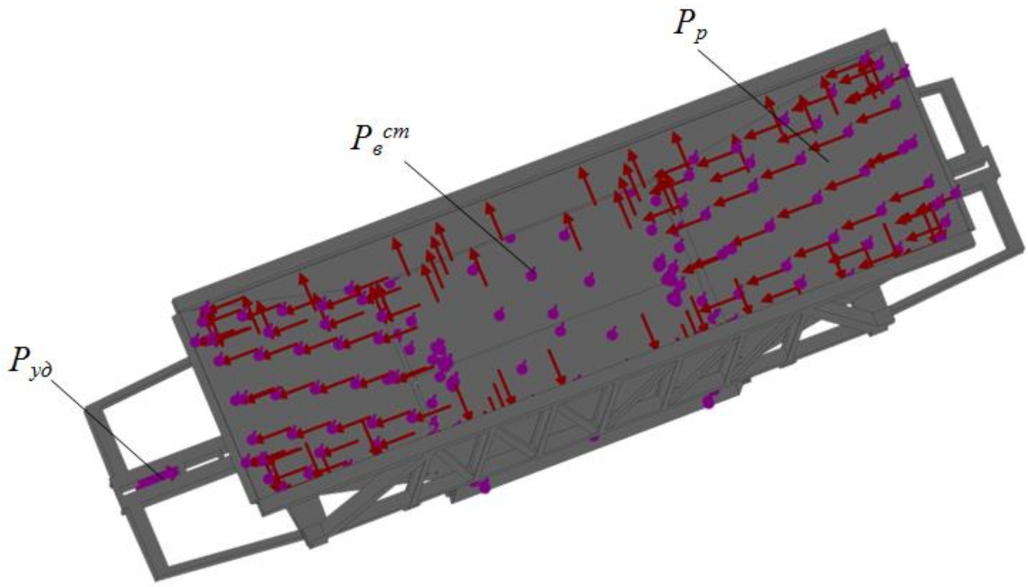

$P_{уД}$ – P_{sp}

$P_{В}^{СТ}$ – P_V^{st}

P_p – P_l

Fig. 2.10 **Calculation diagram of the supporting structure of the hopper car**

Fixing of the model was carried out in the areas where the body rests on the running parts. The material of the load-bearing structure is 09G2S steel, and the hump and upper binding is a composite with a strength limit of 1500 MPa and a density of 2200 kg/m^3. Since steel is an isotropic material, and the composite is anisotropic, the calculation was carried out according to two criteria - Mises and maximum normal stresses. The calculation results are shown in the Figure 2.11.

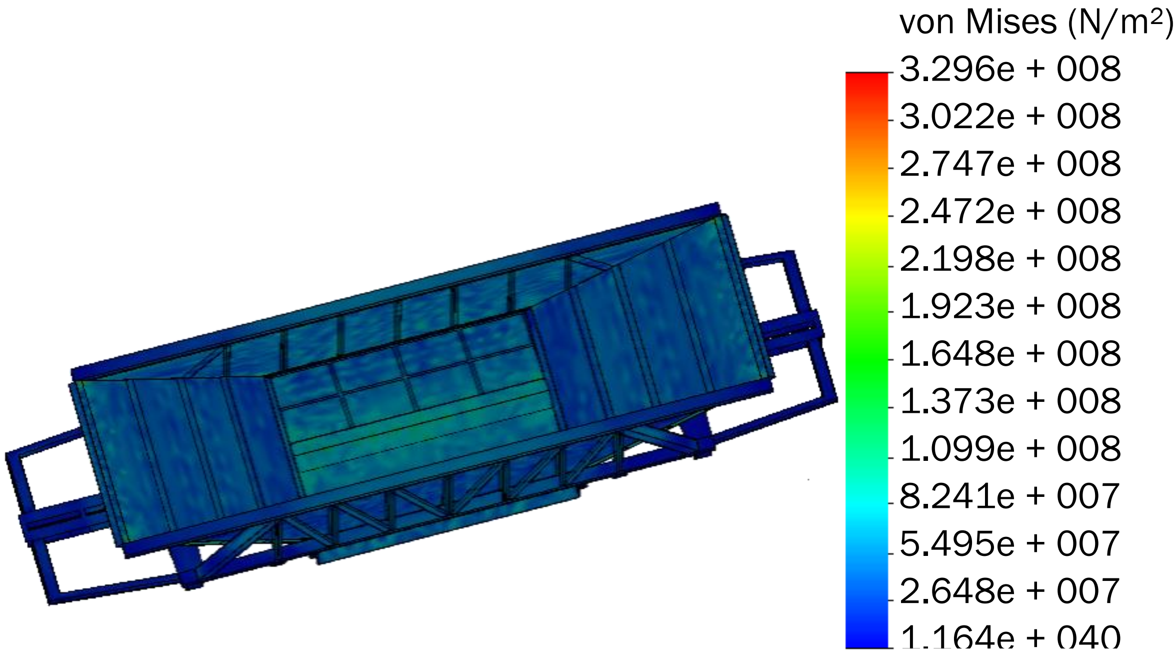

Fig. 2.11 **Stressed state of the supporting structure of the hopper car**

At the same time, the maximum equivalent stresses are concentrated in the zone of interaction of the spinal beam with the pivot beams and amount to 329.6 MPa. The resulting stress value is 3.1% lower than in a typical design. In the hump, the maximum equivalent stress was 322.6 MPa, and in the upper binding, it was 318.4 MPa, which is lower than the permissible values [11, 12].

2.3 Improvement of the load-bearing structure of the hopper car by using cladding made of heat-resistant composite material

The supporting structure of a typical hopper car for transporting pellets and hot sinter consists of a metal frame (Figure 2.12). Unlike other types of wagons, the cladding is not rigidly connected to the frame, but is hung on it. This solution eliminates body warping under the influence of high temperatures and provides easy replacement in case of damage [85].

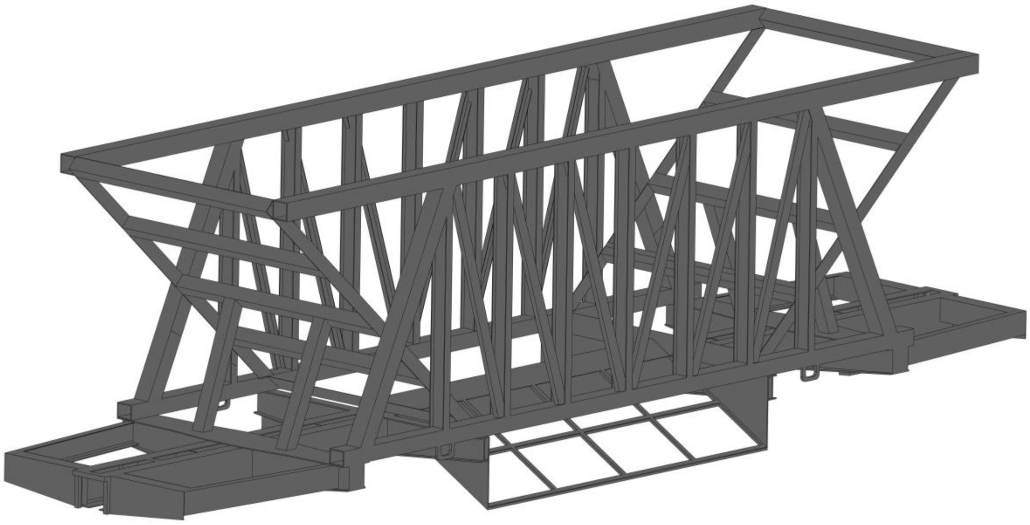

Fig. 2.12 **Load-bearing structure of a hopper car**

In order to improve the strength indicators, including temperature resistance, of the load-bearing structure of the hopper car, it is proposed to improve it by using cladding made of composite material (Figure 2.13). In addition, the use of composite cladding helps to reduce the car container by 5% compared to the prototype.

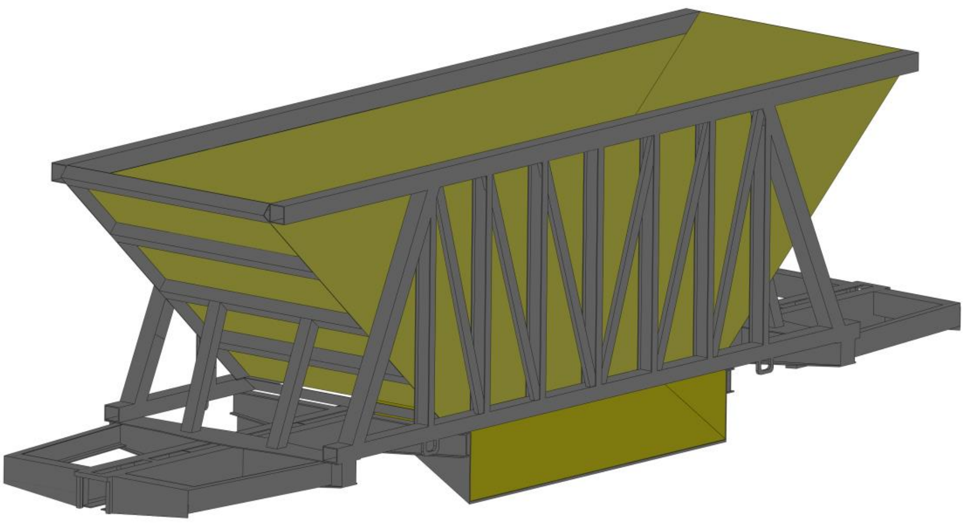

Fig. 2.13 **Improved supporting structure of the hopper car**

At the same time, the proposed improvement can be implemented during the production of new car structures, as well as their modernization in the conditions of wagon repair enterprises.

In connection with the fact that the proposed implementation contributes to the reduction of the car container, the main indicators of its dynamics were determined. The calculation scheme is shown in the Figure 2.14. The hopper car model 20-9749 (Ukraine) was chosen as the prototype.

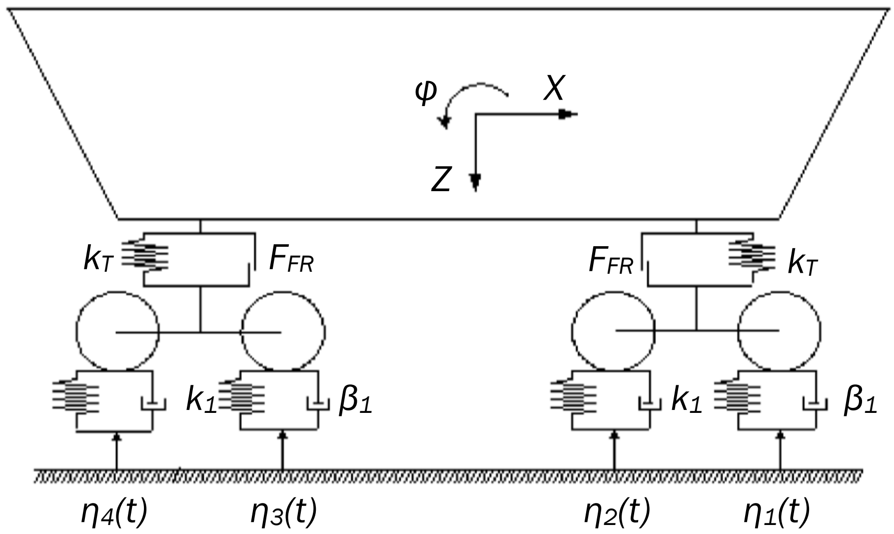

Fig. 2.14 **Calculation diagram of a hopper car**

The bouncing and galloping oscillations are taken into account, as the most common types of wagon oscillations in operation. The model takes into account the technical characteristics of model 18-100 carts.

$$M_1 \cdot \frac{d^2}{dt^2} q_1 + C_{1,1} \cdot q_1 + C_{1,3} \cdot q_3 + C_{1,5} \cdot q_5 =$$

$$= -F_{TP} \cdot \left(sign\left(\frac{d}{dt} \delta_1 \right) + sign\left(\frac{d}{dt} \delta_2 \right) \right), \tag{2.3}$$

$$M_2 \cdot \frac{d^2}{dt^2} q_2 + C_{2,2} \cdot q_2 + C_{2,3} \cdot q_3 + C_{2,5} \cdot q_5 =$$

$$= F_{TP} \cdot l \cdot \left(sign\left(\frac{d}{dt} \delta_1 \right) + sign\left(\frac{d}{dt} \delta_2 \right) \right), \tag{2.4}$$

$$M_3 \cdot \frac{d^2}{dt^2} q_3 + C_{3,1} \cdot q_1 + C_{3,2} \cdot q_2 + C_{3,3} \cdot q_3 + B_{3,3} \cdot \frac{d}{dt} q_3 =$$
$$= F_{TP} \cdot sign\left(\frac{d}{dt}\delta_1\right) + k_1(\eta_1 + \eta_2) + \beta_1\left(\frac{d}{dt}\eta_1 + \frac{d}{dt}\eta_2\right), \tag{2.5}$$

$$M_4 \cdot \frac{d^2}{dt^2} q_4 + C_{4,4} \cdot q_4 + B_{4,4} \cdot \frac{d}{dt} q_4 = -k_1(\eta_1 - \eta_2) - \beta_1 \cdot a \cdot \left(\frac{d}{dt}\eta_1 - \frac{d}{dt}\eta_2\right), \tag{2.6}$$

$$M_5 \cdot \frac{d^2}{dt^2} q_5 + C_{5,1} \cdot q_1 + C_{5,2} \cdot q_2 + C_{5,5} \cdot q_5 + B_{5,5} \cdot \frac{d}{dt} q_5 =$$
$$= F_{TP} \cdot sign\left(\frac{d}{dt}\delta_2\right) + k_1(\eta_3 + \eta_4) + \beta_1\left(\frac{d}{dt}\eta_3 + \frac{d}{dt}\eta_4\right), \tag{2.7}$$

$$M_6 \cdot \frac{d^2}{dt^2} q_6 + C_{6,6} \cdot q_6 + B_{6,6} \cdot \frac{d}{dt} q_6 =$$
$$= -k_1 \cdot a \cdot (\eta_3 - \eta_4) - \beta_1 \cdot a \cdot \left(\frac{d}{dt}\eta_3 - \frac{d}{dt}\eta_4\right), \tag{2.8}$$

F_{Tp} - F_{FR}

where M_1, M_2 *– respectively, the mass and moment of inertia of the supporting structure of the hopper car;*

M_3, M_4 *– the mass and moment of inertia of the first cart in the course of its movement;*

M_5, M_6 *– respectively, the mass and moment of inertia of the second cart in the course of its movement;*

C_{ij} *– characteristics of the elasticity of the components of the oscillating system;*

B_{ij} *– scattering function;*

a – cart semi-base;

q_i *– generalized coordinates corresponding to the translational and angular movements around the vertical axis, respectively, of the body of the hopper car, the first and second cart;*

k_i *– rigidity of spring suspension of carts;*

β_i *– damping coefficient;*

F_{FR} *– frictional force arising in the spring set.*

The calculations made it possible to determine the main indicators of the dynamics of the hopper car: acceleration in the center of mass, acceleration in the areas of support on the carts and the coefficient of vertical dynamics (Figures 2.15 – 2.17).

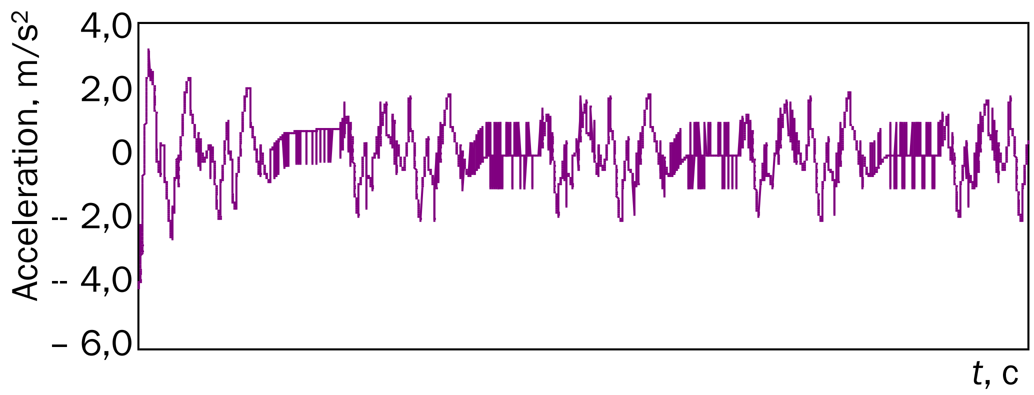

Fig. 2.15 **Acceleration of the supporting structure of the hopper car in the center of mass**

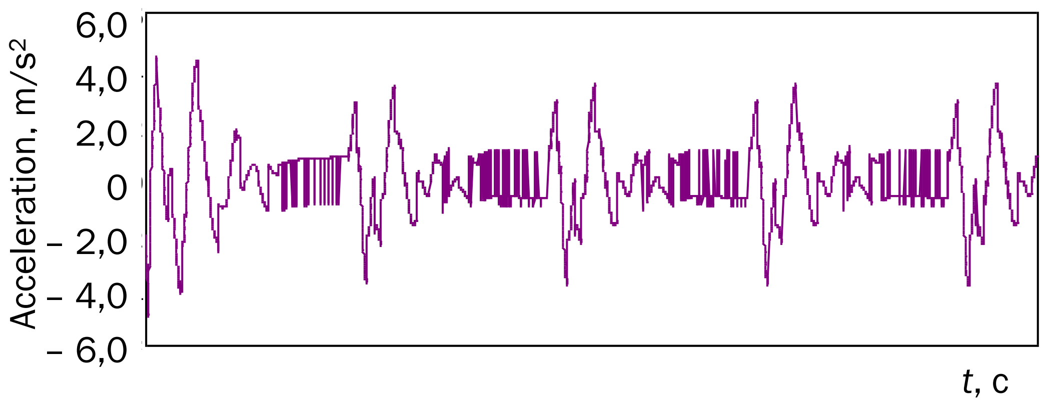

Fig. 2.16 **Acceleration of the supporting structure of the hopper car in the support zones on the carts**

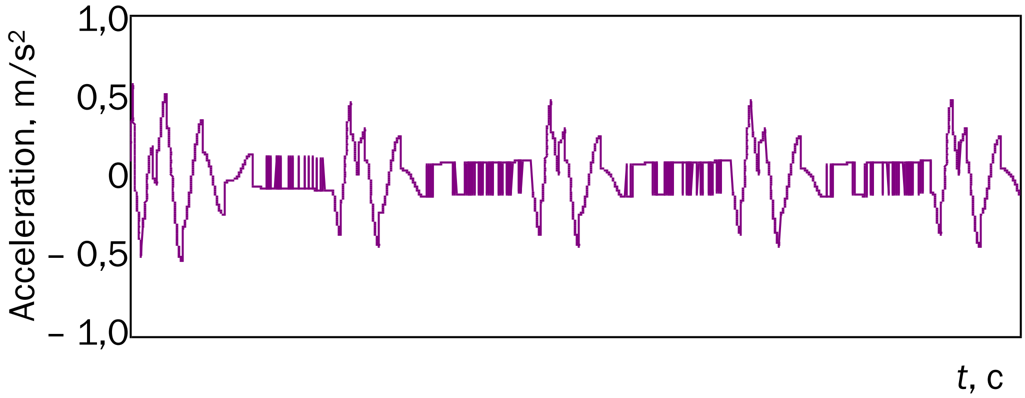

Fig. 2.17 **Coefficient of vertical dynamics of a hopper car**

The calculations of the dynamic loading of the car showed that the determined dynamic indicators do not exceed the permissible values. The acceleration acting on the center of mass of the supporting structure is about 0.4g. The acceleration of the supporting structure of the hopper car in the areas of support on the carts is equal to 0.53g, and the coefficient of vertical dynamics is 0.52. At the same time, the movement of the hopper car is evaluated as "excellent".

To determine the temperature effect on the strength of the supporting structure of the hopper car, a calculation was made in the SolidWorks Simulation software package. At the same time, the finite element method was applied. The mesh was created on a solid body taking into account the curvature. During calculations, isoparametric tetrahedra were used, the optimal number of which was determined by the graphoanalytic method. The number of mesh elements was 373185, nodes – 125608. The maximum size of the mesh element is 60.0 mm, the minimum is 12.0 mm, the maximum aspect ratio of the elements is 543.59, the percentage of elements with an aspect ratio of less than three is 7.64, more than ten - 32.6. The minimum number of elements in a circle is 12, the ratio of the increase in the size of the element is 1.8.

Fixing of the model was carried out by the horizontal parts of the frills, that is, in the areas of abutment on the running parts. The metal structure of the body is made of 09G2S steel, and the cluddage are made of composite. At the same time, the composite has linear elastic orthotropic properties. The strength limit in the direction of the fibers is 1100-1300 MPa, and in the transverse direction – 650 MPa. It is important to say that this composite withstands the strength value at a temperature of 700°C. An example can be a composite with a titanium matrix, which is reinforced with fibers of boron, badger, silicon carbide, beryllium, and molybdenum.

The calculation diagram of the supporting structure of the hopper car to determine its strength indicators is shown in Figure 2.18.

When assembling the model, it is taken into account that the full carrying capacity of the hopper car is used. At the same time, the body is subjected to a vertical static load P_v^{st}, the pressure of the spacer of the bulk cargo P_s, as well as the longitudinal load on the front stop of the auto coupling P_a, which is equal to 2.5 MN. That is, the model takes into account the movement of the car in the *a)*

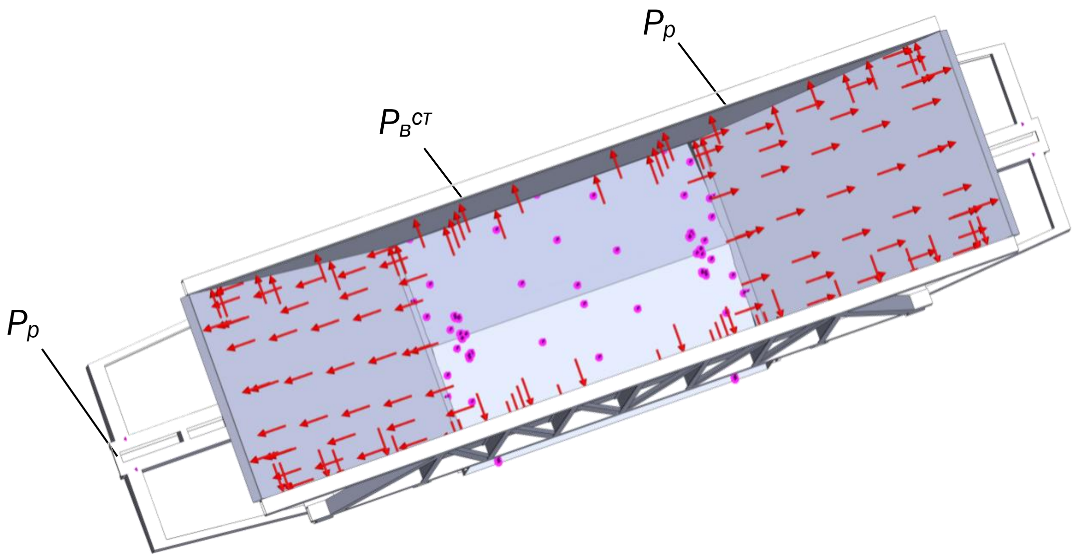

b)

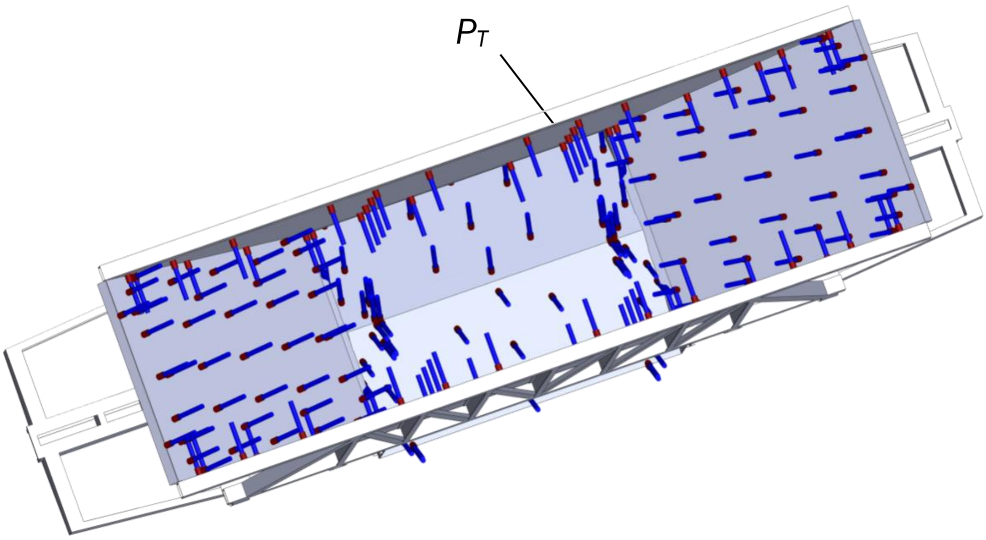

P_T – P_{sp}

P_B^{CT} – P_V^{st}

P_p – P_l

Fig. 2.18 **Calculation diagram of the supporting structure of the hopper car a) force factors; b) temperature load**

train. The model was also subjected to a temperature load RT, which was assumed to be equal to 700 °C.

The results of the strength calculation are shown in the Figure 2.19. It was established that the maximum stress equivalents according to the Mises criterion occur in the zone of interaction of the spinal beam with the pivot beam and are about 290 MPa. Stresses in the shell of a hopper car according to the criterion of maximum normal stresses are about 200 MPa, which is 12% lower than in a typical design (Figure 2.20). At the same time, the trend line y_s describes the distribution of stresses by the height of the rack in the structure of the car with steel cladding, and y_c - with composite cladding.

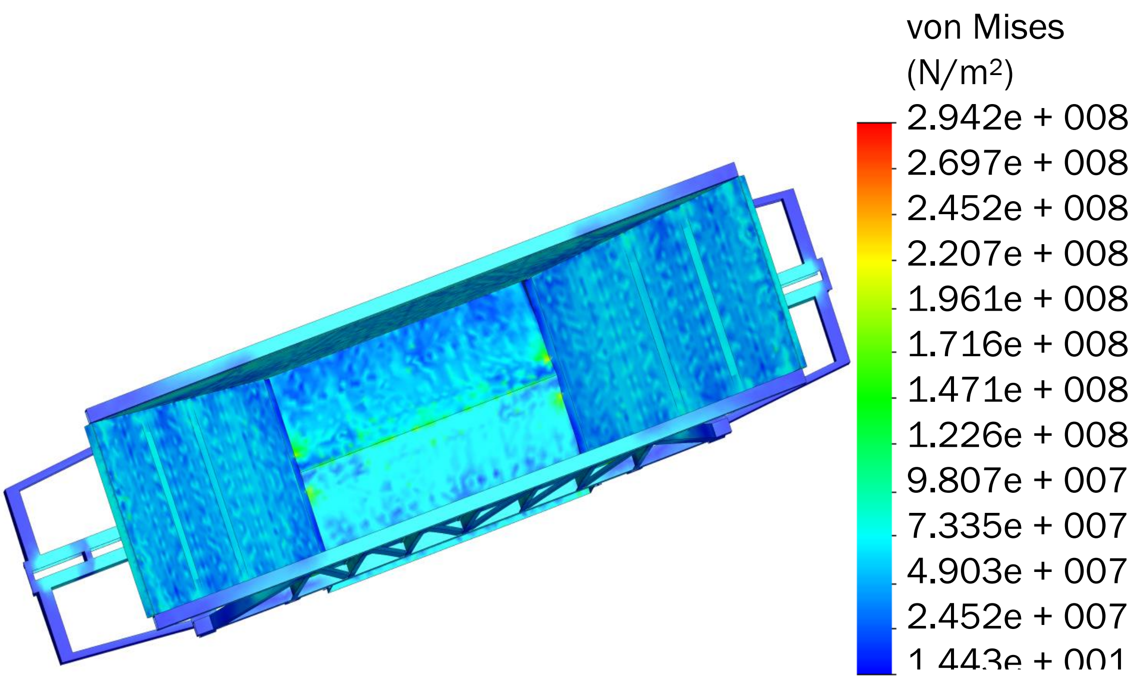

Fig. 2.19 **Stressed state of the supporting structure of the hopper car**

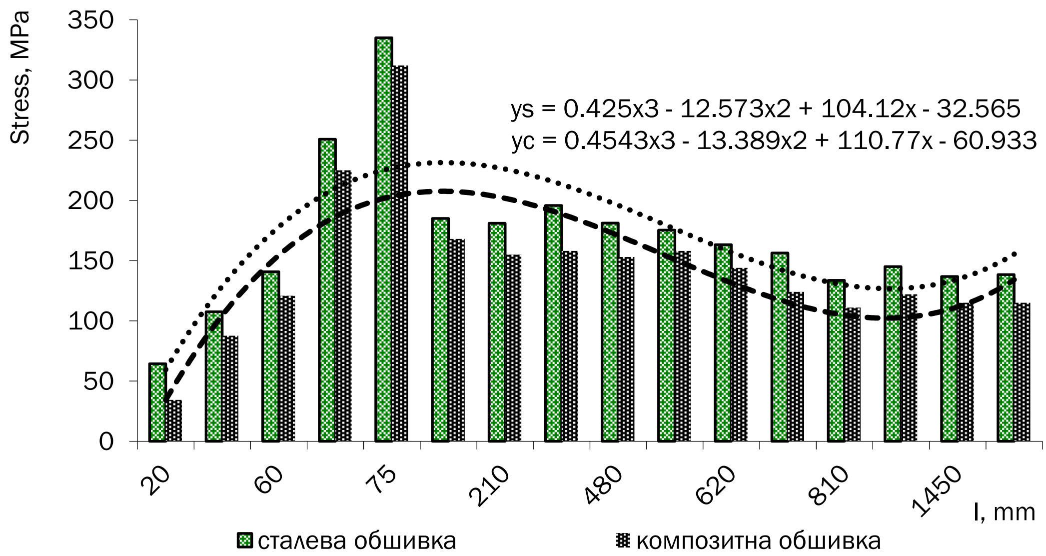

Сталева обшивка – steel cladding

Композитна обшивка – composite cladding

Fig. 2.20 **Stress distribution along the height of the intermediate a strut of the body**

The distribution of stresses along the length of the backbone beam of the frame is shown in the Figure 2.21.

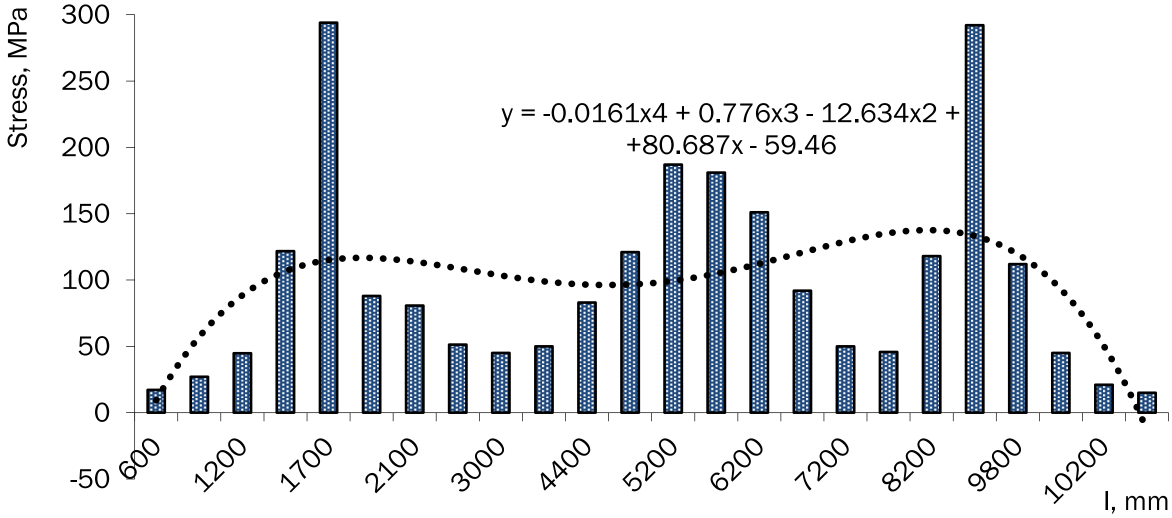

Fig. 2.21 **Distribution of stresses in a spinal beam along its length**

a) *b)*

c) *d)*

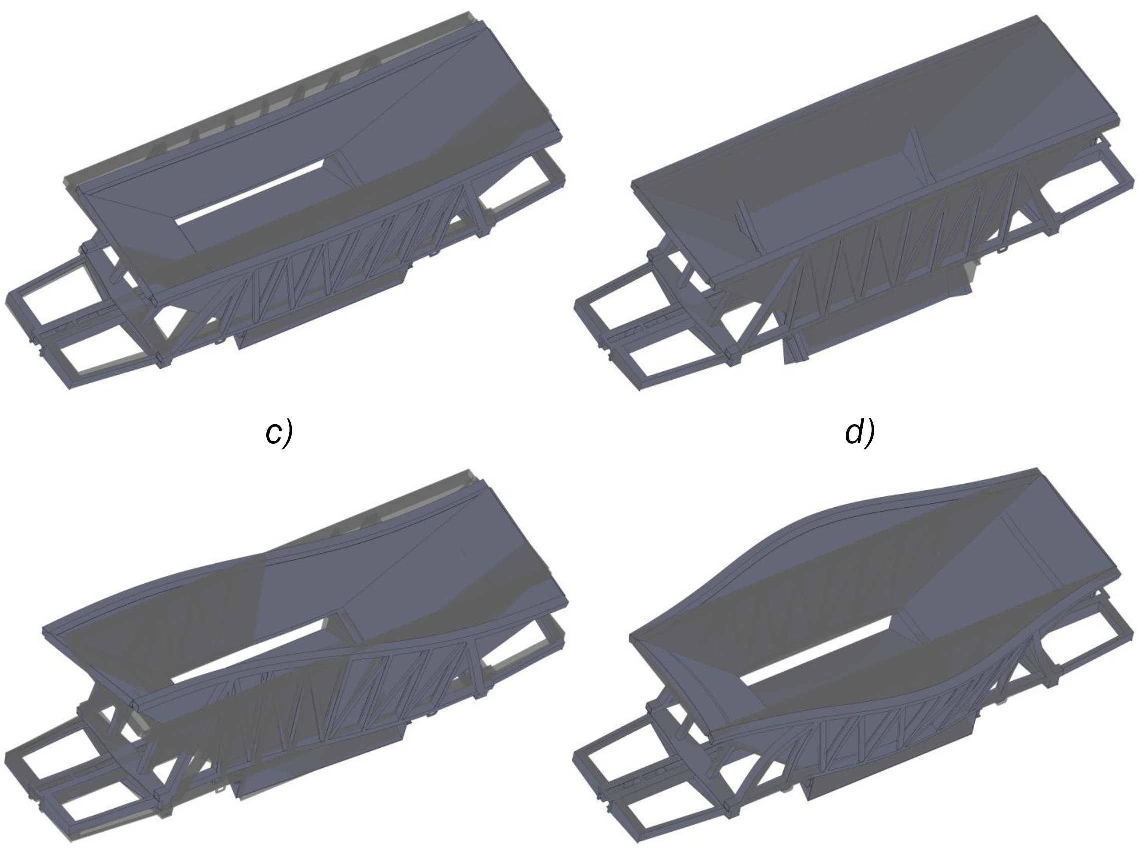

Fig. 2.22 **Some forms of oscillations of the load-bearing structure of the hopper car (deformation scale 20:1)**

a) the first mode; b) the second mode; c) the third mode; d) the fourth mode

At the same time, the maximum stresses occur in the cantilever parts of the frame. In the middle part, they made about 200 MPa.

A modal analysis was conducted to determine the frequencies and forms of natural oscillations of the supporting structure of a hopper car with a composite cladding. The calculation was made according to the calculation scheme shown in the Figure 2.18, a.

Some of the inherent forms of oscillations of the supporting structure of the hopper car are shown in the Figure 2.22.

The results of the calculation of the oscillation frequencies of the load-bearing structure of the hopper car established that the first natural frequency has a value of 11.7 Hz, i.e. not lower than the permissible level of 8 Hz. Therefore, the car movement safety is ensured [20, 21].

Also, within the study, the fatigue resistance of the load-bearing structure of the hopper car was calculated.

Fatigue resistance was calculated taking into account the reserve factor *n* according to the formula [20, 21]:

$$n = \frac{\sigma_{-1Д}}{\sigma_{\mathrm{a},e}} \geq [n], \tag{2.9}$$

Where $\sigma_{a,e}$ – the estimated value of the amplitude of the dynamic stress of the conditional symmetrical cycle, reduced to the base N_0, equivalent in terms of damaging effect to the value of the amplitudes in the real regime of the randon operational stresses during the design service life, MPa;

[n] – allowable safety margin of the the fatigue resistance

Equivalent cumulative dynamic stress amplitude for fatigue calculation $\sigma_{a,e}$ in the case of an intermittent function of distribution of stress amplitudes is determined as follows [20, 21]:

$$\sigma_{\mathrm{a,e}} = \sqrt[m]{\frac{N_{\mathrm{c}}}{N_0} \sum_{i=1}^{k} P_{vi} \, f_{в} \sum_{i=1}^{k} \sigma_{\mathrm{a}i}^{m} P_i}, \tag{2.10}$$

Where N_c – the total number of dynamic stress cycles during the estimated service life;

$p_{\sigma i}$ and p_{vi} – accordingly, the probability of appearance of stresses with the level σ_i in the given speed interval and the share of time for the operation of the car at the speed v_i;

σ_{ai} – level (degree) of stress amplitude, MPa;

$k_{\sigma i}$ and k_{vi} –the number of discretization stages, respectively, stress amplitudes and the range of movement speeds

The results of the calculation of the equivalent summed amplitude of dynamic stresses showed that with the probability of the appearance of stresses with a level of σ_i, which is equal to 0.95 the value $\sigma_{a,e}$= 51.3 MPa. Hence, the safety margin of the fatigue resistance is equal to 4.5. At the same time, due to the lack of experimental data, the permissible value of the safety margim of the fatigue resistance is taken to be equal to 2.2 [30]. Therefore, the condition (2.9) is fulfilled and the fatigue strength of the load-bearing structure of the hopper car is ensured.

2.4 Determining the strength of the load-bearing structure of the gondola car during defrosting of the cargo in it

In winter, convective garages are used to defrost frozen cargo from the load-bearing structures of freight cars (Figure 2.23). When performing the defrosting process, it is important to observe the temperature regimes at which the preservation of the components of the rolling stock is ensured.

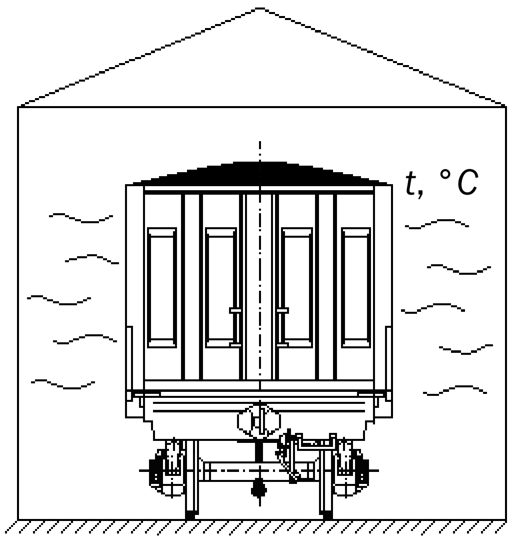

Fig. 2.23 **Defrosting scheme of a car in a convective garage**

An increase in the temperature effect on the components of the load-bearing structure of the car can contribute to its damage and the need for unscheduled repairs. Therefore, determining the permissible temperature effect on the load-bearing structure of cars, in particular a gondola car, as one of the most common types of cars in operation, when defrosting cargo in them is a very relevant issue.

A calculation was made to determine the load bearing structure of the gondola car during the defrosting of the frozen cargo placed in it. At the same time, the finite element method, which is implemented in the SolidWorks Simulation software package, is used. The calculation was made on the example of the load-bearing structure of the universal gondola car model 12-757, built by the PJCS “Kryukiv Wagon Construction Plant”.

When building a spatial model of the load-bearing structure of a gondola car, structural elements that rigidly interact with each other – by welding or using rivets – are taken into account.

When drawing up the calculation scheme, it is taken into account that a vertical static load acts on the load-bearing structure of the gondola car P_V^{st} using the full carrying capacity of a gondola car (Figure 2.24). The model also takes into account the pressure of the spacer of the bulk cargo P_s on the side and end walls. Temperature was applied to the outer surface of the body P_t.

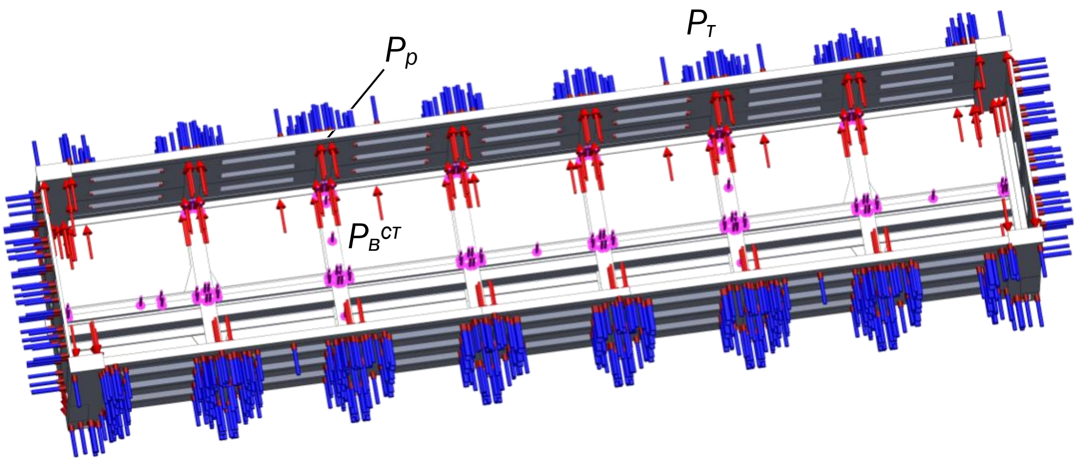

$P_В^{СТ}$ – P_V^{st}

P_p – P_s

P_T - P_t

Fig. 2.24 **Calculation diagram of the supporting structure of the gondola car**

Coal is accepted as bulk cargo. The forces of bulk cargo spacer on the side walls and end doors of the gondola car body are determined according to the method given in [20, 21]. According to this methodology, it is assumed that the load of the bulk cargo strut on the side walls of the car body is distributed according to the law of a triangle with a maximum at its base, and on the end wall – according to the law of a trapezium.

The maximum loads near the bases of the side wall racks are determined [22]

$$q_1 = 0{,}5 \cdot p_a \cdot l_1, \tag{2.11}$$

$$q_2 = 0{,}5 \cdot p_a \cdot (l_1 + l_2), \tag{2.12}$$

$$q_3 = 0{,}5 \cdot p_a \cdot (l_2 + l_3), \tag{2.13}$$

$$q_4 = 0{,}5 \cdot p_a \cdot (l_3 + l_4), \tag{2.14}$$

Where p_a – active (static) pressure of bulk load expansion, which occurs per unit surface area of the vertical wall at floor level, kPa;

l_1 – the distance from the end beam of the frame to the geometric axis of the wagon pivot bearing, m;

l_2 – the distance from the geometric axis of the wagon pivot bearing to the second pillar of the body, m;

l_3 – distance from the second body rack to the third one, m

l_4 – distance from the third rack of the body to the vertical geometric axis of the car body, m

The active pressure of the spacer of the bulk cargo was determined by the formula (2.1).

The pressure of the unevenly distributed load applied to the end door leaf was determined by the formula [22]

$$p = p_a + p_n, \tag{2.15}$$

Where p_n – passive pressure of bulk cargo, which is determined by formula (1), in which the square of the tangent of the difference of two angles is replaced by the square of the tangent of their sum and taking into account the coefficient of vertical dynamics, as well as the angle of natural slope.

The intensity of the trapezoidal load falling on the corner post is determined [22]

$$q_{T1}^{н} = 0{,}5\left(p_a + p_n\right)\cdot b_1; \quad (2.16)$$

$$q_{T1}^{в} = 0{,}5\cdot p_n \cdot b_1; \quad (2.17)$$

on the intermediate rack:

$$q_{T2}^{н} = 0{,}5\left(p_a + p_n\right)\cdot\left(b_1 + b_2\right); \quad (2.18)$$

$$q_{T2}^{в} = 0{,}5\cdot p_n \cdot\left(b_1 + b_2\right); \quad (2.19)$$

on the middle rack:

$$q_{T3}^{н} = 0{,}5\left(p_a + p_n\right)\cdot b_2; \quad (2.20)$$

$$q_{T3}^{в} = 0{,}5\cdot p_n \cdot b_2 \quad (2.21)$$

When assembling the finite-element model of the gondola-car load-bearing structure, isoparametric tetrahedra are used, the optimal number of which is determined by the graphoanalytic method. The main characteristics of the finite element model: the number of elements - 352435, the number of nodes – 116609, the maximum size of the element – 100.0 mm, the minimum size of the element – 20 mm, the maximum aspect ratio of the elements – 38400, the percentage of elements with an aspect ratio of less than three – 18,4, the percentage of elements with an aspect ratio greater than ten is 36.8, the minimum number of elements in a circle is 9, the ratio of the increase in the size of an element is 1.7.

Fixing of the model was carried out in the areas of its abutment on the running parts. 09G2S steel with a yield strength of 345 MPa and a strength limit of 490 MPa was used as the construction material [20, 21].

Based on the calculations, it was established that the maximum equivalent stresses in the supporting structure of the gondola car are within the permissible limits at the defrosting temperature of 91°C (Figure 2.25).

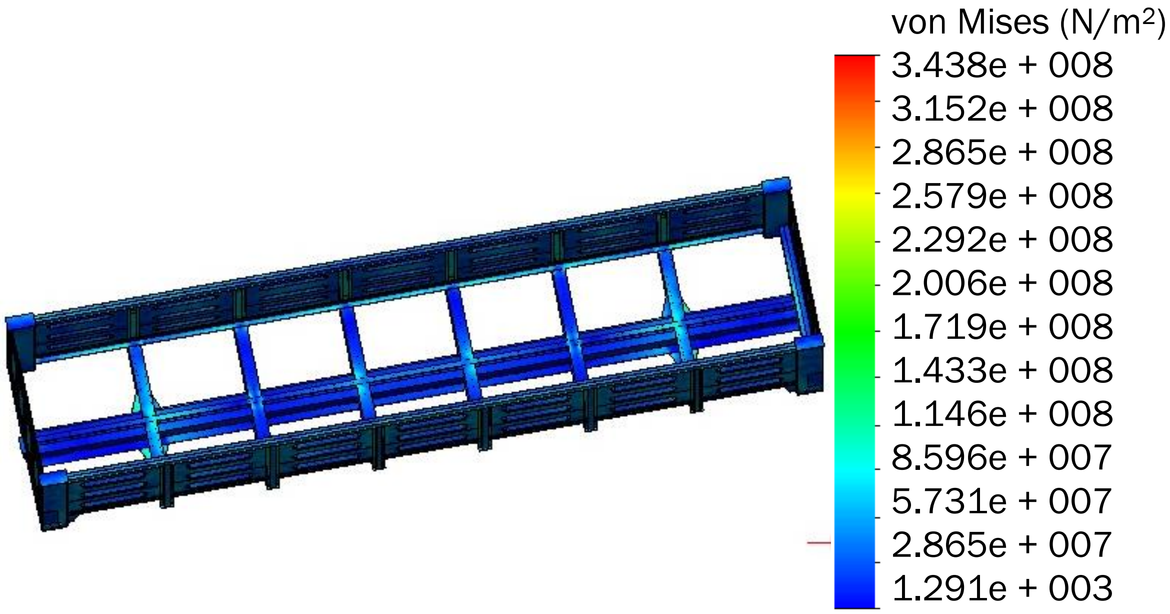

Fig. 2.25 **Stressed state of the supporting structure of a gondola car**

At the same time, the maximum equivalent stresses are recorded in the zone of interaction of the lower binding with the cladding and are equal to 343.8 MPa. The maximum displacements in the supporting structure of the gondola car occur in the middle part of the frame and amount to 3.6 mm (Figure 2.26).

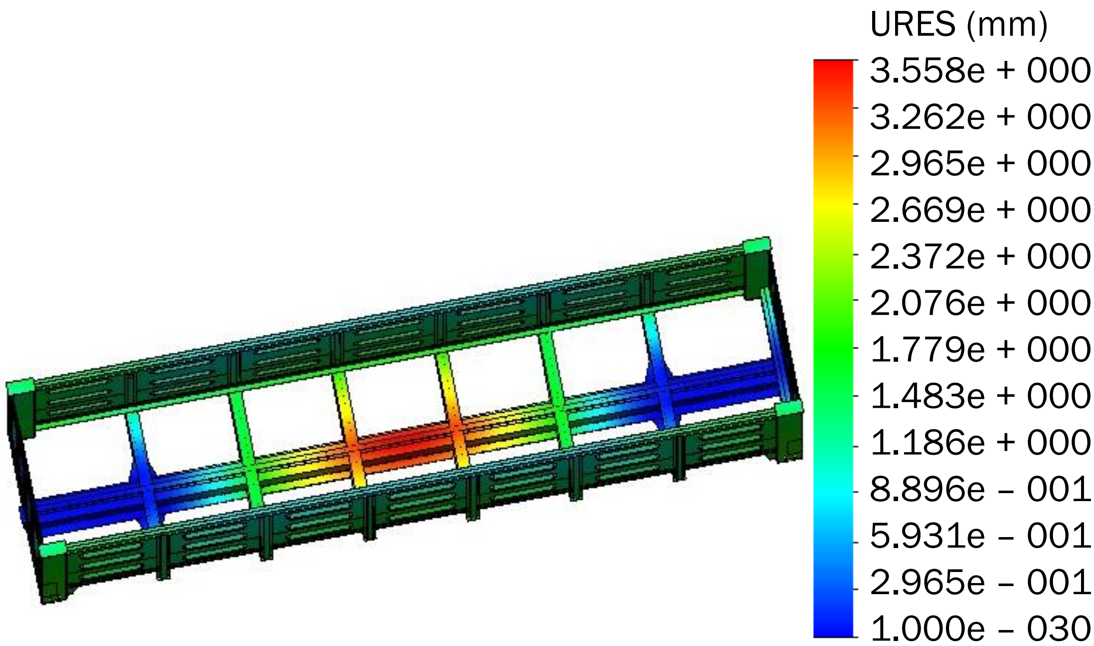

Fig. 2.26 **Movement in nodes of the load-bearing structure**

According to the calculation scheme shown in the Figure 2.24, the most loaded zones of the load-bearing structure of the gondola car during defrosting of the cargo are determined (Figure 2.27).

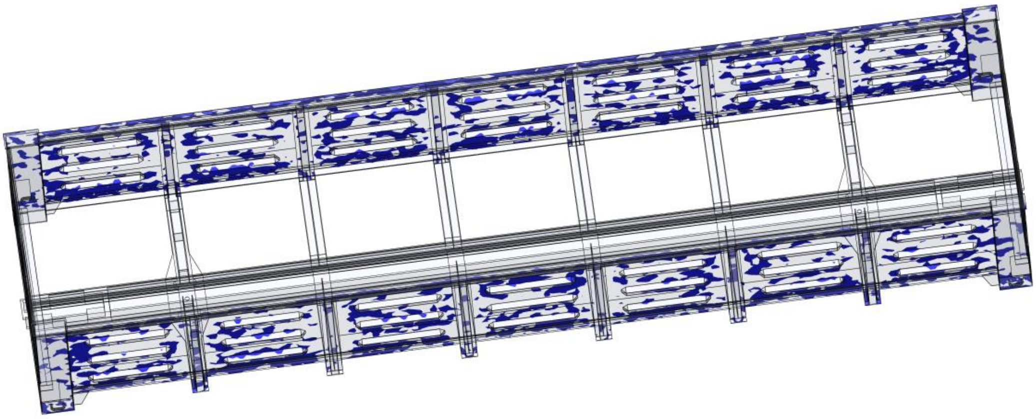

Fig. 2.27 **The most loaded zones of the load-bearing structure of the gondola-car during defrosting of the cargo in it**

They include cladding of the side and end walls. When creating new designs of wagons, it is necessary to take this factor into account in order to improve their technical and economic indicators.

2.5 Adaptation of load-bearing structures of gondola cars for transportation of high-temperature cargoes

2.5.1 Determining the load bearing structure of gondola car when transporting high-temperature cargoes in it

To determine the possibility of using a gondola car for the transportation of high-temperature cargoes, the load of its supporting structure was determined. The 12-757 gondola car was chosen as the prototype. When compiling the spatial model, structural elements that rigidly interact with each other - by welding or rivets - are taken into account.

Fastening of the supporting structure of the gondola car took place in the areas where it rests on the carts. 09G2S steel, which has a yield strength of 345 MPa and a strength limit of 490 MPa [20, 21], was used as the construction material.

The finite-element model of the supporting structure of the semi-car is formed by isoparametric tetrahedra. The optimal number of tetrahedra is calculated by the graphic-analytic method. The number of grid elements was 352435, nodes – 116609. The maximum size of the grid element is 100 mm, the minimum is 20 mm, the maximum aspect ratio of the elements is 38400, the percentage of elements with an aspect ratio of less than three is 18.4, more than ten is 36.8. The number of elements in the circle was 9. The ratio of the increase in the size of the elements is 1.7.

When drawing up the calculation scheme, it is taken into account that a vertical static load acts on the load-bearing structure of the gondola car P_v^{st} using the full carrying capacity of gondola car (Figure 2.28). The model also takes into account the longitudinal load acting on the front stops of the auto coupling P_l, i.e., the movement of a car in a train was simulated. In addition, the pressure of the spacer of the bulk cargo is taken into account P_s. Temperature was applied to the inner surface of the components of the load-bearing structure P_t at the level of 700°C from the transported cargo.

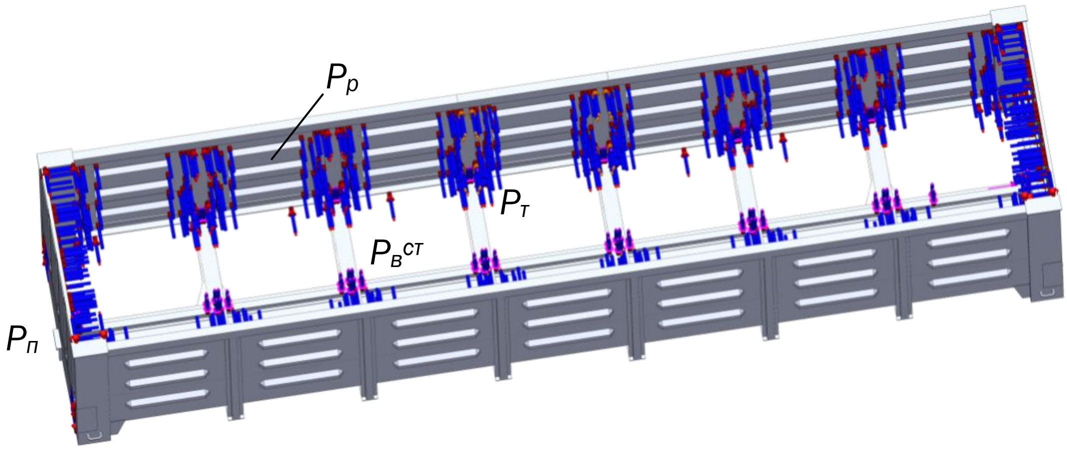

P_p – P_s

P_n – P_l

$P_в^{ст}$ – P_v^{st}

$P_т$ – P_t

Fig. 2.28 **Calculation diagram of the supporting structure of the gondola car**

Based on the calculations, it was established that the maximum equivalent stresses in the load-bearing structure of the gondola car are about 3800 MPa, which means that they significantly exceed the allowable ones (Figure 2.29).

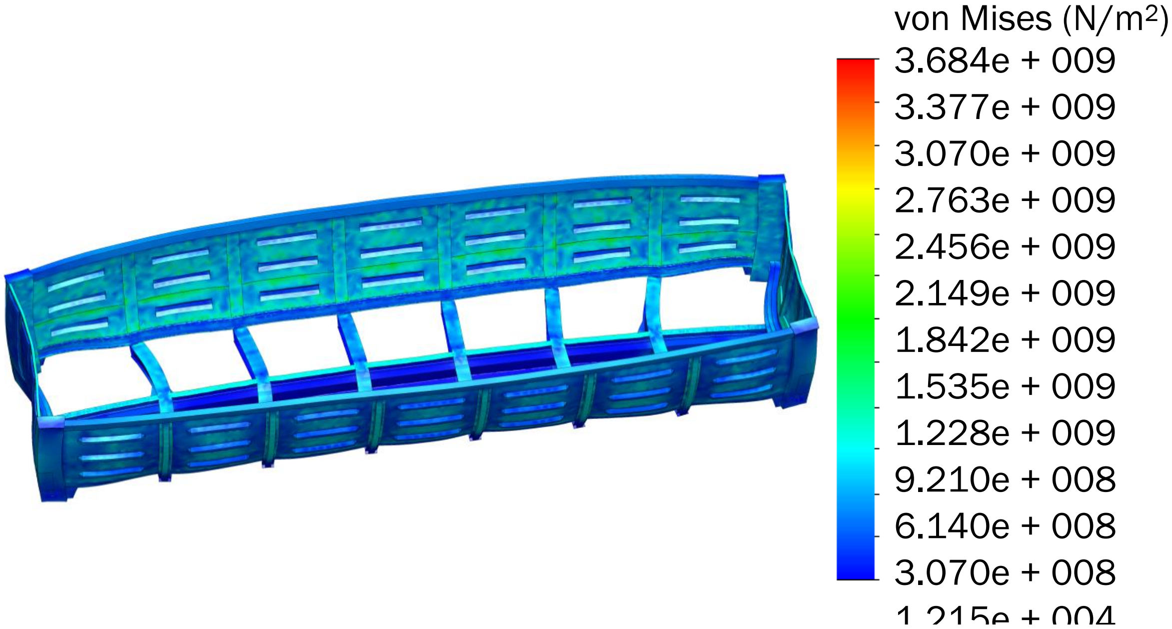

Fig. 2.29 **Stressed state of the supporting structure of the gondola car (scale of deformations – 40:1)**

The calculation was also carried out for other values of the temperature load. The calculation results are shown in the Figure 2.30.

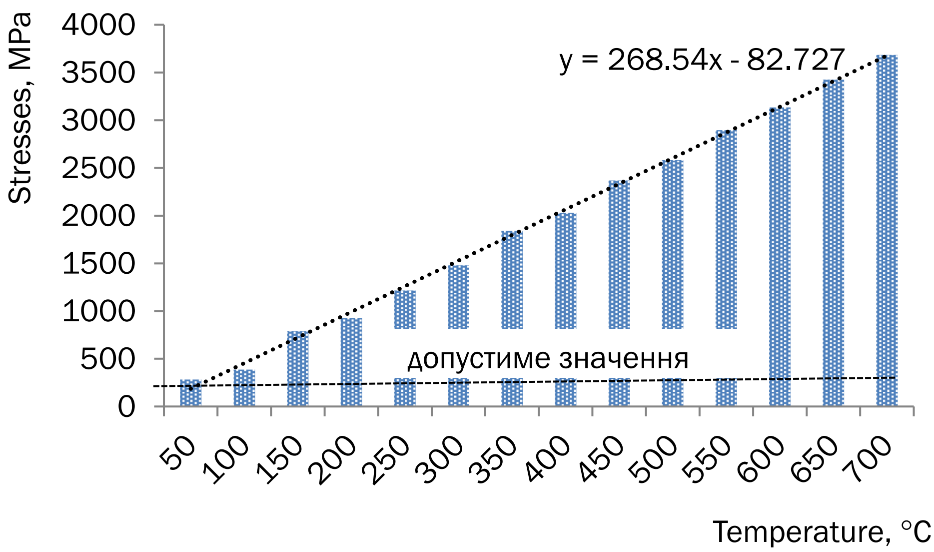

Fig. 2.30 **Dependence of stresses in the load-bearing structure of the gondola car on the temperature of the cargo transported in it**

It can be seen from the Figure 2.30 that the permissible stresses in the load-bearing structure of the gondola car are observed at a temperature of the transported cargo of 94°C. At the same time, the temperature of the sinter transported in railway cars has much higher values.

2.5.2 Measures to adapt the load-bearing structure of the gondola car to the transportation of high-temperature cargo

In order to use gondola cars for transportation of cargoes with an elevated temperature, it is possible to place them in open-type heat-resistant containers, i.e. flats (Figure 2.31).

a)

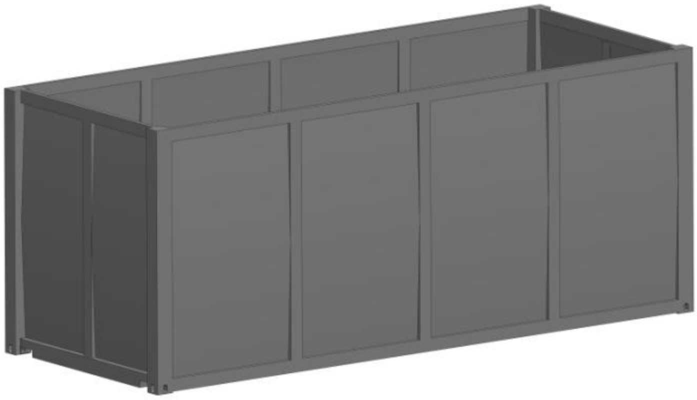

b)

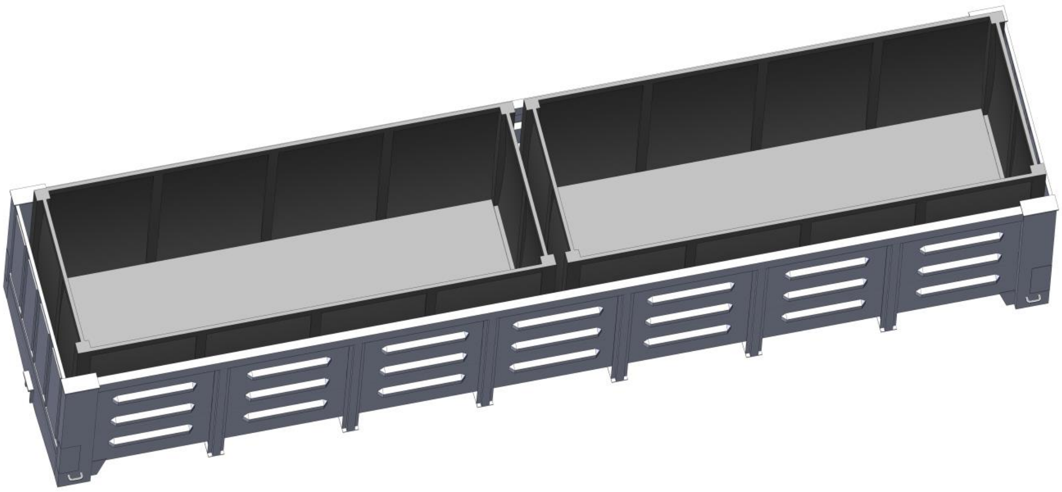

Fig. 2.31 **Open type container for transportation of hot sinter**
a) spatial model; b) placement of containers in a gondola car

A feature of the proposed flat is that its walls have a convex configuration. This configuration of the side walls makes it possible to increase the useful volume of the container by 8% compared to the prototype. The amount of deflection of the side and end walls is determined for technological reasons, namely, on the condition that the dimensions of the flat are preserved in accordance with the prototype. A composite with heat-resistant properties is used as the flat material, which can withstand a heating temperature of 700°C and has a strength limit: in the direction of the fibers – 1100 – 1300 MPa, across the fibers – 650 MPa. The container was secured by the horizontal parts of the fittings.

To substantiate the proposed decision, a calculation was made for the strength of the flat. When constructing a finite-element model of an open-type container, flats used isoparametric tetrahedra. The number of mesh elements is 47846, nodes – 14599. The maximum size of the mesh element is 120 mm, the minimum size is 24 mm, the maximum aspect ratio is 8330.9, the percentage of elements with an aspect ratio of less than three is 5.84, more than ten is 84.9. The number of elements in the circle makes up to 9, and the ratio of the increase in the size of the elements is 1.7.

The calculation scheme is shown in the Figure 2.32.

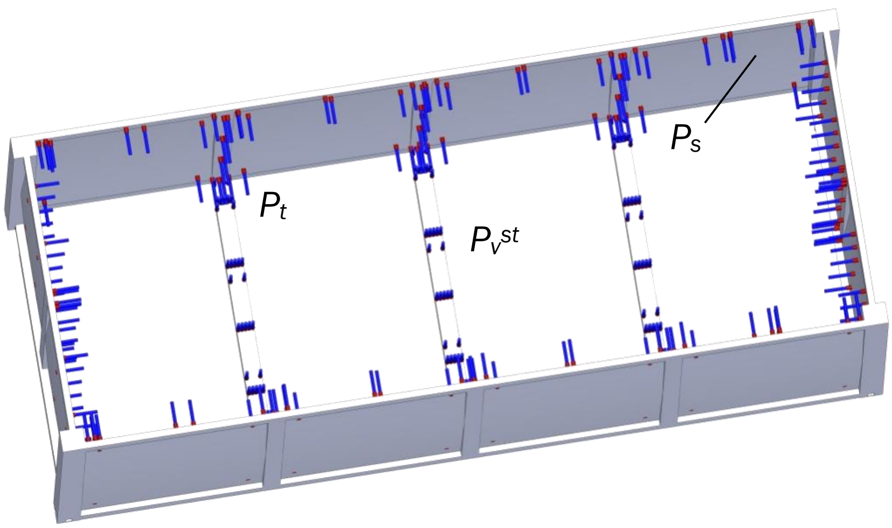

Fig. 2.32 **Calculation scheme of the flat**

When drawing up the calculation scheme, it is taken into account that a vertical static load P_v^{st} acts on the flat, pressure of load spreader P_s, as well as temperature load P_t.

The load spreader pressure was determined by the formula (2.1).

The calculation results showed that the maximum equivalent stresses in the load-bearing structure of the flat do not exceed the permissible ones (Figure 2.33).

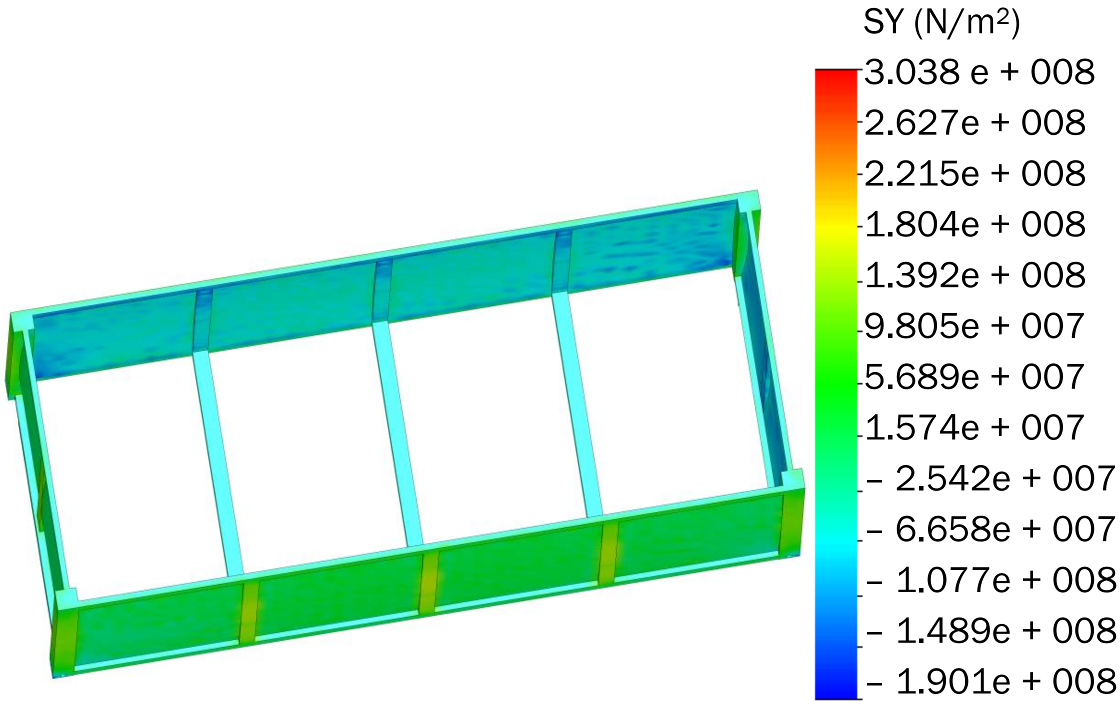

Fig. 2.33 **Stressed state of the container**

At the same time, the maximum stresses are about 300 MPa and are concentrated in the flat struts. In the cladding, the maximum equivalent stresses were about 260 MPa. In the transverse beams – 210 MPa.

To determine the main indicators of the dynamics of a gondola car loaded with flats, a calculation of the dynamic load was carried out. The studies were carried out in a flat coordinate system. It is taken into account that the car moves along a joint unevenness with elastic-viscous properties. When compiling the differential equations of motion, it is taken into account that the flats do not have their own degree of freedom and move together with the car body.

The calculation diagram of the gondola car is shown in the Figure 2.34.

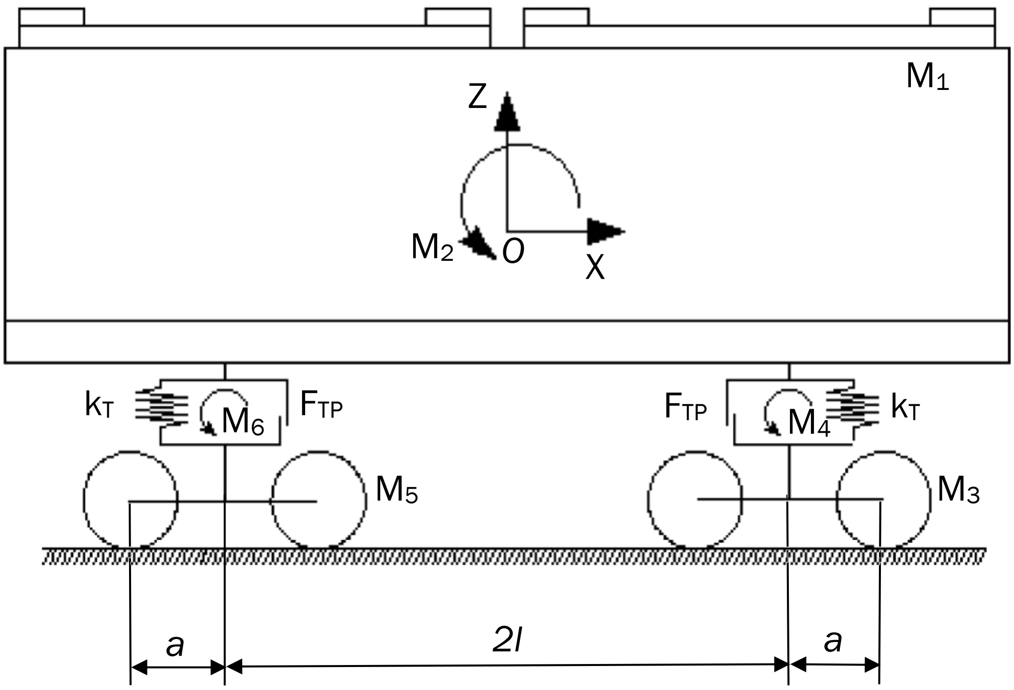

Fig. 2.34 **Calculation diagram of a gondola car**

The equations of motion of the gondola car have the following form [24, 25]:

$$M_1 \cdot \frac{d^2}{dt^2} q_1 + 2k_T \cdot q_1 - k_T \cdot q_3 - k_T \cdot q_5 = P_z, \tag{2.22}$$

$$M_2 \cdot \frac{d^2}{dt^2} q_2 + \left(2 \cdot l^2 \cdot k_T\right) \cdot q_2 + \left(l \cdot k_T\right) \cdot q_3 - \left(l \cdot k_T\right) \cdot q_5 = P_\varphi, \tag{2.23}$$

$$M_3 \cdot \frac{d^2}{dt^2} q_3 - k_T \cdot q_1 + \left(l \cdot k_T\right) \cdot q_2 + \left(k_T + 2 \cdot k_1\right) \cdot q_3 + 2 \cdot \beta_1 \cdot \frac{d}{dt} q_3 = P_{T_1}^z, \tag{2.24}$$

$$M_4 \cdot \frac{d^2}{dt^2} q_4 + \left(2 \cdot a^2 \cdot k_1\right) \cdot q_4 + 2 \cdot \beta_1 \cdot \frac{d}{dt} q_4 = P_{T_1}^\varphi, \tag{2.25}$$

$$M_5 \cdot \frac{d^2}{dt^2} q_5 - k_T \cdot q_1 - l \cdot k_T \cdot q_2 + \left(k_T + 2 \cdot k_1\right) \cdot q_5 + 2 \cdot \beta_1 \cdot \frac{d}{dt} q_5 = P_{T_2}^z, \tag{2.26}$$

$$M_6 \cdot \frac{d^2}{dt^2} q_6 + \left(2 \cdot a^2 \cdot k_1\right) \cdot q_6 + 2 \cdot \beta_1 \cdot \frac{d}{dt} q_6 = P_{T_2}^\varphi, \tag{2.27}$$

$$P_z = -F_{TP} \cdot \left(sign\left(\frac{d}{dt}\delta_1 \right) + sign\left(\frac{d}{dt}\delta_2 \right) \right), \tag{2.28}$$

$$P_\varphi = F_{TP} \cdot l \cdot \left(sign\left(\frac{d}{dt}\delta_1 \right) + sign\left(\frac{d}{dt}\delta_2 \right) \right), \tag{2.29}$$

$$P_{T_1}^z = F_{TP} \cdot sign\left(\frac{d}{dt}\delta_1 \right) + k_1\left(\eta_1 + \eta_2\right) + \beta_1\left(\frac{d}{dt}\eta_1 + \frac{d}{dt}\eta_2 \right), \tag{2.30}$$

$$P_{T_1}^\varphi = -k_1 \cdot a \cdot \left(\eta_1 - \eta_2\right) - \beta_1 \cdot a \cdot \left(\frac{d}{dt}\eta_1 - \frac{d}{dt}\eta_2 \right), \tag{2.31}$$

$$P_{T_1}^z = F_{TP} \cdot sign\left(\frac{d}{dt}\delta_2 \right) + k_1\left(\eta_3 + \eta_4\right) + \beta_1\left(\frac{d}{dt}\eta_3 + \frac{d}{dt}\eta_4 \right), \tag{2.32}$$

$$P_{T_2}^\varphi = -k_1 \cdot a \cdot \left(\eta_3 - \eta_4\right) - \beta_1 \cdot a \cdot \left(\frac{d}{dt}\eta_3 - \frac{d}{dt}\eta_4 \right), \tag{2.33}$$

Where M_1, M_2 – respectively, the mass and moment of inertia of the load-bearing structure of the gondola car during jumping and galloping oscillations;

M_3, M_4 – respectively, the mass and moment of inertia of the first cart in the course of its movement during jumping and galloping oscillations;

M_5, M_6 – respectively, the mass and moment of inertia of the second cart in the course of its movement during jumping and galloping oscillations;

a – half of the cart base (model 18-100);

q_i – generalized coordinates corresponding to consistent movement relative to the vertical axis and angular movement around the vertical axis;

k_i – stiffness of the spring suspension of the gondola car;

β_i – damping coefficient;

F_{TP} – absolute friction force in the spring assembly;

$\eta(t)$ – periodic function that describes the contact inequality.

The calculation results are shown in the figures 2.35, 2.36.

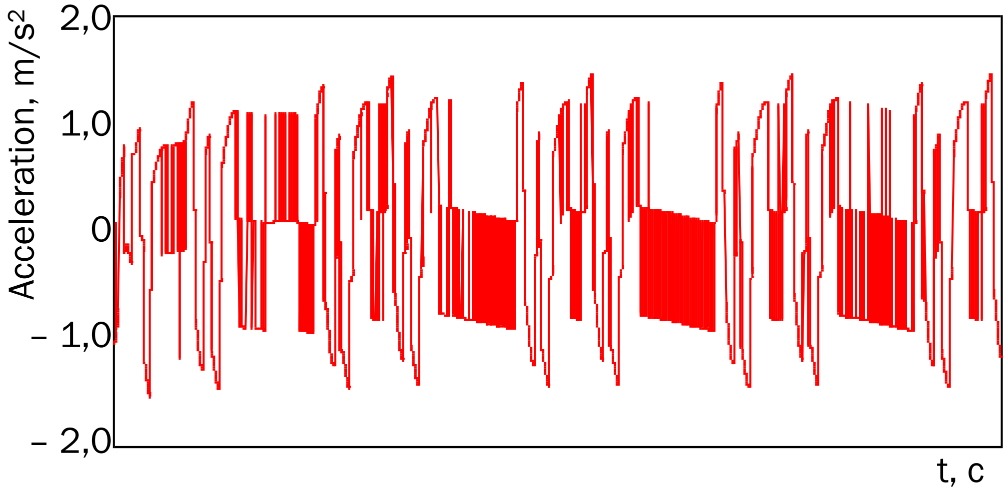

Fig. 2.35 **Accelerations that act in the center of mass of the load-bearing structure of the gondola car**

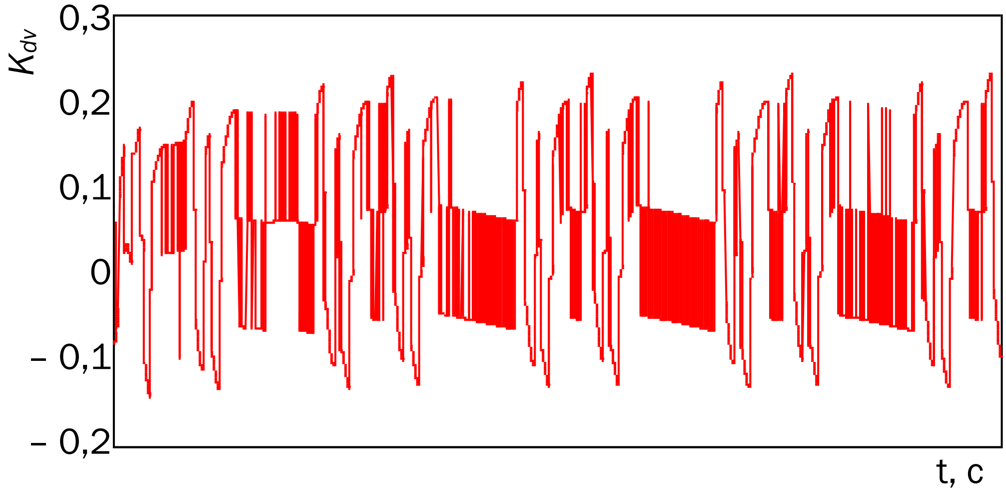

Fig. 2.36 **Coefficient of vertical dynamics**

At the same time, the accelerations acting in the center of mass of the load-bearing structure of the gondola car amounted to about 1.5 m/s2 (0.15g). The coefficient of vertical dynamics is equal to 0.22. That is, the calculated dynamics indicators are within the limits of permissible values, and the movement of the car is evaluated as "excellent" [20, 21].

2.6 Design features and determination of the load-bearing structure of the car for the transportation of high-temperature, bulk/liquid cargo during operational modes

An increase in the competitive environment in the transportation market requires the introduction of highly efficient rolling stock into operation. This causes the need for additional capital investments. Therefore, it is possible to update the existing fleet of vehicles for the transportation of the specified cargo nomenclature.

A rational solution in this case is the introduction into operation of multi-functional wagon designs intended for the transportation of a wide range of cargoes. At the same time, it is necessary to study also the possibility of transportation of high-temperature cargo, the segment of which takes place at industrial enterprises. Such cargoes are transported by specialized rolling stock. Due to its lack, wagons that are not intended f or these purposes may be used. This leads to their damage, the need for unscheduled repairs, and, accordingly, maintenance costs. In addition, such a circumstance threatens the safety of cargo transportation by rail. Therefore, there is a need to carry out research on the design, as well as the modernization of existing train structures to ensure their multi-functionality. This will help increase the efficiency of railway transport operation and the transport industry as a whole.

In order to ensure the multi-functionality of wagons in order to expand the range of goods transported in them, the modernization of existing structures is proposed (Appendix A). A feature of modernization is the use of an open-type boiler made of heat-resistant material on wagons, the load-bearing structure of which is represented by a frame (Figure 2.37). It is possible to install such a boiler on the frames of a tank car or a platform car. It is also possible to modernize tank cars by trimming the boiler and covering it with heat-resistant material.

To prevent splashing of the transported cargo, it is recommended to use a removable cover, which is attached to the upper part of the boiler (Figure 2.38).

a)

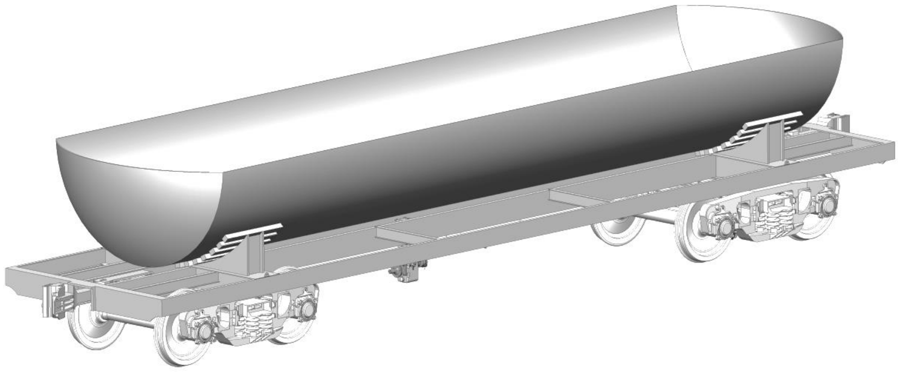

b)

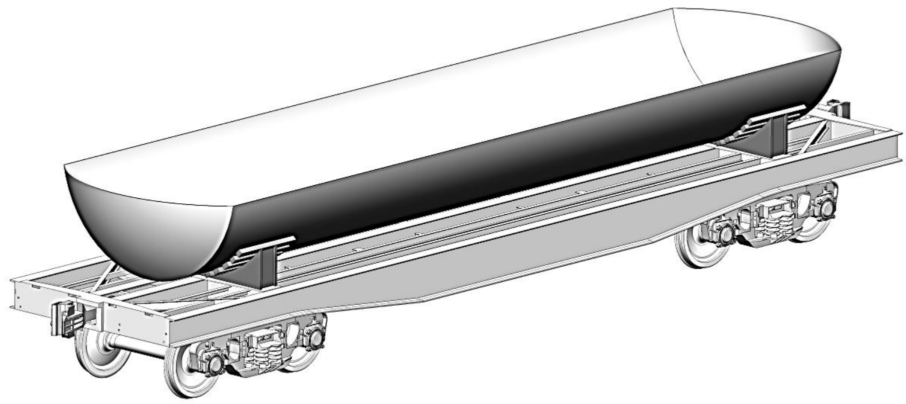

Fig. 2.37 **Multifunctional car**

a) created on the basis of a tank car; b) created on the basis of a platform car

a)

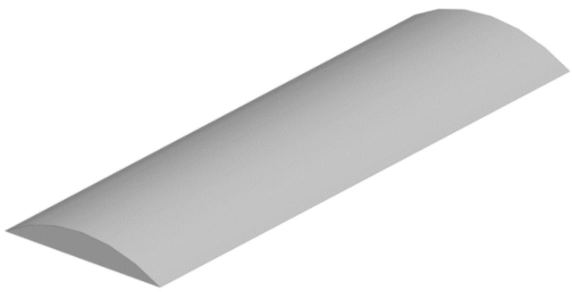

b)

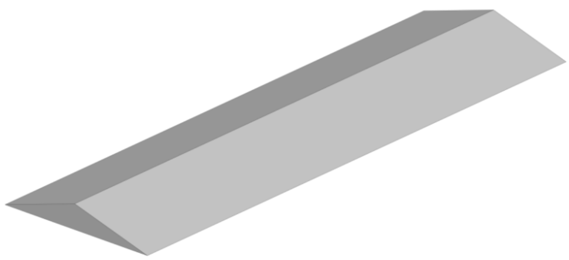

c)

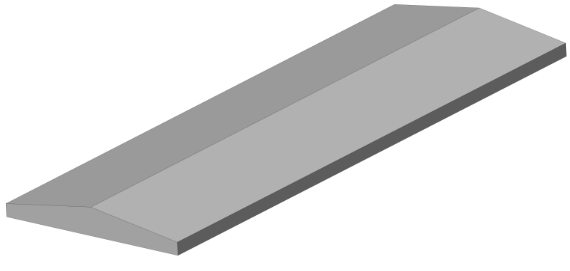

d)

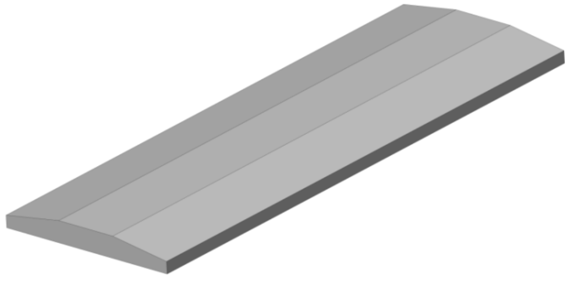

Fig. 2.38 **Possible versions of removable covers**

a) the first option; b) the second option; c) the third option; d) the fourth option

If necessary, removable covers can be equipped with devices for maintenance and storage.

In the proposed wagon, it is possible to transport not only bulk cargo, but also liquid cargo.

To determine the strength of the boiler under vertical loading, taking into account the transportation of bulk cargo in it (I load scheme), a calculation was made.

The SolidWorks (France) software package was used to create a spatial model of the multifunctional design of the car. In order to determine the strength of the boiler, the method of finite elements was used. The calculation was carried out in the SolidWorks Simulation software (France). At the same time, the theory of maximum normal stresses is applied.

It is taken into account that the boiler is made of a composite that has linear elastic orthotropic properties. The strength limit in the direction of the fibers is 1100-1300 MPa, and in the transverse direction - 650 MPa. The composite withstands the strength value at a temperature of 700 °C. The number of layers of material is assumed to be equal to 2. The calculation of the strength of the boiler is carried out as for a thin-walled shell. Fixing of the model took place in the areas where the boiler rests on the wooden supports of the gutters. At the same time, the model was rigidly fixed. That is, the possible frictional forces between the wooden bars and the boiler are not taken into account.

Tetrahedrons were used when compiling the finite-element model, the number of which was calculated by the graphoanalytic method.

The number of grid elements was 40478, nodes – 20573. The maximum size of the grid element is 80 mm, the minimum is 16 mm.

The calculation scheme of the boiler is shown in the Figure 2.39. When compiling it, it is taken into account that the boiler is subjected to a vertical static load P_v^{st} taking into account the use of the full load capacity of the boiler, as well as the pressure of the bulk cargo P_{pl}.

The pressure of bulk cargo is calculated according to the formula [22]:

$$P_{гідр} = \rho \cdot g \cdot h, \qquad (2.34)$$

$P_{гідр}$ - P_{hydr}

Where ρ – density of bulk cargo, kg/m³;

h – height of load distribution relative to the boiler, m.

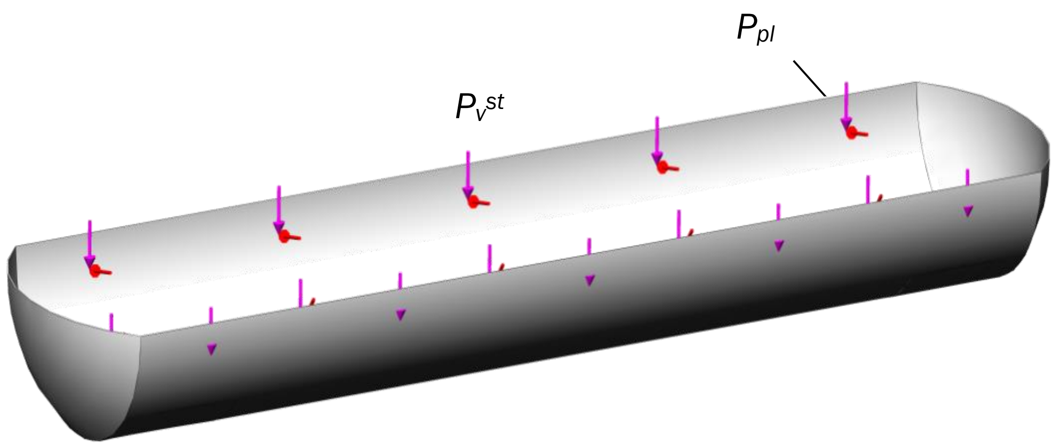

Fig. 2.39 **Calculation scheme of the boiler (I load scheme)**

The calculation results are shown in the Figure 2.40.

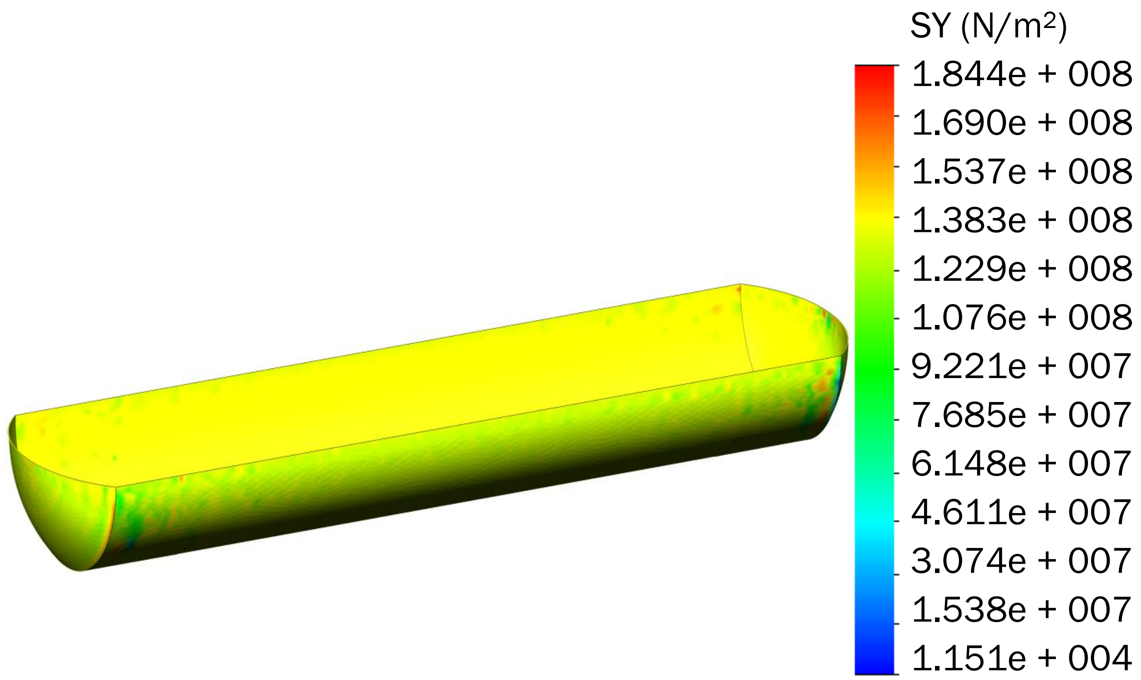

Fig. 2.40 **Stressed state of the boiler (I load scheme)**

At the same time, the maximum stresses recorded in the zones of interaction of the cylindrical part of the boiler with the bottoms were 184.4 MPa, that is, they do not exceed the allowable ones.

To determine the longitudinal load of the boiler (II load scheme), the calculation scheme shown in the Figure 2.41 was drawn up. The calculation was carried out in quasi-statics.

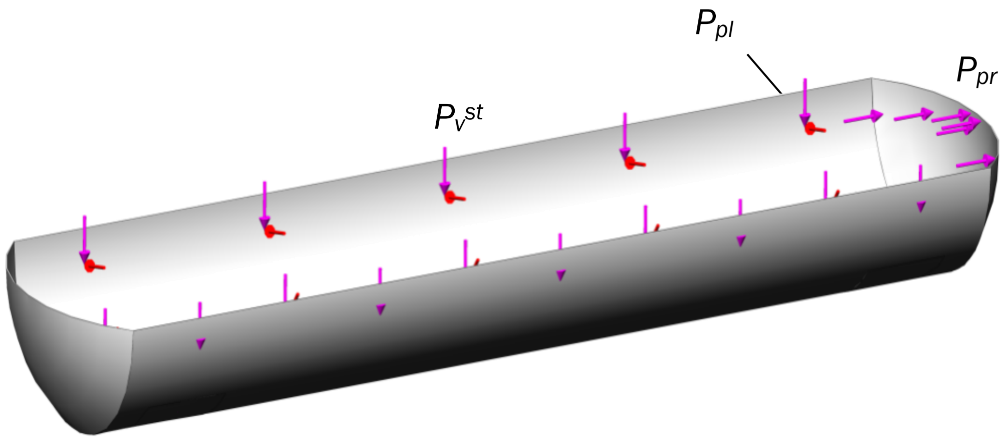

Fig. 2.41 **Calculation scheme of the boiler (II load scheme)**

The value of the maximum pressure from water impact is determined by the ratio of the inertia force of the cargo to the area of the vertical projection of the bottom [22]:

$$P_{пр} = N \cdot \frac{m_{в}}{m_{бр}} \cdot \frac{1}{F}, \tag{2.35}$$

$P_{пр}$ - P_{pr}

$m_{в}$ - m_{c}

$m_{бр}$ - m_{gr}

Where N – force of impact on the automaticle coupling, MN;;

m_c – weight of the cargo in the boiler, kg;

m_{gr} – car gross weight, kg;

F – internal cross-sectional area of the boiler, m^2.

The calculation results are shown in the Figure 2.42. At the same time, the maximum stresses occur in the middle part of the bottom and amount to 307.4 MPa, that is, they do not exceed the permissible ones.

At the next stage of the study, the possibility of transporting high-temperature bulk cargo in the boiler was determined (III load scheme). The calculation scheme of the boiler is identical to that shown in the Figure 2.41. At the same time, the pressure of the liquid cargo is replaced by the pressure of the bulk cargo. Also, a temperature load R_T equal to 700 °C was applied to the inner surface of the boiler (Figure 2.43).

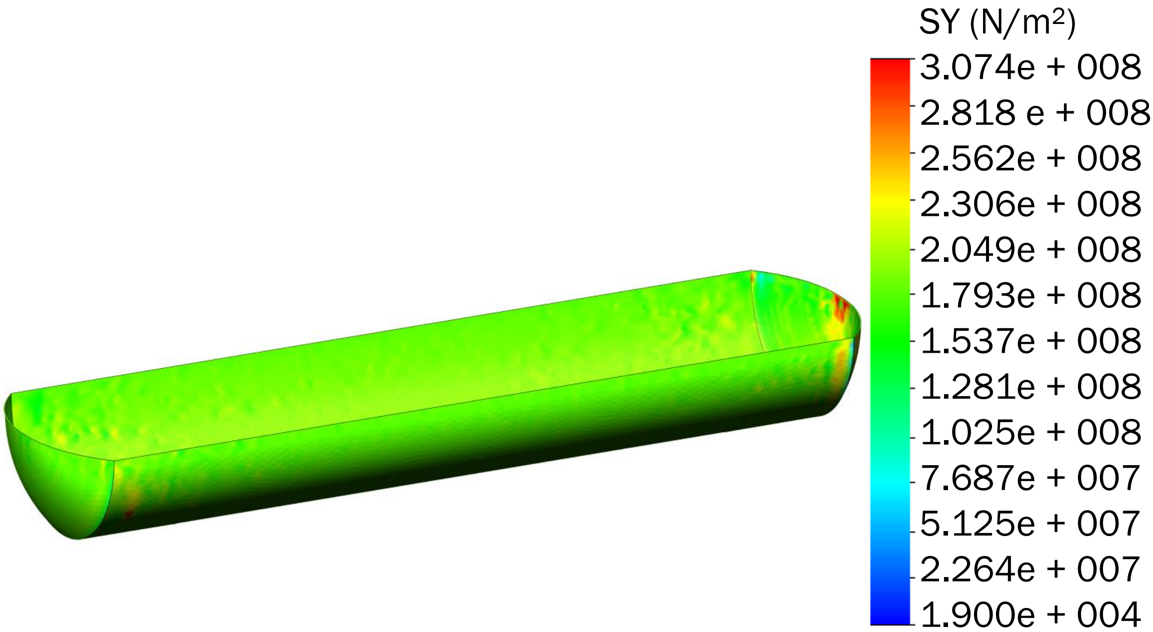

Fig. 2.42 **Stressed state of the boiler (II load scheme)**

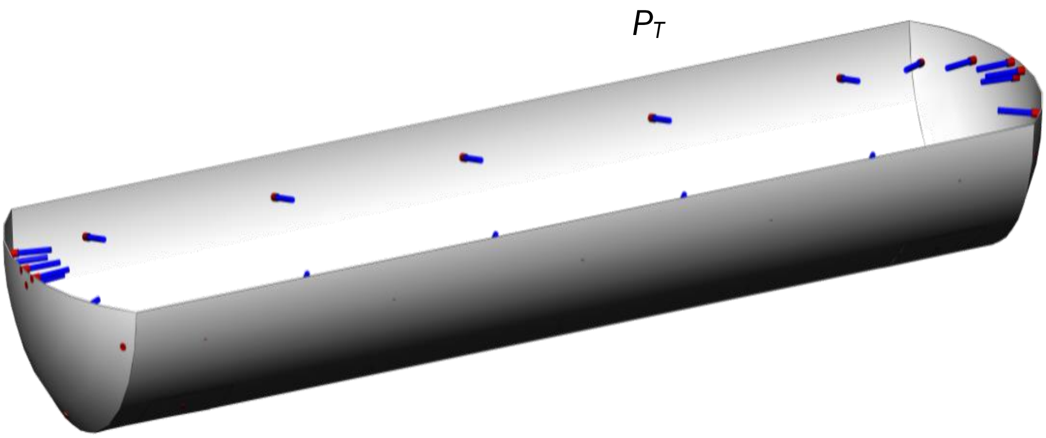

Fig. 2.43 **Scheme of applying temperature load to the boiler (III load scheme)**

To determine the loads that act on the boiler when the longitudinal force acts on the car, mathematical modeling was carried out. In this case, the mathematical model given in [23] was used. However, as the part of this study, it was modified by adapting it to determine the load capacity of the proposed car design. The case of a shunting collision of a car taking into account the effect of a load of 3.5 MN on the rear axle of the coupling is taken into account.

It is taken into account that the car is loaded to its full carrying capacity with conditional cargo. The movement of the cargo when the wagon was hit was not taken into account. The blow is considered absolutely hard. The modelling took into account the frictional forces that arise between the wooden bars and the boiler. When carrying out the calculations, it was taken into account that the car rests on model 18-100 carts with the appropriate stiffness characteristics of the spring sets. When determining the inertia coefficients, the nominal parameters of the components of the load-bearing structure of the car were taken into account.

The calculation scheme for determining the longitudinal load of the car is shown in the Figure 2.44.

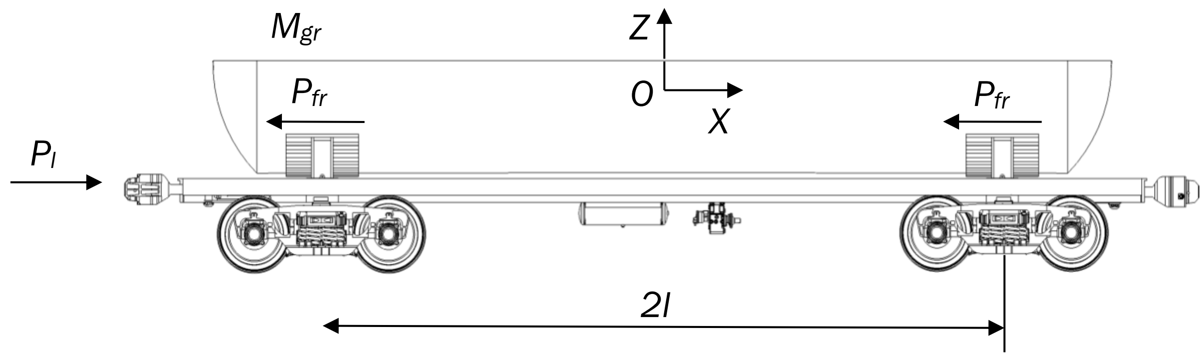

Fig. 2.44 **Calculation scheme for determining the longitudinal car load**

In this case, the system of differential equations (2.2) was used.

The solution of the system of differential equations was carried out using the Runge-Kutta method under initial conditions which are equal to zero.

The calculation results established that the maximum acceleration acting on the boiler is 36.5 m/s^2, has a negative value and occurs at the moment of impact (Figure 2.45).

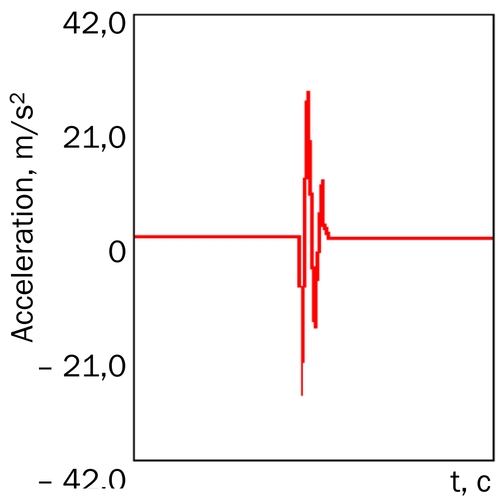

Fig. 2.45 **Accelerations that act on the load-bearing structure of the car under its longitudinal load**

The obtained acceleration value is taken into account in strength calculations as a component of the dynamic load acting on the boiler when it is longitudinally loaded.

The calculation results are shown in the Figure 2.46. At the same time, the maximum stresses occur in the zones of interaction of the bottoms with the cylindrical parts of the boiler and are 314.5 MPa, so they are within the permissible limits.

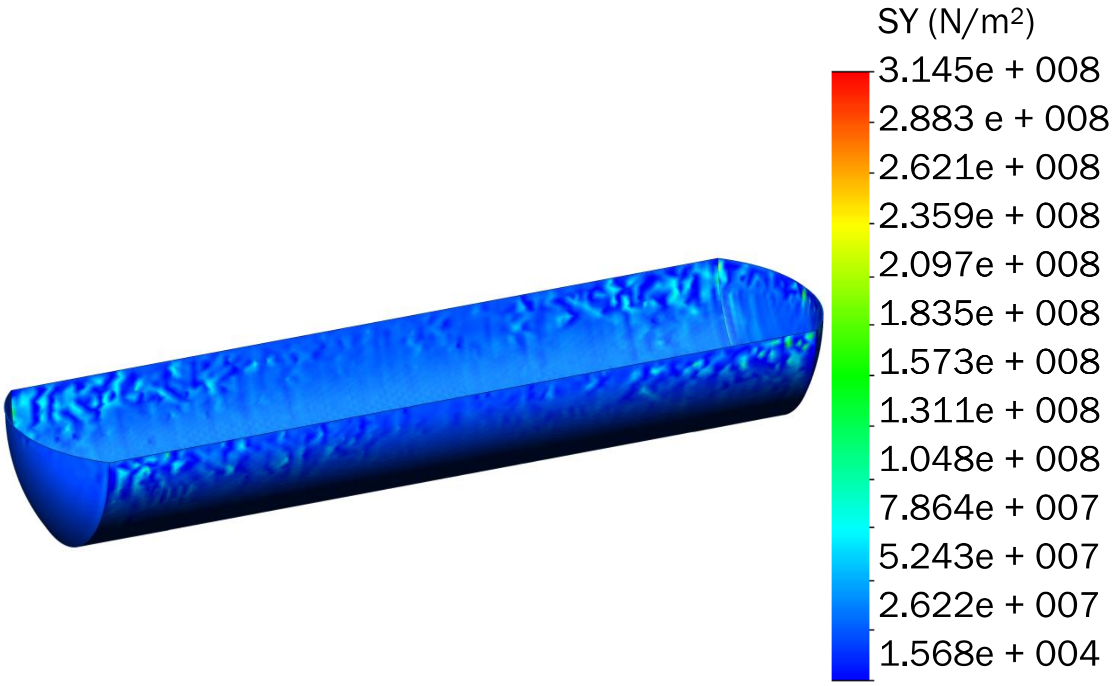

Fig. 2.46 **Stressed state of the boiler (III load scheme)**

According to the calculation scheme shown in the Fig. 3, the dislocation fields of the accelerations acting on the boiler are defined, as well as their numerical values. The calculation was made using the options of the SolidWorks Simulation software packag. The calculation results are shown in the Figure 2.47.

The maximum acceleration acting on the boiler is concentrated in the bottom and is 37.4 m/s^2. In the cylindrical part of the boiler, the acceleration value is in the range of 28.0 m/s^2 - 12 m/s^2.

Appropriate calculations were made to verify the obtained results. As a variation parameter, the impact force of the car on the automatic coupling is taken into account. The output parameter of the model is the acceleration of the load-bering structure of the car.

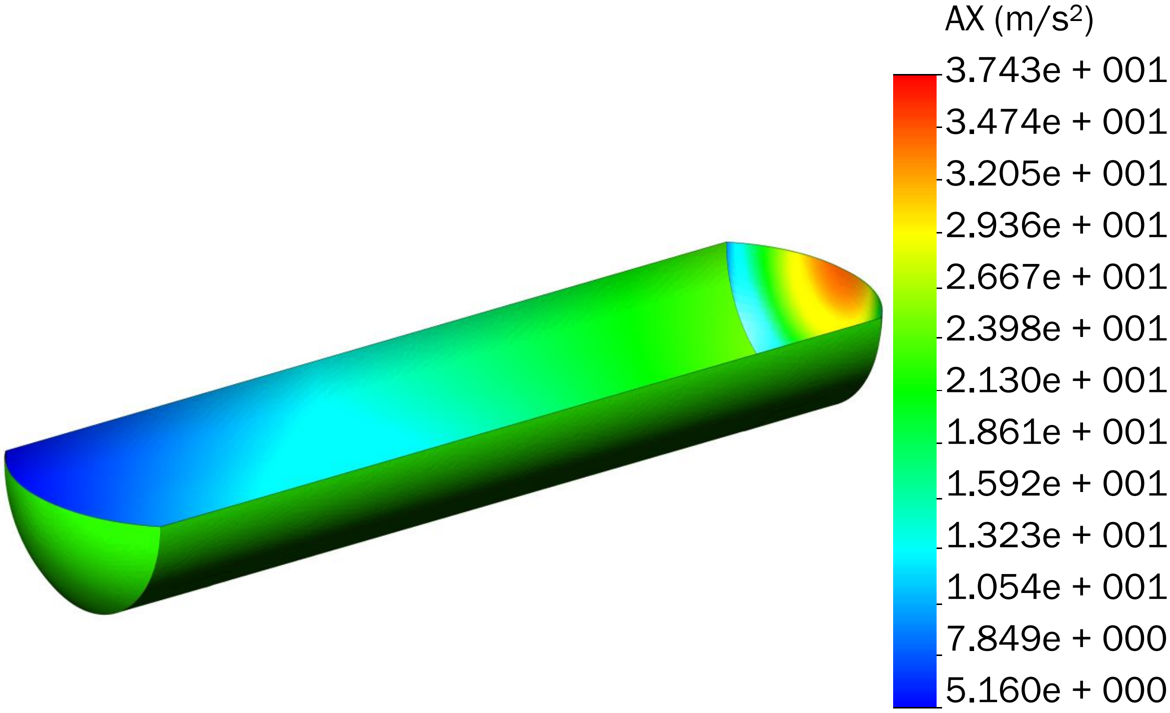

Fig. 2.47 **Dislocation fields of accelerations relative to the boiler**

To determine the optimal number of experiments for the purpose of subsequent verification of the model, the Student's criterion was applied [26]:

$$n = \frac{t^2 \cdot \sigma^2}{\delta^2}, \tag{2.36}$$

Where t – table value of Student's criterion;

σ – mean square deviation of a random variable;

δ^2 – absolute error of the measurement result.

On the basis of variational calculations, the accelerations that act on the boiler at different impact forces on the car automatic coupling were obtained. The results of the calculations are shown in the Figure 2.48.

It was established that the number of conducted experiments is sufficient to obtain the adequacy of the result. At the same time, the calculation error was 5.45%.

Using the results of the calculations shown in the Figure 2.48, the dynamic load model of the boiler was verified according to the F-criterion by comparing two dispersions [27 – 29]

$$F_p = \frac{S_{ад}^2}{S_y^2}, \tag{2.37}$$

$S_{аД}$ – S_{ad}

S_y – S_r

Where S_{ad} – adequacy dispersion;

S_r – reproducibility dispersion.

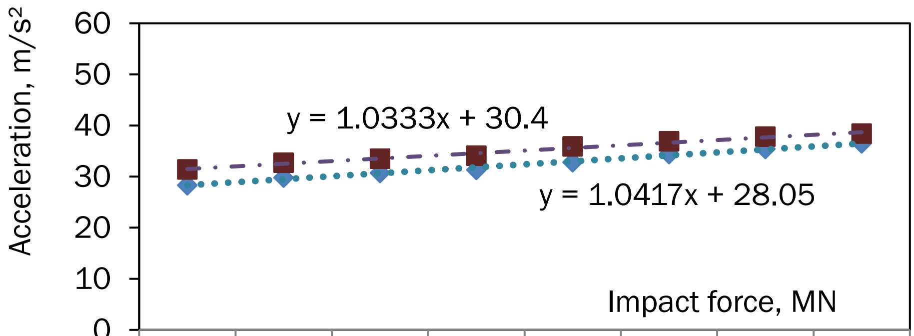

	2,8	2,9	3	3,1	3,2	3,3	3,4	3,5
математична модель	28,3	29,8	30,7	31,3	32,8	34,4	35,4	36,5
комп'ютерна модель	31,4	32,7	33,5	34,1	35,9	36,9	37,8	38,4

математична модель - mathematical model

компютерна модель – computer model

Fig. 2.48 **Simulation results of dynamic boiler load**

Adequacy dispersion was determined

$$S_{ад}^2 = \frac{\sum_{i=1}^{n}\left(y_i - y_i^p\right)}{\left(N - q\right)}, \tag{2.38}$$

$S_{аД}$ – S_{ad}

Where y_i^p – the calculated value obtained by modeling;

f_i – the number of degrees of freedom;

N – the number of experiments in the planning matrix;

q – the number of the equation coefficients.

The reproducibility dispersion was calculated

$$S_y^2 = \frac{1}{N}\sum_{i=1}^{n} S_i^2, \tag{2.39}$$

S_y – S_r

Where S_i^2 *– dispersion in each line where parallel experiments were performed.*

It was established that with the dispersion of adequacy S_{ad}=8.23 and reproducibility dispersions S_r=6.44, the actual value of the F-criterion F_p=1.27, which is less than the table value F_t=3.58 at the level of significance α=0.05. Therefore, the hypothesis of adequacy is not denied.

CONCLUSIONS TO THE SECTION 2

1. The load bearing structure of the hopper car due to temperature influence was determined. It was established that the maximum equivalent stresses in the supporting structure of the hopper car are about 340 MPa and are concentrated in the zone of interaction of the backbone beam with the pivot beam. The maximum stresses in the load-bearing structure of the hopper car, which are caused by the temperature load, occur in the vertical racks and humps and amount to 335 MPa, which is 3% lower than the yield stress of the structural material.

The influence of the temperature load on the maximum equivalent stresses in the load-bearing structure of the hopper car was determined. It was established that this dependence is linear. The maximum equivalent stresses at the temperature of the transported cargo of 700°C are almost equal to the yield point of the construction material. With a slight increase in the temperature effect on the supporting structure, its strength indicators will not be ensured. Therefore, there is a need to improve the load-bearing structure of the hopper car to ensure its durability in operation.

2. Measures are proposed to improve the load-bearing structure of the hopper car to ensure its durability in operation by using a two-tube backbone beam and composite components. The dynamic load capacity of the supporting

structure of the hopper car was determined, taking into account improvement measures. The results of the calculations showed that the maximum accelerations acting on the supporting structure of the hopper car are equal to 37.6 m/s^2 (0.37g).

The main indicators of strength of the load-bearing structure of the hopper car have been determined. It was established that the maximum equivalent stresses amount to 329.6 MPa and are concentrated in the zone of interaction of the spinal beam with the pivot beams. At the same time, the obtained stress value is 3.1% lower than in a typical design.

3. The possibility of improving the load-bearing structure of the hopper car by using cladding made of heat-resistant composite material to improve its strength indicators was considered. It also contributes to the reduction of the car's container by 5% compared to the prototype.

The dynamic load capacity of the improved design of the hopper car was determined. The results of the calculations showed that the determined dynamics indicators do not exceed the permissible values. The acceleration acting on the center of mass of the load-bearing structure is about 0.4g. The acceleration of the supporting structure of the hopper car in the areas of support on the carts is 0.53g, and the coefficient of vertical dynamics is 0.52. At the same time, the movement of the hopper car is evaluated as "excellent".

The main strength indicators of the improved design of the hopper car were determined. The maximum stress equivalents occur in the zone of interaction of the spinal beam with the pivot beam and are about 290 MPa. At the same time, the stresses in the shell of the hopper car are about 200 MPa, which is 12% lower than in a typical design. That is, the strength of the supporting structure is ensured.

A modal analysis was conducted and the fatigue resistance coefficient of the load-bearing structure of the hopper car was determined. The calculation results established that the first natural frequency has a value of 11.7 Hz, which is not lower than the permissible value of 8 Hz. Therefore, the safety of the carriage is ensured.

The coefficient of the reserve of fatigue resistance of the load-bearing structure of the hopper car was 4.5, which is almost twice as high as permissible.

4. The strength of the load-bearing structure of the semi-car during defrosting of the cargo in it was determined. At the same time, the permissible temperature effect on the load-bearing structure of the gondola car should not exceed 91°C. The maximum equivalent stresses are recorded in the zone of interaction of the lower binding with the cladding and are equal to 343.8 MPa. The maximum movements in the load-bearing structure of the gondola car are concentrated in the middle part of the frame and amount to 3.6 mm.

The most heavily loaded zones of the load-bearing structure of the gondola car during defrosting of the cargo in it were determined. Such areas include cladding of side and end walls.

5. Measures to adapt the load-bearing structures of gondola cars to the transportation of high-temperature cargoes are considered. The load-bearing structure of the gondola car was determined when transporting high-temperature cargo in it. It was established that the maximum equivalent stresses in the load-bearing structure of the gondola car when transporting sinter with a temperature of 700 °C in it are about 3800 MPa, which means that they significantly exceed the permissible ones.

At the same time, permissible stresses in the supporting structure of the gondola car are observed at a temperature of the cargo transported in it of 94°C.

Measures are proposed to adapt the load-bearing structure of the gondola car to the transportation of high-temperature cargoes by placing them in heat-resistant flats made of composite material.

The calculation of the strength of the flat, taking into account the 700°C temperature effect on it, established that the maximum equivalent stresses are about 300 MPa and do not exceed the permissible values. In the cladding, the maximum equivalent stresses were about 260 MPa. In the transverse beams – 210 MPa.

6. The main indicators of the dynamics of the load-bearing structure of a gondola car loaded with flats with high-temperature cargo are determined. Accelerations acting in the mass center of the supporting structure of the gondola car amounted to about 1.5 m/s^2 (0.15g). The coefficient of vertical dynamics is equal to 0.22. Therefore, the calculated dynamics indicators are within the limits of permissible values, and the movement of the wagon is assessed as "excellent".

7. The load-bearing structure of the car for the transportation of high-temperature, bulk/liquid cargoes is proposed. The strength of the boiler of the car for the transportation of high-temperature, bulk/liquid cargoes under operational conditions was determined. The vertical load of the boiler is taken into account, taking into account the transportation of liquid cargo (I scheme); longitudinal (II scheme), as well as the effect of temperature load (III scheme). In the case of the first load scheme, the maximum stresses recorded in the zones of interaction of the cylindrical part of the boiler with the bottoms were 184.4 MPa. With the II scheme, the maximum stresses occur in the middle part of the bottom and amount to 307.4 MPa. The maximum stresses in the III scheme occur in the zones of interaction of the bottoms with the cylindrical parts of the boiler and amount to 314.5 MPa. Therefore, with all considered load regimes, the maximum stresses are within the permissible limits.

The dynamic loading of the boiler of the car for the transportation of high-temperature, bulk/liquid cargoes was determined. The results of mathematical modeling of dynamic load established that the maximum acceleration acting on the boiler is 36.5 m/s^2.

The results of computer modeling of the dynamic load of the boiler showed that the maximum acceleration acting on it is concentrated in the bottom and is 37.4 m/s^2. In the cylindrical part of the boiler, the acceleration value is in the range of 28.0 m/s^2 – 12 m/s^2.

Verification of dynamic load models of the boiler of the car for transportation of high-temperature, bulk/liquid cargo was carried out. The calculation was made according to the F-criterion. It was established that with the dispersion of adequacy S_{ad}=8.23 and reproducibility dispersion S_y=6.44, the actual value of the F-test F_p=1.27, which is less than the table value F_t=3.58 at the level of significance α=0.05. Therefore, the hypothesis of adequacy is confirmed.

SECTION 3
IMPROVEMENT OF ELEMENTS OF TRIBOTECHNICAL PAIRS OF BRAKES OF MOVING VEHICLES

3.1 Study of the load of brake pads under temperature influence

In the process of braking, the elements of tribotechnical pairs experience temperature stress due to friction. In this regard, their damage may occur, which affects the safety of traffic, environmental friendliness and efficiency of operation of rolling stock. Therefore, it is important to create measures to increase the efficiency of the elements of tribotechnical pairs of rolling stock brakes.

One of the most common tribotechnical pairs on broad-gauge railways is the "pad-wheel" pair (Figure 3.1).

a) *b)*

Fig. 3.1 **Tribotechnical pair "pad - wheel"**
a) brake pad; b) interaction of the pad with the wheel

To determine the fields of stress distribution on the surface of the pad under the influence of temperature load, a calculation was carried out using the finite element method. For this purpose, its spatial model was built (Figure 3.2).

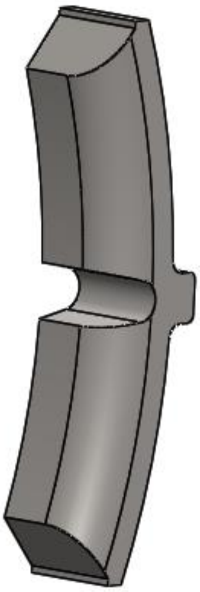

Fig. 3.2 **Spatial model of the brake pad**

The calculation is implemented in the environment of the CosmosWorks software package. Finite elements were modeled by spatial isoparametric tetrahedra (Figure 3.3). The number of model elements was 7,730, nodes – 12,224. The model was fixed in the areas where the block was installed in the shoe.

The temperature that was applied to the pad is taken as equal to 600°C in accordance with [41] (Figure 3.4).

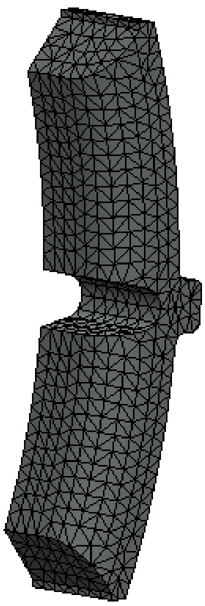

Fig. 3.3 **Finite element model of the brake pad**

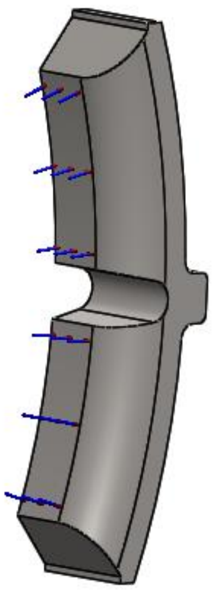

Fig. 3.4 **Calculation scheme of the brake pad**

The calculation results are shown in Figures 3.5, 3.6.

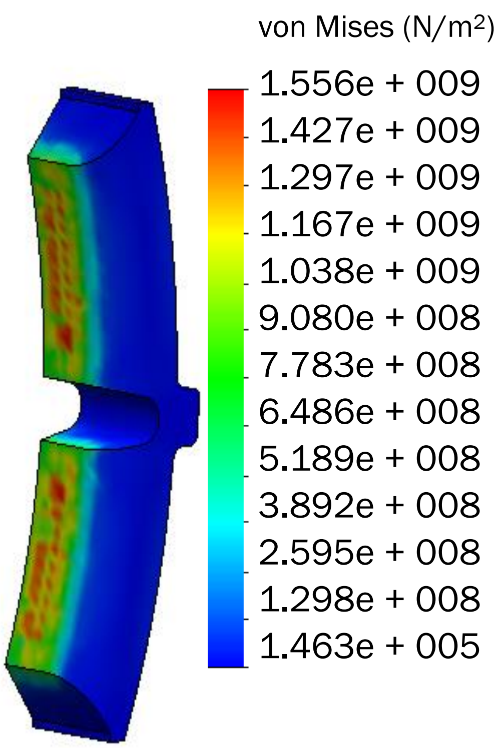

Fig. 3.5 **Stressed state of the brake pad**

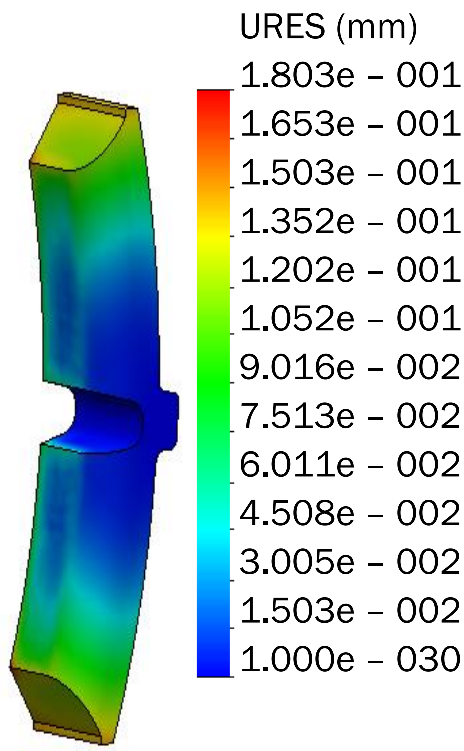

Fig. 3.6 **Movement in brake pad assemblies**

At the same time, the maximum equivalent stresses exceed the permissible ones.

In order to reduce the uncoupling of wagons for unscheduled repairs, as well as the costs of their repairs, work is being carried out to improve the friction pair. One of the possible options for this modernization is the use of brake pads with filters (Figure 3.7) [36].

Such pads were made to ensure braking efficiency at high speeds. A very significant factor is that the temperature of the brake pad is related to the coefficient of friction and the inclusion of filters in the brake pad prevents its temperature from increasing and increases the coefficient of friction.

They also found the use of blocks with foam-ceramic inserts (Figure 3.8). Testing of these brake pads in real operating conditions has shown good results. Therefore, the use of foreign experience in the introduction of powders into the pad material can significantly help in the development of a universal pad. At the same time, such blocks have a significant drawback - a significant manufacturing cost compared to typical pads.

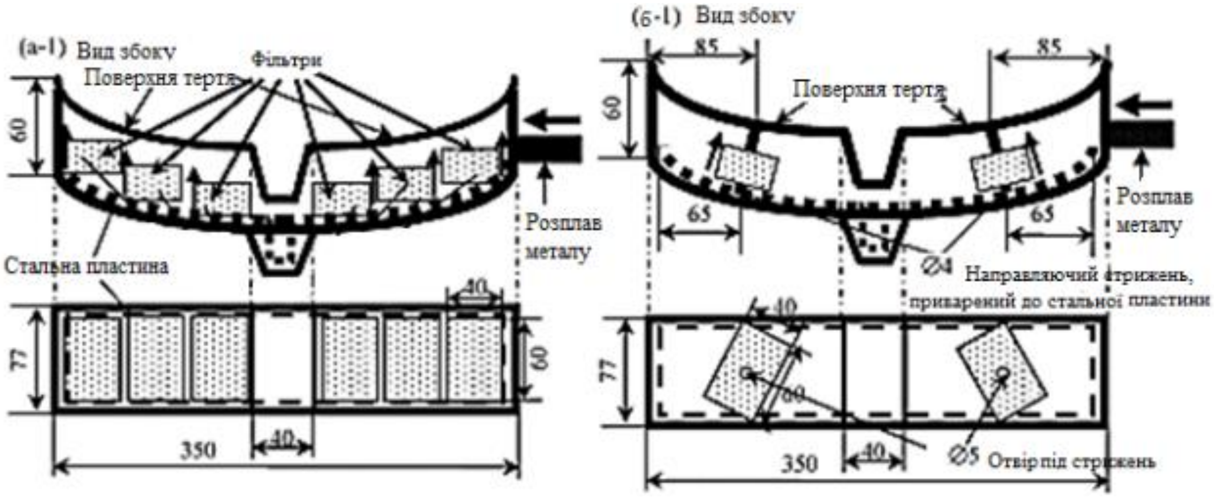

Вид збоку – side view

Фільтри – filters

Поверхня тертя – friction surface

Стальна пластина – steel plate

Розплав металу – metal melt

Направляючий стрижень, приварений до стальної пластини - Guide rod welded to a steel plate

Fig. 3.7 **Structure of brake pads with filters [36]**

a) b) c) d)

Fig. 3.8 **Foam-ceramic inserts in the pad material**
a) aluminum + AlPO4; b) aluminum; c) aluminum titanate; d) silicon carbide [36]

In this regard, in order to increase the efficiency of operation of braking systems, the justification of the use of brake pads with metal-ceramic inserts was carried out. There is positive experience in the operation of pads on broad-gauge rolling stock. A calculation was made to justify the use of these blocks on cars.

To determine the stress distribution fields on the surface of a cast iron block with ceramic inserts, its spatial model was built (Figure 3.9).

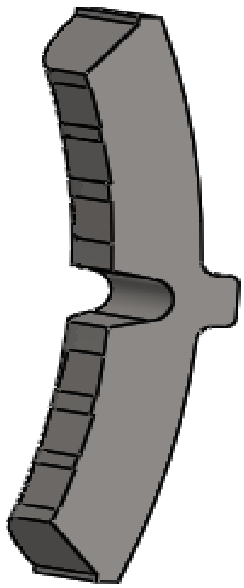

Fig. 3.9 **Spatial model of the brake pad**

Finite elements were modeled by spatial isoparametric tetrahedra (Figure 3.10). The number of model elements was 8415, nodes – 13247. The model was fixed in the areas where the pads was installed in the shoe.

The temperature that was applied to the pad was taken as equal to 600°C in accordance with [41]. The calculation scheme of the pad is shown in Figure 3.11.

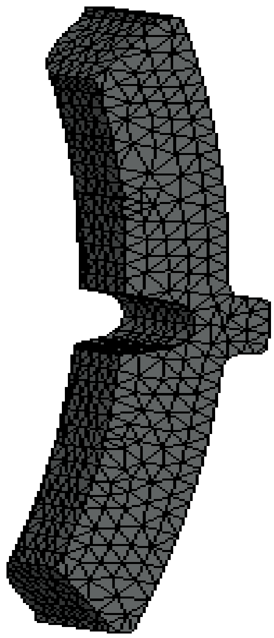

Fig. 3.10 Finite element model of the brake pad

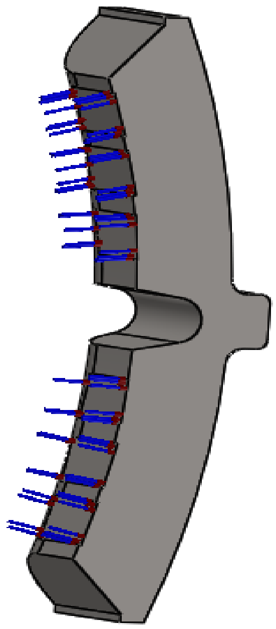

Fig. 3.11 **Calculation scheme of the brake pad**

The calculation results are shown in figures 3.12, 3.13. At the same time, the maximum equivalent stresses do not exceed the permissible ones.

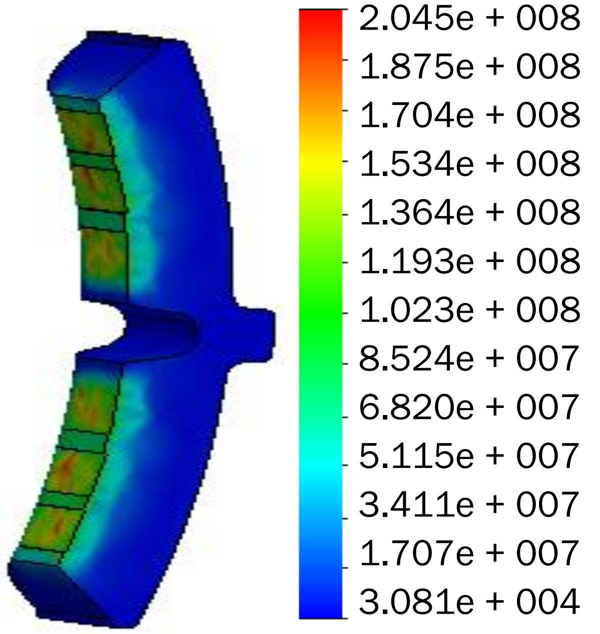

Fig.3.12 **Stressed condition of the brake pad**

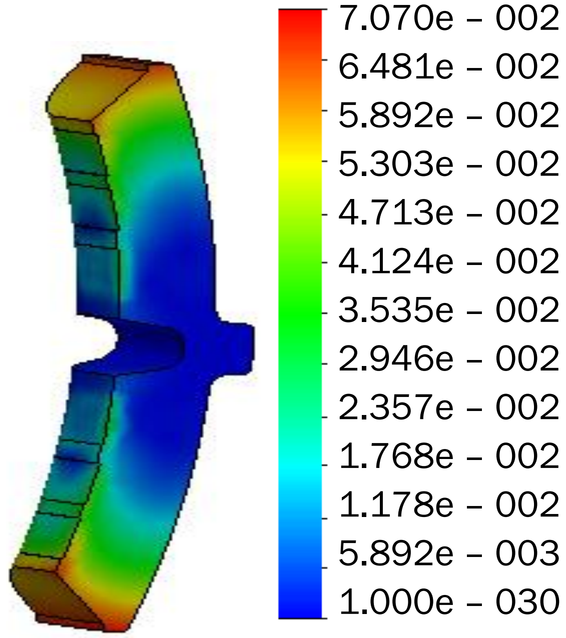

Fig.3.13 **Movement in brake pad assemblies**

The conducted research substantiates the expediency of using these pads on freight rolling stock.

3.2 Calculations of the thermal regime and wear of brake pads

During braking, the train's kinetic energy is converted into thermal energy, heating the brake pads (or discs) and wheels [41]. Therefore, it is important to determine the permissible pressure force on the block.

The permissible amount of pressure $K_t^ч$, кН on a cast-iron brake pad is determined from the expression:

$$K_t^ч = \frac{\left[80\Phi(t) - 70,2v_0 m_v\right] + \sqrt{\left[80\Phi(t) - 70,2v_0 m_v\right]^2 + 4500 v_0 m_v \Phi(t)}}{2,25 v_0 m_v}, \qquad (3.1)$$

where

$$\Phi(t) = \frac{F_к \Delta\tau_{\max}\alpha_0}{1 - e^{-0,155\alpha_0\sqrt{t}}}, \qquad (3.2)$$

$$\alpha_0 = 0{,}004 + 0{,}005\sqrt{v_0}, \tag{3.3}$$

$$m_v = 0{,}6\frac{3{,}6v_0 + 100}{18v_0 + 100}, \tag{3.4}$$

where v_0 *– initial braking speed, m/s;*

$\Delta\tau_{\max}$ *– the maximum permissible temperature of the brake pad during braking, °C (for cast iron – 600 °C, for composite ones – 400 °C);*

α_0 *– coefficient of heat transfer to the environment.*

For composite circles, this value is determined by the expression given in [41].

The duration of braking *t* (c) with the length of the braking distance S_r (м) known according to the standards on the given slope with the initial braking speed v_0 is based on the assumption of uniformly decelerated motion:

$$t = \frac{2S_r}{v_0}. \tag{3.5}$$

Taking into account the calculations carried out for a conditional unit of rolling stock, the dependence of the permissible amount of pressure on the initial braking speed was obtained (Figure 3.14).

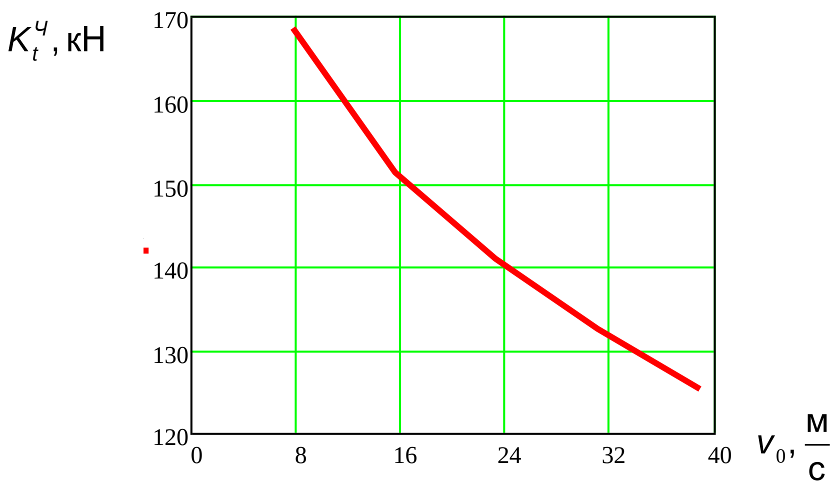

Fig. 3.14 **Dependence of the permissible amount of pad pressure on the initial braking speed**

At the same time, the amount of wear for one braking ΔH can be calculated for cast iron pads according to the following formula [41]

$$\Delta H = \frac{0,04}{\left(\frac{5 \cdot 10^9 F_K}{\alpha_K B_\Gamma v t} - \frac{525}{\sqrt{t}} \right) Y}, \tag{3.6}$$

Where $F_к$ *- geometric area of pad friction, m²;*

α_K *- heat flow distribution coefficient in the pad (0.2 - 0.3 with one block per wheel and 0.35 with double-sided pressing of single and sectional blocks);*

t - duration of braking, c;

B_Γ *- average braking force over time t, H;*

v *- average speed of the wagon, m/s;*

Y *- pad quality factor (when meeting the requirements of the pad manufacturing standard,* Y *=1).*

Herewith,

$$B_\Gamma = 0,5\left(i_c - w''_{cp}\right) q_0, \tag{3.7}$$

where w''_{cp} *— average specific resistance to movement (2 N/kN is assumed).*

The critical time t_{KP} безперервного гальмування, of continuous braking, after which the catastrophically rapid wear of the brake pad occurs, is equal to

$$t_{KP} = \left(\frac{95 \cdot 10^5 \cdot F_к}{\alpha_K \cdot B_\Gamma \cdot v} \right)^2. \tag{3.8}$$

Composite brake pads have different patterns of wear.

The minimum thickness of brake pads on rolling stock, respectively, for plain and mountain profiles with protracted steep slopes, is calculated according to the following expression [41]:

$$\Delta H_{\min} = 0,01 + 0,00015 S_T'', \tag{3.9}$$

$$\Delta H_{\min} = 0,01 + 0,00003 \sum_{i=1}^{n} L_i, \tag{3.10}$$

Where S_T'' *—total distance traveled by the train in braking mode (determined by speed measuring tapes), km*

$\sum_{i=1}^{n} L_i$ *— the sum of the multiplication of the lengths of the path sections in kilometers by their slope in thousands measurement units.*

The wear of brake pads by thickness (m) on a long section with long slopes can be determined by the formula [41]:

$$\Delta H = A \sum_{i=1}^{n} L_i, \tag{3.11}$$

where $\sum_{i=1}^{n} L_i$ *— the sum of the multiplications of the lengths (km) of all sections of the path with a descent along which the train travels, by the amount of the descent.*

Based on the calculations, a graph of the dependence of brake pad wear on the initial braking speed was obtained (Figure 3.15).

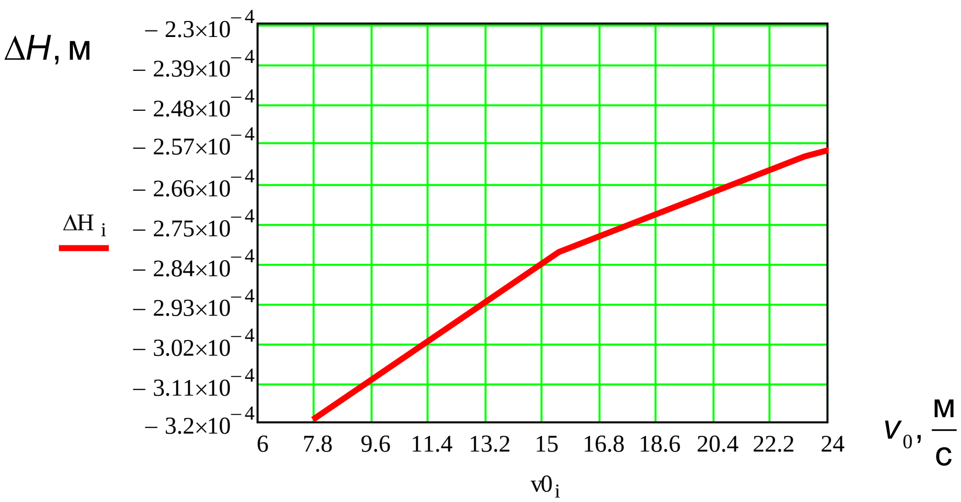

Fig. 3.15 **Chart of dependence of brake pad wear on initial braking speed**

The chart of the dependence of the critical time of continuous braking on the initial braking speed is shown in Figure 3.16.

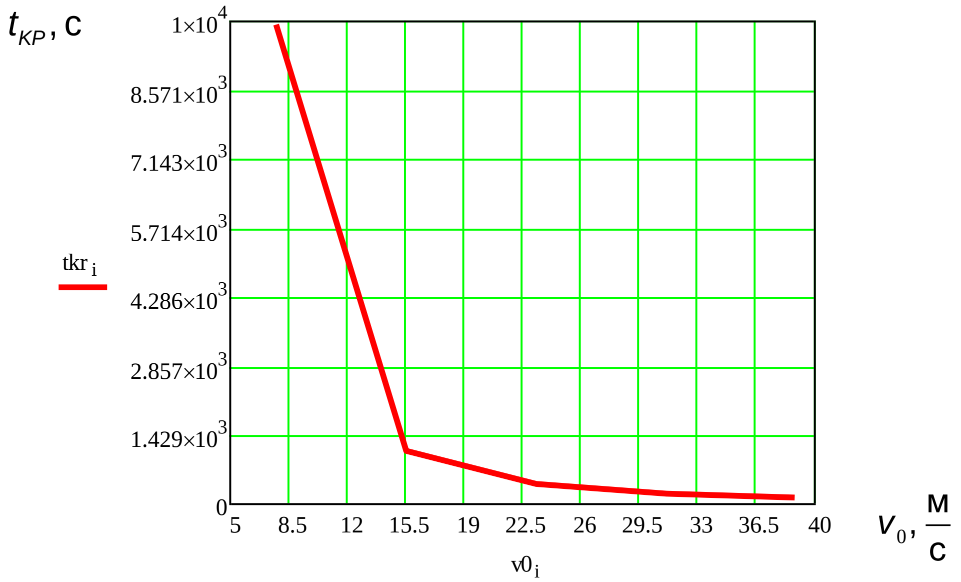

Fig. 3.16 **Chart of the dependence of the critical time of continuous braking from the initial braking speed**

During braking, the process of friction between the brake pad and the wheel occurs at the points of their actual contact [41].

The temperature (˚C) at any moment of the braking time on the wheel surface can be determined by the expression [41]:

$$\Delta\tau_n = \frac{q_T}{\alpha_0}\left[1-e^{-\frac{2\alpha_0}{\sqrt{\pi\lambda\gamma c}}\sqrt{t}\left(1-\frac{2}{3}\cdot\frac{t}{t_B}\right)}\right]. \tag{3.12}$$

The highest temperature during braking on the surface of the wheel is reached in the middle of this process $t = 0{,}5t_B$:

$$\Delta\tau_{n\max} = \frac{q_T}{\alpha_0}\left[1-e^{-0{,}9433\frac{\alpha_0}{\sqrt{\pi\lambda\gamma c}}\sqrt{t_B}}\right]. \tag{3.13}$$

The temperature on the surface of the wheel at the time the train stops $t = t_B$:

$$\Delta\tau_{nK} = \frac{q_T}{\alpha_0}\left[1 - e^{-0{,}667\frac{\alpha_0}{\sqrt{\pi\lambda\gamma c}}\sqrt{t_B}}\right]. \tag{3.14}$$

Set braking temperature (at constant speed):

$$\Delta\tau_{n\infty} = \frac{q_T}{\alpha_0}\left[1 - e^{-2\frac{\alpha_0}{\sqrt{\pi\lambda\gamma c}}\sqrt{t_B}}\right], \tag{3.15}$$

Where q_T *– heat flow density,* $\text{ккал}/\left(\text{м}^2\cdot{}^\circ\text{C}\right)$*; (kCal/(m² · °C);*

λ *– thermal conductivity coefficient,* $\text{ккал}/\left(\text{м}\cdot{}^\circ\text{C}\right)$ *(kCal/(m · °C);*

γ *– specific weight, kN/m³;*

c *– specific heat capacity,* $\text{ккал}/\left(\text{кгс}\cdot{}^\circ\text{C}\right)$ *(kCal/(kgs · °C);*

t_B *– braking time to a complete stop, seconds.*

The heat flux density at the initial moment of braking is determined by the expression:

$$q_T = \frac{\alpha_R \cdot b_\Gamma \cdot q_0 \cdot v_0}{17080\pi \cdot R \cdot h_K}, \tag{3.16}$$

Where α_R *– heat flow distribution coefficient;*

h_K *– width of the wheel friction surface, m (should be taken 0.09 m).*

The above formulas are obtained for the conditions of heating a semi-confined body, that is, when the heat flow does not yet reach the surface that limits the heating body from the side opposite to the heat supply.

Due to the fact that the braking force changes in the process of filling the brake cylinders and when the speed of movement changes, the value b_Γ is calculated based on the length of the actual braking distance S_Γ and brake preparation time t_Π [41]:

$$b_Г = \frac{108 \cdot v_0}{2\left(S_Г - v_0 t_П\right)} - w_0 - i_c, \tag{3.17}$$

Where w_0 *– the main specific resistance of the train movement (assume 2 N/kN).*

Time t at the same time, in the expression for thermal regime calculations, it is taken as reduced by the time of preparation $t_П$, if $t \geq t_П$.

To determine the diameter of the wheel D_K, which provides the necessary convection of heat to avoid overheating during emergency braking, the following expression is used:

$$D_K = \frac{\alpha_R \cdot b_Г \cdot q_0 \cdot v_0}{8540\pi h_K \cdot \Delta\tau_{nK} \cdot \alpha_0}\left(1 - e^{-0{,}9433\frac{\alpha_0}{\sqrt{\pi\lambda\gamma c}}\sqrt{t_B}}\right). \tag{3.18}$$

The dependence of the heating temperature of the cast iron pad on the braking time is shown in the Figure 3.17.

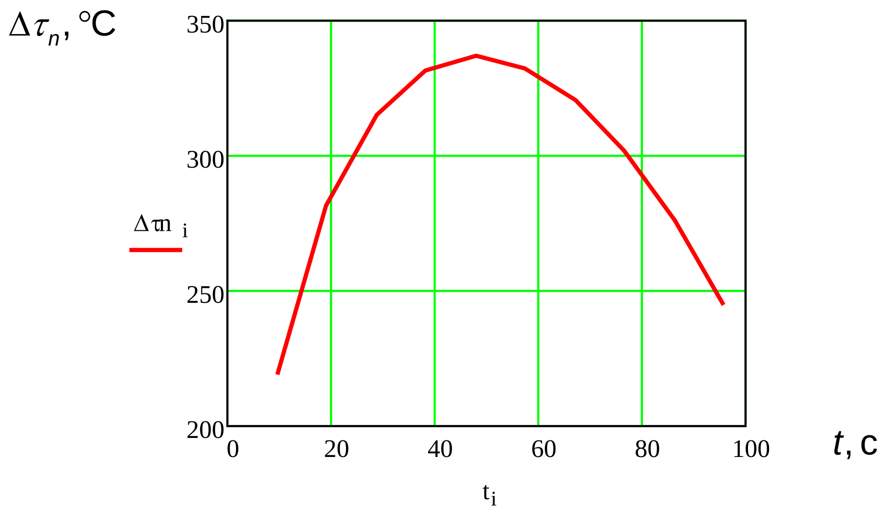

Fig. 3.17 **Dependence of the heating temperature of the cast iron pads by braking time**

At the same time, the chart of dependency $D_K = f\left(v_0, q_0\right)$ has the form shown in Figure 3.18.

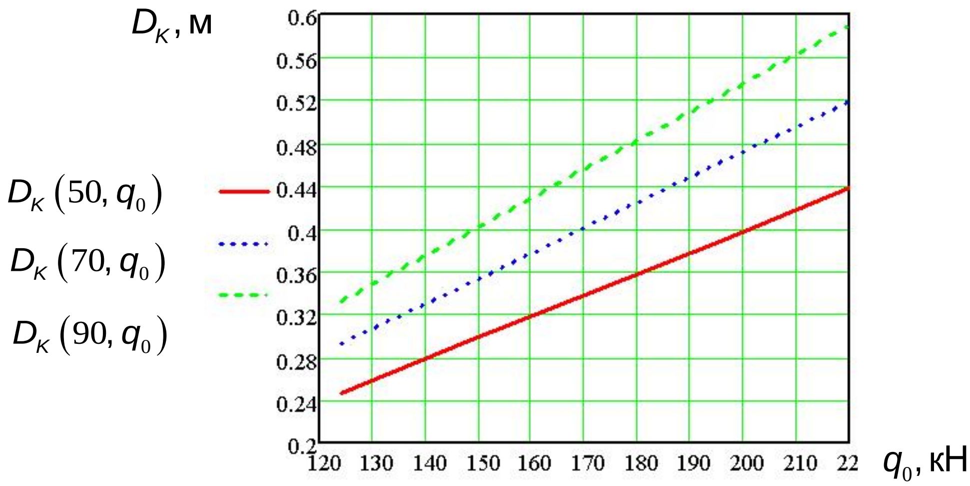

Fig. 3.18 **Chart of dependency of wheel diameter on braking speed and axial load**

Figure 3.18 shows that this dependency is linear. At the same time, the smallest wheel diameter is observed at a speed of 90 km/h and an axial load of 220 kN/axle.

3.3 Justification of the creation of promising disc brakes for passenger cars

One of the most important conditions for the safety of high-speed train movement, both in case of failure or impossibility of applying the electrodynamic brake, and in case of automatic (emergency) braking is the dissipation of the kinetic energy of the train by the mechanical brake [37, 38]. A disc brake refers to mechanical friction brakes. It is similar to a pad brake, but differs in that the brake linings are not pressed against the rolling surface of the wheels, as in a pad brake, but to special brake discs (figures 3.19) [38].

The brake of the domestic KVZ-TsNII cart for passenger cars consists of four claw mechanisms, each of which has a brake cylinder 1, two paired levers 2 with tightening 3 and a lock 4 and two shoes 6 with friction linings 5. Two brake discs are placed on one pair of wheels 7 with a diameter of 620 mm with a friction surface width of 120 mm [86].

Each disk consists of two halves connected by bolts 9. The disk is attached to the hub, pressed onto the axle of the wheel pair, by radially located bolts 8 with split bushings and plate springs. For better heat dissipation, the discs are equipped with ribs and ventilation windows.

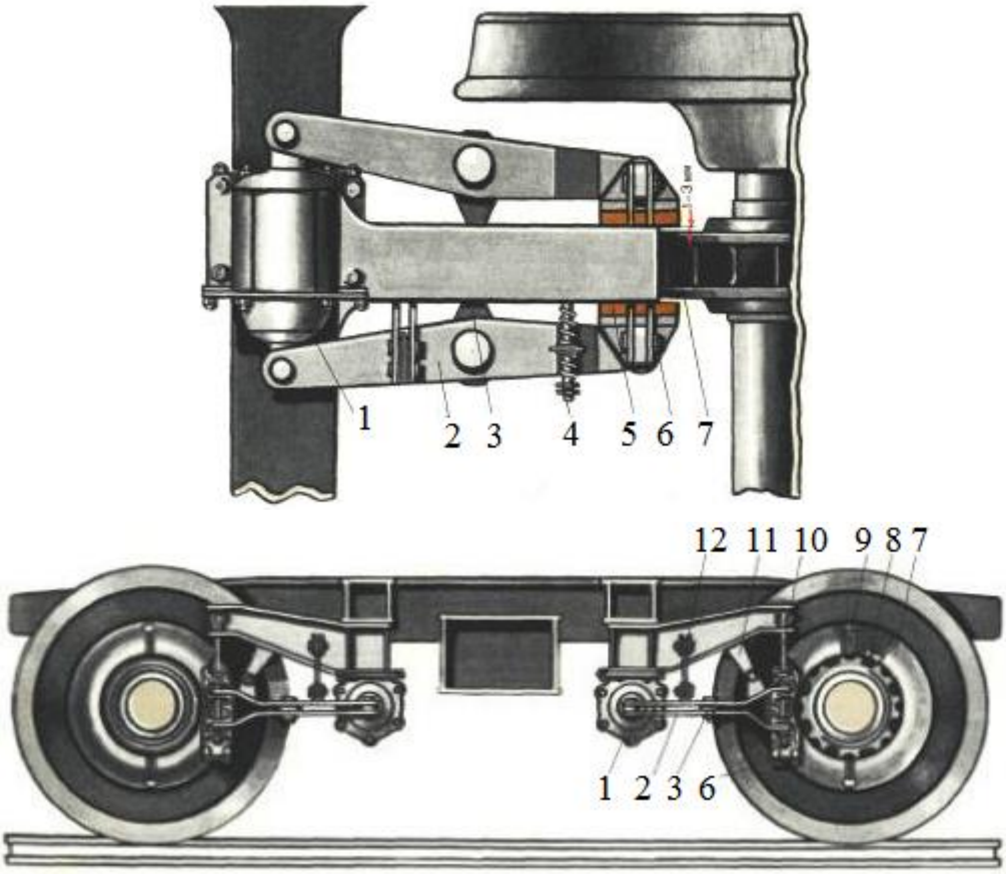

Fig. 3.19 **General view of a rolling stock disc brake**

Shoes with overlays are suspended from the console of the cross beam of the cart on hinged suspensions 12. The shoes are hingedly connected to levers 2 with vertical rollers 10, which are attached to the same console as the shoe suspensions by suspensions 12. Four brake cylinders 1 with a diameter of 8" are installed on each cart. Each of the cylinders serves one pair of brake shoes 6. The brake linings are made of composite material [38].

Brake discs are placed on the middle part of the axle of the wheel pair. During operation, they experience significant temperature loads. This contributes to the appearance of defects on the surface of the disc. The most common among such defects are cracks (Figure 3.20).

The reason for the appearance of cracks can be significant temperatures that occur in the zone of interaction of the disc with the linings, a change in the structure of the metal, increased forces of pressing the pad on the wheel, etc. This makes it necessary to implement measures to modernize disc brakes of cars.

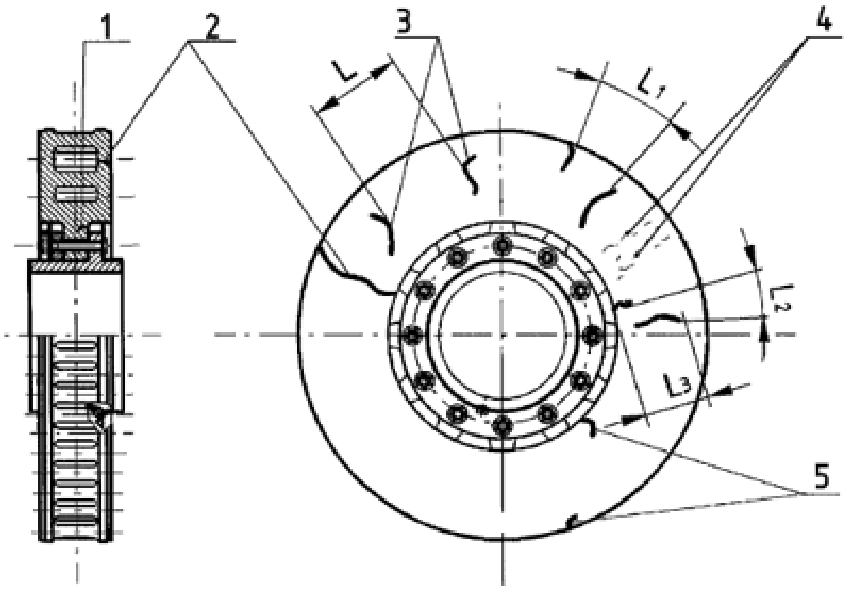

1 – cracks located in the zone of attachment of the friction ring to the hub;
2 – through cracks; 3 – cracks in the middle part of the friction ring;
4 – microcracks (hairline cracks) located on the working surface of the friction ring;
5 – cracks extending to the outer or inner edge of the friction ring

Fig. 3.20 **Types of defects on the surface of the brake disc crown**

In order to reduce the costs of repairing disc brakes, it is suggested to use a sectional design of the brake disc (Figure 3.21).

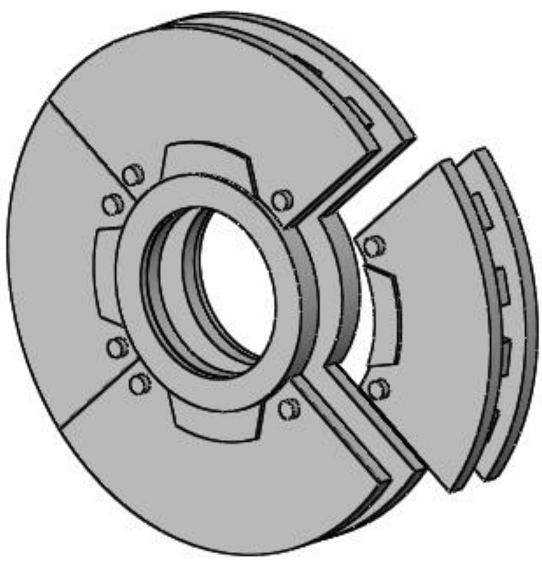

Fig. 3.21 **Sectional brake disc**

This design makes it possible to replace the worn sector with a new one and increase the overall resource of the brake disc.

To increase the stiffness of the disc, and accordingly ensure its strength, it is suggested to install reinforcing ribs between the outer and inner rings, which have holes for cooling and reducing the total weight of the brake disc (Figure 3.22).

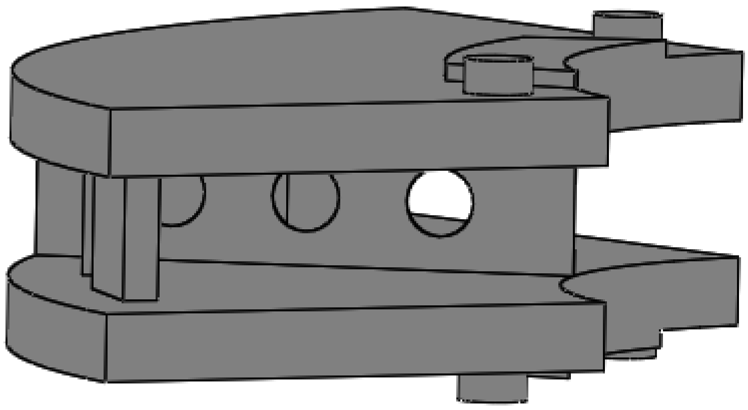

Fig. 3.22 **Section of a brake disc with a reinforcing diaphragm**

The proposed design of the brake disc has a 15% higher moment of resistance compared to the typical design. And therefore it can withstand greater stresses.

At the same time, the mass of the proposed disc is 3.5% greater than the mass of a typical one.

To determine the numerical values of the stresses that develop in the brake disk, taking into account the proposed solutions, the calculation of temperature conditions was carried out in the CosmosWorks software.

The calculation diagram of the brake disc is shown in the Figure 3.23. At the same time, the temperature was applied to the pad, which simulated a brake pad. The numerical value of the temperature was 600°C [41]. The results of the calculations are shown in the Figure 3.24.

The calculations showed that the maximum equivalent stresses in the brake disc under the influence of temperature loads, taking into account improvement measures, decreased by 13%. The conducted research will contribute to increasing the service life of brake discs by reducing their load during operating modes.

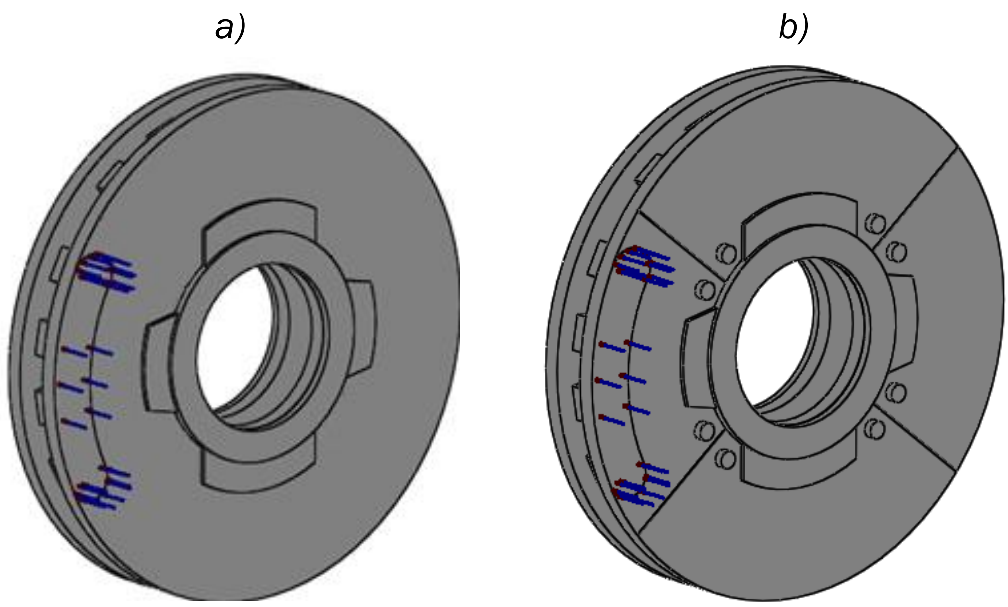

Fig. 3.23 **Calculation scheme of the brake disc**
a) typical design; b) improved design

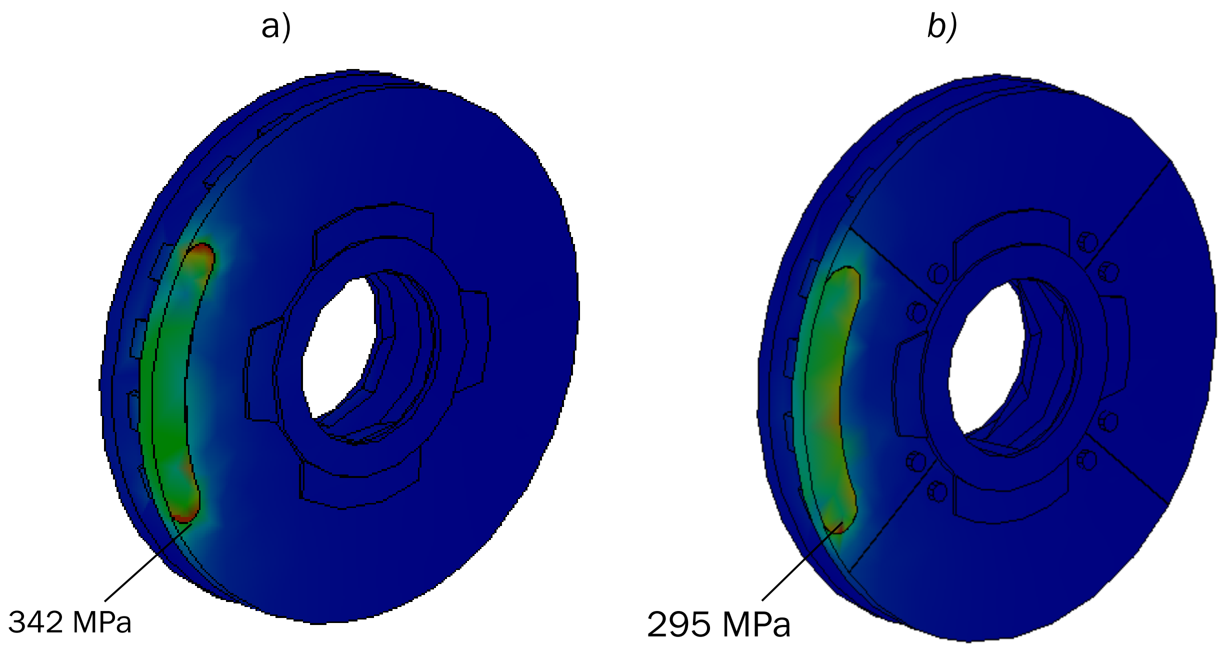

Fig. 3.24 **Stress in the brake disc**
a) typical design; b) improved design

CONCLUSIONS TO THE SECTION 3

1. Measures are proposed to improve the elements of tribotechnical pairs of rolling stock brakes. To increase the efficiency of operation of braking

systems, the use of brake pads with metal-ceramic inserts is proposed. In order to justify the use of these pads on rolling stock, a strength calculation was performed in the Cosmos Works software environment. The temperature that was applied to the pad is assumed to be equal to 600°C. The results of the calculations showed that the maximum equivalent stresses do not exceed the allowable ones. The conducted research substantiates the expediency of using these pads on a rolling stock.

2. The theoretical aspects of calculating the thermal regime and wear of brake pads are presented. An example of such a calculation for a cast iron brake pad is also presented. The dependences of the permissible amount of pad pressure on the initial braking speed, brake pad wear on the initial braking speed, the critical time of continuous braking on the initial braking speed, the heating temperature of the pad on the braking time, as well as the wheel diameter on the braking speed and axial load are given.

3. The design features of rolling stock disc brakes are considered. The main defects of disks and their causes in operation are determined.

The need to improve the design of disc brakes is substantiated. In order to reduce the cost of repairing disc brakes, it is suggested to use a sectional design of the brake disc. To increase the stiffness of the disc, and accordingly ensure its strength, it is suggested to install reinforcing ribs between the outer and inner rings, which have holes for cooling and reducing the total weight of the brake disc.

The calculation of the strength of the proposed disk design under temperature influence was carried out. The numerical value of the temperature, which was taken into account during the calculations, was taken equal to 600°C. The results of the calculations showed that the maximum equivalent stresses in the brake disc under the influence of temperature loads, taking into account improvement measures, decreased by 13%. The conducted research will contribute to increasing the service life of brake discs by reducing their load during operating modes.

GENERAL CONCLUSIONS

1. The structural features and main characteristics of hopper cars for the transportation of hot pellets and sinter have been studied. At the same time, the designs of hopper cars of Ukrainian production were considered.

A patent analysis of the supporting structures of hopper cars for the transportation of pellets and hot sinter was carried out. At the same time, the analysis was carried out in relation to Ukrainian inventions and useful models.

Literary sources on the determination of the temperature effect on the components of the rolling stock were analyzed. The main operational situations of occurrence and effect of temperature load on the components of rolling stock structures are determined. Measures regarding the improvement of components of the rolling stock to ensure their heat resistance during operational modes are considered.

The main labor protection measures and features of the repair of the supporting structures of hopper cars for the transportation of hot pellets and sinter are considered.

2. The load bearing structure of the hopper car was determined and measures were proposed to increase the efficiency of high-temperature cargo transportation.

At the first initial stage of the research, the load bearing structure of the hopper car due to temperature effects was determined. The maximum stresses in the load-bearing structure of the hopper car, which are caused by the temperature load, occur in the vertical racks and humps and amount to 335 MPa, which is 3% lower than the yield stress of the material of the structure.

Measures are proposed to improve the load-bearing structure of the hopper car to ensure its durability in operation by using a two-tube backbone beam and composite components. The dynamic load capacity of the supporting structure of the hopper car was determined, taking into account improvement measures. The results of the calculations showed that the maximum accelerations acting on the load-bearing structure of the hopper car are equal to 37.6 m/s^2 (0.37g).

The calculation of the strength of the load-bearing structure of the hopper car was carried out. The maximum equivalent stresses at the end were 329.6

MPa and were concentrated in the zone of interaction of the spinal beam with the pivot beams. It is important to say that the obtained stress value is 3.1% lower than in a typical design structure.

The improvement of the load-bearing structure of the hopper car through the use of sheathing made of heat-resistant composite material to improve its strength is substantiated. The dynamic load capacity of the improved design of the hopper car was determined. The results of the calculations showed that the determined dynamics indicators do not exceed the permissible values.

The strength of the improved supporting structure of the hopper car was calculated. The maximum equivalent stresses are provided in the zone of interaction of the spinal beam with the pivot beam and are about 290 MPa. At the same time, the stresses in the coating of the hopper car are about 200 MPa, which is 12% lower than in a typical design. Therefore, the strength of the supporting structure is ensured.

A modal analysis was conducted and the fatigue resistance coefficient of the load-bearing structure of the hopper car was determined. The calculation results established that the first natural frequency has a value of 11.7 Hz, which is not lower than the permissible value of 8 Hz. Therefore, the safety of the carriage is ensured. The coefficient of the reserve of fatigue resistance of the load-bearing structure of the hopper car was 4.5, which is almost twice as high as the permissible.

The strength of the load-bearing structure of the gondola car during defrosting of the cargo in it was determined. At the same time, the permissible temperature effect on the load-bearing structure of the gondola car should not exceed 91°C. It was established that the maximum equivalent stresses occur in the zone of interaction of the lower binding with the cladding and are equal to 343.8 MPa.

The most heavily loaded zones of the load-bearing structure of the gondola car during defrosting of the cargo in it were determined.

Measures are proposed to adapt the load-bearing structures of gondola cars to the transportation of high-temperature cargoes. The load-bearing structure of the gondola car was determined when transporting high-temperature cargo in it. The maximum equivalent stresses in the load-bearing structure of the gondola car when transporting sinter with a temperature of 700

°C in it are about 3800 MPa, so they significantly exceed the allowable ones. At the same time, permissible stresses in the supporting structure of the gondola car are observed at a temperature of the cargo transported in it of 94°C.

Measures are proposed to adapt the load-bearing structure of the gondola car to the transportation of high-temperature cargoes by placing them in heat-resistant flats made of composite material.

The calculation of the strength of the flat, taking into account the temperature effect on it at 700°C, established that the maximum equivalent stresses are about 300 MPa and do not exceed the permissible values.

The main indicators of the dynamics of the load-bearing structure of a gondola car loaded with flats with high-temperature cargo are determined. It was established that the calculated dynamics indicators are within the limits of permissible values, and the movement of the wagon is assessed as "excellent".

A load-carrying structure of the car for transportation of high-temperature, liquid/bulk cargoes is also proposed.

The results of calculations on the strength of the car's boiler for transportation of high-temperature, bulk/liquid cargo under operating conditions are given. At the same time, the vertical load of the boiler is taken into account, taking into account the transportation of bulk cargo (I scheme); longitudinal (II scheme), as well as the effect of temperature load (III scheme). In the case of the first loading scheme, the maximum stresses recorded in the zones of interaction of the cylindrical part of the boiler with the bottoms were 184.4 MPa. With the II scheme, the maximum stresses occur in the middle part of the bottom and amount to 307.4 MPa. The maximum stresses in the III scheme occur in the zones of interaction of the bottoms with the cylindrical parts of the boiler and amount to 314.5 MPa. Therefore, with all considered load regimes, the maximum stresses are within the permissible limits.

The dynamic loading of the boiler of the car for the transportation of high-temperature, liquid/bulk cargoes was determined. According to the results of mathematical modeling of dynamic loading, it was established that the maximum acceleration acting on the boiler is 36.5 m/s^2. The results of computer modeling of the dynamic load of the boiler showed that the maximum acceleration acting on it is concentrated in the bottom and is 37.4 m/s^2.

The dynamic load models of the car's boiler for the transportation of high-temperature, liquid/bulk cargoes have been verified. It was established that the hypothesis of adequacy is confirmed.

3. Measures are proposed to improve the elements of tribotechnical pairs of rolling stock brakes by using brake pads with metal-ceramic inserts. The strength calculation of the proposed brake pad design is given. The results of the calculations showed that the maximum equivalent stresses do not exceed the allowable ones. The conducted research substantiates the expediency of using these pads on a rolling stock.

Theoretical aspects are presented, as well as an example of calculating the thermal regime and wear of a cast iron brake pad.

The design features of rolling stock disc brakes are considered. The main defects of discs and their causes in operation are determined.

In order to reduce the cost of repairing disc brakes, it is proposed to use a sectional design of the brake disc. A special feature of the disc is the presence of reinforcing ribs between the outer and inner rings, which have holes for cooling and reducing the total weight of the brake disc. Such a decision helps to increase the rigidity of the disk, and accordingly, to ensure its strength.

The calculation of the strength of the proposed disk structure under temperature influence was carried out using the finite element method, implemented in the CosmosWorks software package. The numerical value of the temperature, which was taken into account in the calculations, was taken as equal to 600 °C. It was established that the maximum equivalent stresses in the brake disc under the influence of temperature loads, taking into account improvement measures, decreased by 13%. The conducted research will contribute to increasing the service life of brake discs by reducing their load during operating modes.

REFERENCES

1. http://transport.in.ua/informatsiya/inform-zhd-perevozki/vagony-harakteristiki/hopper-okatyshej-20-471/
2. Kharitonov M. I., Pankin V. N. Freight cars. Part I (gondola cars and covered wagons): Tutorial for laboratory work / M. I. Kharitonov, V. N. Pankin. – Khabarovsk: Publishing House of the Far Eastern State University of Communications, 2003. – 96 p.: 45 illustrations.
3. https://www.kvsz.com/index.php/ua/produktsiya/vantazhne-vagonobuduvannya/vagoni-khoperi/item/2902-vahon-khoper-dlia-perevezennia-okatyshiv-model-20-7032
4. https://vagon.by/model/20-480
5. http://www.dvmash.biz/ru/hoperi/6-2010-06-15-13-11-34/48-20-4015-20-4015-01.html
6. https://ukrailtrans.com.ua/4-osnyj-vagon-dlya-okatyshej-model-20-4015-01/
7. https://vagon.by/model/20-9749
8. https://vagon.by/model/20-471
9. https://dmz-karpaty.com/services/car-building/19-9982
10. https://ukrailtrans.com.ua/4-osnyj-vagon-dlya-okatyshej-model-20-793/
11. Railway hopper gondola car for hot pellets and sinter: patent 122540 of Ukraine, IPC (2017.01) B61D 7/00 B61D 3/00. u2017 08482; application date 18.08.17; published on 10.01.18, Bull. No. 1.
12. Railway hopper gondola car for hot coils and sinter: pat. 101213 of Ukraine, IPC (2013.01) B61D 7/00 B61F 1/02 (2006.01) B61D 7/16 (2006.01) B61D 06/17 (2006.01) B61D 08/17 (2006.01). a2011 03663; application date 28.03.11; published on 11.03.13, Bull. No. 5.
13. Hopper car of the articulated type: pat. 145805 of Ukraine, IPC (2021.01)
14. B61D 17/06 (2006.01) B61D 7/00. a2011 03663; application date 03.07.20; published on 06.01.21, Bull. No. 1.
15. Hopper car with elastic elements in the load-bearing structure: pat. 148947 of Ukraine, IPC (2021.01) B61D 7/00. u2020 04026; application date 20.01.2021; published on 05.10.21, Bull. No. 40.
16. Railway open hopper car: pat. 118389 of Ukraine, IPC (2006.01) B61F 1/02 (2006.01) B61F 1/10 (2006.01) B61D 7/00. a2017 01810; application date 06/26/2018; published on 10.01.2019, Bul. No. 1.
17. Hopper car: pat. 98764 of Ukraine, IPC (2015.01) B61D 7/00. u2014 11358; application date 17.10.14; published on 12.05.15, Bul. No. 9.
18. UA 98764 U, 12.05.2015
19. http://um.co.ua/11/11-9/11-97694.html
20. https://ua.all.biz/vagon-dlya-okatyshej-modeli-20-9839-gp-71tn-vkuz-g1828828

21. DSTU 7598:2014. Freight cars. General requirements for calculations and design of new and modernized wagons of 1520 mm gauge (non-self-propelled). Kyiv, 2015. 162 p.
22. GOST 33211–2014. Freight cars. Requirements for strength and dynamic qualities. Moscow, 2016. 54 p.
23. Lukin V.V., Shadur L.A., Koturanov V.I., Khokhlov A.A., Anisimov P.S. Construction and calculation of wagons. Moscow, 2000. 731 p.
24. Bogomaz G. I., Mekhov D. D., Pylypchenko O. P., Chernomashentseva Y. G. Loading of container-tanks located on a railway platform when hitting a car coupling. Collection of science works “Dynamics and motion control of mechanical systems”. Kyiv: Academy of Science, Institute of Technical Mechanics. 1992. P. 87–95.
25. Dyomin Yu. V., Chernyak G. Yu. Fundamentals of wagon dynamics: tutorial Kyiv: Kyiv University of Economics and Transport Technologies, 2003. 269 p.
26. Fomin Oleksij, Lovska Alyona. Establishing patterns in determining the dynamics and strength of a covered freight car, which exhausted its resource // Eastern-European Journal of Enterprise Technologies. 2020. Vol. 6. Issue 7 (108). P. 21 – 29. doi: 10.15587/1729-4061.2020.217162
27. Kosmin V.V. Fundamentals of scientific research: Textbook. Moscow: GOU "Educational and methodological center for education in railway transport", 2007. 271 p.
28. Matalytsky M. A., Khatskevich G. A. Probability theory and mathematical statistics: textbook. Minsk: Higher School, 2017. 591 p.
29. Ivchenko G. I., Medvedev Yu. I. Mathematical statistics: textbook. M.: Knizhny Dom “LIBROKOM”, 2014. 352 p.
30. Rudenko V. M. Mathematical statistics: textbook. Kyiv: Center of Educational Literature, 2012. 304 p.
31. Ustych P. A., Karpych V. A., Ovechnikov M. N. Reliability of rail non-traction rolling stock. Moscow, 1999. 415 p.
32. https://promvest.info/ru/otrasli-i-predpriyatiya/na-uvz-vpervyie-izgotovlen-vagon-hopper-modeli-20-5197-dlya-perevozki-okatyishey-i-aglomerata/
33. http://vmz.com.ua/index.php/vagony-menu/khoppery/9-uncategorised/123-vagon-khopper-dlya-okatyshej
34. https://vagon.by/model/20-9916-01
35. https://vagon.by/model/19-9809
36. https://vagon.by/model/19-1241
37. Yamshinskyi, M.M., Nazarenko, V.S., and Kravchenko, K.O. (2015). Analysis of brake pads and ways of evaluating their perspective. Structural analysis of brake pads and ways of evaluation. *Bulletin of the East Ukrainian National University named after Volodymyr Dahl*, pp. 204 – 209.
38. Babaev A. M., Dmytriev D. V. Principle of operation, calculations and basics of

operation of railway rolling stock brakes: textbook - Kyiv: State Economic and Technological University of Transport, 2007, p.176.
39. Lovska A. O., Ravlyuk V. G. Synopsis of lectures on the discipline "Modern brake wagon systems" (part II). Synopsis of lectures. Kharkiv: Ukrainian State University of Railway Transport, 2019, p. 61.
40. Gallagher R. (1984). Method of finite elements. Moscow: Mir, p. 428.
41. Sham Tyku. Effective work SolidWorks 2005. Official manual. Petersburg, 2006, p. 0.
42. Martynov I. E., Ravlyuk V. G., Afanasenko I. M. Methodical instructions for the performance of the control work in the discipline "New brake technology". Kharkiv: Ukrainian State University of Railway Transport, 2014. p. 41.
43. Guoshun Wang, Rong Fu. Impact of Brake Pad Structure on Temperature and Stress Fields of Brake Disc // Advances in Materials Science and Engineering. – 2013. – Vol. 2013, Article ID 872972, http://dx.doi.org/10.1155/2013/872972
44. Aurelio Somà, Marco Aimar, Nicolò Zampieri. Simulation of the Thermal Behavior of Cast Iron Brake Block during Braking Maneuvers // Applied Science. – 2021. – Vol. 11(11), 5010; https://doi.org/10.3390/app11115010
45. Jay Prakash Srivastava, Prabir Kumar Sarkar, Vinayak Ranjan. Effects of thermal load on wheel–rail contacts: A review // Journal of Thermal Stresses. – 2016. – Vol. 39, Issue 11. P. 1389 – 1418. https://doi.org/10.1080/01495739.2016.1216060
46. Azadeh Haidari Parisa, Hosseini Tehrani. Thermal load effects on fatigue life of a cracked railway wheel // Latin American Journal of Solids and Structures. – 2015. – Vol.12 (6), June. https://doi.org/10.1590/1679-78251658
47. Qing Wu, Colin Cole, Maksym Spiryagin. Preload on draft gear in freight trains // Proceedings of the Institution of Mechanical Engineers, Part F: Journal of Rail and Rapid Transit. – 2018. – Vol. 232, Issue 6. https://doi.org/10.1177/0954409717738849
48. Andrew Nikitchenko, Viktor Artiukh, Denis Shevchenko, Vera Murgul. Modeling of Operation of Elastic-frictional Draft Gear by NX Motion Software // Procedia Engineering. – 2017. – Vol. 187, P. 790 – 796.
49. Hyun-Ah Lee, Seong-Beom Jung, Hwan-Hak Jang, Dae-Hwan Shin, Jang Uk Lee, Kwang Woo Kim, Gyung-Jin Park. Structural-optimization-based design process for the body of a railway vehicle made from extruded aluminum panels // Proceedings of the Institution of Mechanical Engineers, Part F: Journal of Rail and Rapid Transit. – 2016. – Vol. 230, Issue 4. – P. 1283 – 1296.
50. D.Ya. Antipin, D.Yu Racin, S.G. Shorokhov. Justification of a Rational Design of the Pivot Center of the OpenTop Wagon Frame by means of Computer Simulation // Procedia Engineering. – 2016. – Vol. 150. – P. 150 – 154
51. Tomasz Kuczek, Bartosz Szachniewicz. Topology Optimization of Railcar Composite Structure // Inderscience Enterprises Ltd. 2014, January.

52. Bain D.G. (2019). Analysis of the stress state of the load-bearing floor covering of a four-axle half-car with a hollow body. *Bulletin of the Bryansk State Technical University, 1(29)*, p.47–51.
53. Determination of the dynamic load of the carrying structure of the hopper wagon with the actual dimensions of structural elements / Oleksij Fomin, Alyona Lovska, Pavel Skok, Ivan Rogovskii // Technology audit and production reserves. – 2021. – № 1/1(57). – P. 6 – 11. doi: 10.15587/2706-5448.2021.225458
54. Mrzyglod M., Kuczek T. Uniform crashworthiness optimization of car body for high-speed trains // Structural and Multidisciplinary Optimization . 2014, Vol. 49. P. 327–336.
55. Avent R. R., Mukai D. J., Robinson P. F. Effect of heat straightening on material properties of steel // Journal of Materials in Civil Engineering. – 2000. – Vol. 12, Issue 3. – P. 188 – 195.
56. Alessio Gullino, Paolo Matteis, Fabio D'Aiuto. Review of Aluminum-To-Steel Welding Technologies for Car-Body Applications // Metals. – 2019. – Vol. 9, Issue 315. doi:10.3390/met9030315
57. Chandra Prakash Shukla, P. K. Bharti. Study and Analysis of Doors of BCNHL Wagons // International Journal of Engineering Research & Technology (IJERT). 2015. Vol. 4. Issue 04. P. 1195 – 1200.
58. Alexandru Ionut Patrascu, Anton Hadar, Stefan Dan Pastrama. Structural Analysis of a Freight Wagon with Composite Walls // Materiale plastic. 2019. Vol. 57(2). P. 140 – 151. doi: 10.37358/MP.20.2.5360
59. George Edward Street, Preetum Jayantilal Mistry, Michael Sylvester Johnson. Impact Resistance of Fibre Reinforced Composite Railway Freight Tank Wagons // Journal of Composites Science. 2021. Vol. 5. Issue 152. https://doi.org/10.3390/jcs5060152
60. Mariusz Kosobudzki, Krzysztof Jamroziak, Mirosław Bocian, et al. The analysis of structure of the repaired freight wagon // AIP Conference Proceedings. 2018. Vol. 2029. 020030. https://doi.org/10.1063/1.5066492
61. Marek Płaczek, Andrzej Wróbel, Maciej Olesiejuk. Modelling and arrangement of composite panels in modernized freight cars // MATEC Web of Conferences. 2017. Vol. 112. 06022. doi: 10.1051/matecconf/201711206022
62. Yuansong Liu, Mingjie Guan. Selected physical, mechanical, and insulation properties of carbon fiber fabric-reinforced composite plywood for carriage floors // European Journal of Wood and Wood Products. 2019. Vol. 77(03). doi: 10.1007/s00107-019-01467-y
63. Zaynitdinov Olmos Irikovich, Rahimov Rustam Vyacheslavovich, Waail Mahmod Lafta, Ruzmetov Yadgor Ozodovich. Development of new polymer composite materials for the flooring of rail carriage // International Journal of Engineering & Technology. 2020. Vol. 9 (2). P. 378 – 381.
64. Antipin D.Ya. (2019). Improvement of the calculation method for the strength of

the upper linings of the side walls of gondola cars. *Bulletin of the Bryansk State Technical University, 3(76),* pp. 58 – 64. DOI: 10.30987/article_5c8b5ceb111c58.12769482

65. Domenico Gattuso, Giancarla Cassone, Antonio Lucisano, Maurizio Lucisano, Francesco Lucisano. Automated rail wagon for new freight transport opportunities // IEEE International Conference on Models and Technologies for Intelligent Transportation Systems (MT-ITS). 2017. DOI: 10.1109/MTITS.2017.8005581
66. Pavol Šťastniak, Lukáš Smetanka, Marián Moravčík. Structural Analysis of a Main Construction Assemblies of the New Wagon Prototype Type Zans // Manufacturing Technology. 2018. Vol. 18. No. 3. P. 510 – 515.
67. S. Slavchev, V. Stoilov, S. Purgic. STATIC Strength Analysis Of The Body Of A Wagon, Series Zans // Journal of the Balkan Tribological Association. 2015. Vol. 21. No 1. P. 3 – 57.
68. Wenfei Liu, Yuming Wang, Tianyou Wang. Box Girder Optimization by Orthogonal Experiment Design and GA-BP Algorithm in the Gondola Car Body // Processes. 2022. Vol. 10. Issue 74. https://doi.org/10.3390/pr10010074
69. Rúben Silva, Diogo Ribeiro, Cássio Bragança, Cristina Costa, António Arêde, Rui Calçada. Model Updating of a FreightWagon Based on Dynamic Tests under Different Loading Scenarios // Applied Science. 2021. Vol. 11. 10691. https://doi.org/10.3390/app112210691
70. Cheng Wei, Cai Kaiwu, Qu Fukang, Xiao Jin. Study on Fatigue Strength and Life of Freight Car Frame after Making Holes // MATEC Web of Conferences. 2018. Vol. 175. 01035. https://doi.org/10.1051/matecconf/2018175
71. Andrzej Buchacz, Andrzej Baier, Marek Płaczek, Krzysztof Herbuś, Piotr Ociepka, Michał Majzner. Development and analysis of a new technology of freight cars modernization // Journal Of Vibroengineering. 2018. Vol. 20. Issue 8. P. 2978 – 2997.
72. Fomin Oleksij, Lovska Alyona. Determination of dynamic loading of bearing structures of freight wagons with actual dimensions // Eastern-European Journal of Enterprise Technologies. 2021. Vol. 2/7 (110). P. 6 – 15. doi: https://doi.org/10.15587/1729-4061.2021.220534
73. Fomin Oleksij, Lovska Alyona. Establishing patterns in determining the dynamics and strength of a covered freight car, which exhausted its resource // Eastern-European Journal of Enterprise Technologies. 2020. Vol. 6. Issue 7 (108). P. 21 – 29. doi: 10.15587/1729-4061.2020.217162
74. Putyato A.V., Konovalov E.N., Afanaskov P.M. (2016). Forecasting the final resource of a hopper-doser car after long-term operation taking into account the actual physical and mechanical characteristics of the material of the supporting structure. *Mechanics of machines, mechanisms and materials, 1(34)*, pp. 26 - 35.
75. Improvement of the design of the hopper car for grain transportation / Kebal Y. V., Shatov V. A., Tyokotev O. M., Murashova N. G. // Collection of scientific papers

State Economic and Technological University of Transport. "Transport systems and technologies" series, 2017, Issue. 30, pp.113 – 122.
76. Substantiating the optimization of the loadbearing structure of a hopper car for transporting pellets and hot agglomerate / O. Fomin, A. Lovska, I. Skliarenko, Yu . Klochkov // Eastern-European Journal of Enterprise Technologies. – 2020. – № 1/7 (103) – P. 65 – 74. doi: 10.15587/1729-4061.2020.193408
77. George Edward Street, Preetum Jayantilal Mistry, Michael Sylvester Johnson. Impact Resistance of Fibre Reinforced Composite Railway Freight Tank Wagons // Journal of Composites Science. – 2021, Vol. 5 (6), Issue 152, https://doi.org/10.3390/jcs5060152
78. Zaynitdinov Olmos Irikovich, Ruzmetov Yadgor Ozodovich, Rustam Rahimov, Waail Mahmod Lafta. Development of new polymer composite materials for the flooring of rail carriage // International Journal of Engineering and Technology. – 2020. – Vol. 9(2). P. 378 – 381.
79. Alexandru Ionut Patrascu, Anton Hadar, Stefan Dan Pastrama. Structural Analysis of a Freight Wagon with Composite Walls // MATERIALE PLASTICE. – 2020. – Vol. 57 (2). P. 140 – 151. https://doi.org/10.37358/MP.20.2.5360
80. Nicholas Fantuzzia, Michele Bacciocchiab, David Benedettic, Jacopo Agnelli. The use of sustainable composites for the manufacturing of electric cars // Composites Part C. – 2021. – Vol. 4. 100096. https://doi.org/10.1016/j.jcomc.2020.100096
81. Tautvydas Pravilonis, Edgar Sokolovskij. Analysis of composite material properties and their possibilities to use them in bus frame construction // Transport. – 2020. – Vol. 35, Issue 4. P. 368 – 378. https://doi.org/10.3846/transport.2020.13018
82. I. D. Ibrahima, T. Jamirua, E. R. Sadikub, W. K. Kupolatic, K. Mpofud, A. A. Ezea, C. A. Uwa. Production and Application of Advanced Composite Materials in Rail Cars Development: Prospect in South African Industry // Procedia Manufacturing. – 2019. – Vol. 35. P. 471 – 476.
83. Kondratiev A. Improving the mass efficiency of a composite launch vehicle head fairing with a sandwich structure // Eastern-European Journal of Enterprise Technologies. 2019. Vol. 6. No. 7 (102). P. 6 – 18. https://doi.org/10.15587/1729-4061.2019.184551
84. A. Kondratiev, V. Gaidachuk, T. Nabokina, V. Kovalenko. Determination of the influence of deflections in the thickness of a composite material on its physical and mechanical properties with a local damage to its wholeness // Eastern-European Journal of Enterprise Technologies. 2019. Vol. 4. No. 1 (100). P. 6 – 13. https://doi.org/10.15587/1729-4061.2019.174025.
85. Parunakyan V. E., Jenchako V. G. (2010). Investigation of the defrosting process of iron-containing raw materials in wagons with the use of computer technology "Data mining". *Bulletin of the Azov State Technical University, 20,* p. 267 - 274.
86. Oleksij Fomin, Alyona Lovska, Vadym Dzhenchako, Olexandr Zhylinkov, Anna

Fomina, Andrii Lytvynenko. (2022). Determining the features of temperature influence on the load-bearing structure of a hopper car with a composite cladding when transporting pellets to metallurgical enterprises. *Eastern-European Journal of Enterprise Technologies, Vol. 1/7 (115)*, pp. 32 – 41.

87. Krylov V.I., Klykov V.Ye., and Yasentsev V.F. (1980). Rolling stock brakes: textbook. Moscow: Transport, p. 271.
88. Karyagina N.S., Medvedev V.V. (1978). Occupational safety in the wagon industry. Moscow: Transport, p. 222.

APPENDIX A

PATENT DESIGNS OF TEMPERATURE-RESISTANT COMPONENTS OF ROLLING STOCK

IPC B 61 D 3/00

HOPPER CAR FOR TRANSPORTATION OF PELLETS AND HOT SINTER

The useful model refers to wagon construction and can be used for railway transportation of heterogeneous bulk and bulk cargoes that do not require protection from atmospheric precipitation.

A well-known open-type hopper car, the structure of which consists of a crew part module containing two two-axle carts, a self-coupling module, a braking equipment module, a frame module that includes backbone, end, pivot and intermediate beams, an unloading equipment module, a body module that contains two vertical side walls including top and bottom strapping, vertical and inclined struts, and two inclined end walls that include top and bottom strapping, functions of typical harnesses to absorb energy arising from the action of operational loads, transferred to the spinal beam of the changed (new) design, namely, which includes an intermediate adapter consisting of a thrust part on which a support plate of a typical design is placed, while the thrust part of the adapter is connected through a rod to a piston in which there are two throttle valves – inlet and outlet, viscous damping and anti-corrosion material is placed on the left and right sides of the piston, and in order to create the pressure of the viscous damping anti-corrosion material when moving the piston during the perception of the impact load, a bottom is provided in the spine beam, which is welded to the spine beam from the inside along its diameter, in order to limit the movements of the adapter during "jerk-stretching", a limiter is provided, which is welded to the backbone beam on the side of the coupling housing, as well as upper and lower bindings of the side walls, which are made of round pipes and filled with a viscous material with damping and anti-corrosion properties, as well as the execution of the end, pivot and intermediate beams of the frame module of the upper and lower bindings, vertical and inclined racks of the side walls and upper and lower bindings of the walls of the end module of the body from round pipes, which are filled with a viscous material with damping and anti-corrosion properties (UA 118389 C2, 10.01.2019).

The disadvantage of this design of the hopper car is the presence of a large number of components included in it, which requires an increase in the costs of maintaining the car.

It is also known the design of a railway hopper car, which contains a body with vertical longitudinal walls, a frame with brake, clutch and unloading devices mounted on carts. The body is made of three sections. At the same time, the cantilever sections are made movable relative to the fixed middle, connected to it by hinges with the location of the axes of rotation perpendicular to the longitudinal axis of the body, and the outer width of each cantilever part of the body is smaller than the inner width of the fixed part (UA 98764 U, 12.05.2015).

The disadvantage of this design of the hopper car is the insufficient strength of the losad-bearing structure under the action of operational loads, and as a result, the appearance of cracks in it.

The closest to the proposed object is an open-type railway hopper car (model 20-9749, TU U35.2-01124454-035:2005), the design of which consists of a crew part module containing double two-axle bogies, an auto-coupling module with typical harnesses, a brake equipment module, a frame module consisting of backbone, end, pivot and intermediate beams, an unloading equipment module and a body module consisting of two side vertical walls that include upper and lower strapping, vertical and inclined struts, two end inclined walls, which include upper and lower strapping, and two bunkers with two unloading hatches.

The reasons preventing the achievement of the required technical result are the insufficient strength of the supporting structure of the hopper car under operational loads.

The basis of the useful model is the task of increasing the strength of the load-bearing structure of the hopper car, and as a result, the operational resource.

The task is solved by the fact that in a hopper car, the design of which consists of a crew unit module containing two two-axle carts, a self-coupling module with typical coupling devices, a brake equipment module, a frame module consisting of backbone, end, pivot and intermediate beams, the unloading equipment module and the body module, which consists of two side vertical walls, which include upper and lower strapping, vertical and inclined racks, two end inclined walls, which include upper and lower strapping, and two hoppers with two unloading hatches, the backbone beam consists of two pipes of rectangular cross-section along the length of which the reinforcing diaphragm is placed, and the hump and upper strapping of the side and end walls are made of composite heat-resistant material.

The introduction of new features in interaction with the known ones ensure an increase in the strength of the load-bearing structure of the hopper car by reducing the load under the action of operational loads.

Сутність корисної моделі пояснюється кресленнями, де

на фіг. 1 показаний загальний вид запропонованого вагона-хопера;

на фіг. 2 – модуль кузова вагона-хопера;

на фіг. 3 – переріз обв'язування верхнього;

на фіг. 4 – модуль рами вагона-хопера;

на фіг. 5 – переріз хребтової балки;

на фіг. 6 – переріз горбиля.

The essence of the useful model is explained by the drawings, where

in the fig. 1 – the general view of the proposed hopper car;

in the fig. 2 – hopper car body module;

in the fig. 3 – cross-section of the upper strapping;

in the fig. 4 – hopper car frame module;

in the fig. 5 – cross-section of the spinal beam;

in the fig. 6 – cross-section of a humpback.

The proposed hopper car (Fig. 1) consists of a crew part module 1, which contains double two-axle carts, a self-coupling module 2, a braking equipment module 3, a body module 4 and a frame module 5. The body module includes the side walls with the top 6 and lower 7 strapping, vertical 8 and inclined 9 racks (Fig. 2), and end walls with upper 10 and lower 11 strapping. At the same time, the upper strapping of 6 side walls and 10 end walls is made of a composite material with heat-resistant properties (Fig. 3). The frame module (Fig. 4) includes a spinal beam 12, which consists of two pipes 13 of rectangular section along the length of which the reinforcing diaphragm 14 (Fig. 5) is placed. A hump 15 made of composite material with heat-resistant properties is placed on top of the spinal beam (Fig. 6). The frame structure also includes pivot beams 16, end beams 17 and intermediate transverse beams 18 (Fig. 4).

The proposed hopper car works as follows. To form a freight railway train, the hopper car is connected to the rear car and the front car (or locomotive) through the coupling device module 2 (Fig. 1), and to the train brake line through the brake equipment module 3. Vertical loads from the transported cargo, which placed in the hopper car, are transmitted to the frame module (Fig. 4) and then to the axles of the wheel pairs of two two-axle carts (Fig. 1) of the crew unit module 1.

ABSTRACT

HOPPER CAR FOR TRANSPORTATION OF PELLETS AND HOT SINTER

1. *Object of the invention*: a utility model.

2. *Field of application*: the useful model refers to wagon construction and can be used for rail transportation of heterogeneous bulk and bulk cargoes that do not require protection from atmospheric precipitation.

3. *Essence of the invention* is that the spinal beam consists of two pipes of rectangular section along the length of which the reinforcing diaphragm is placed, and the hump and upper strapping of the side and end walls are made of composite heat-resistant material.

4. *Technical result*: increasing the strength of the supporting structure of the hopper car due to the reduction of the load under the action of operational loads.

Claim of the utility model

A hopper car, the design of which consists of a crew unit module containing double two-axle bogies, a self-coupling module with typical coupling devices, a brake equipment module, a frame module consisting of backbone, end, pivot and intermediate beams, an unloading equipment module and a body module, which consists of two side vertical walls, which include upper and lower binding, vertical and inclined struts, two end inclined walls, which include upper and lower strapping, and two hoppers with two unloading hatches, **differs in** that the beam is ridged consists of two pipes of rectangular cross-section along the length of which the amplifying diaphragm is placed, and the hump and upper strapping of the side and end walls are made of composite heat-resistant material.

Hopper car for transporting pellets and hot sinter

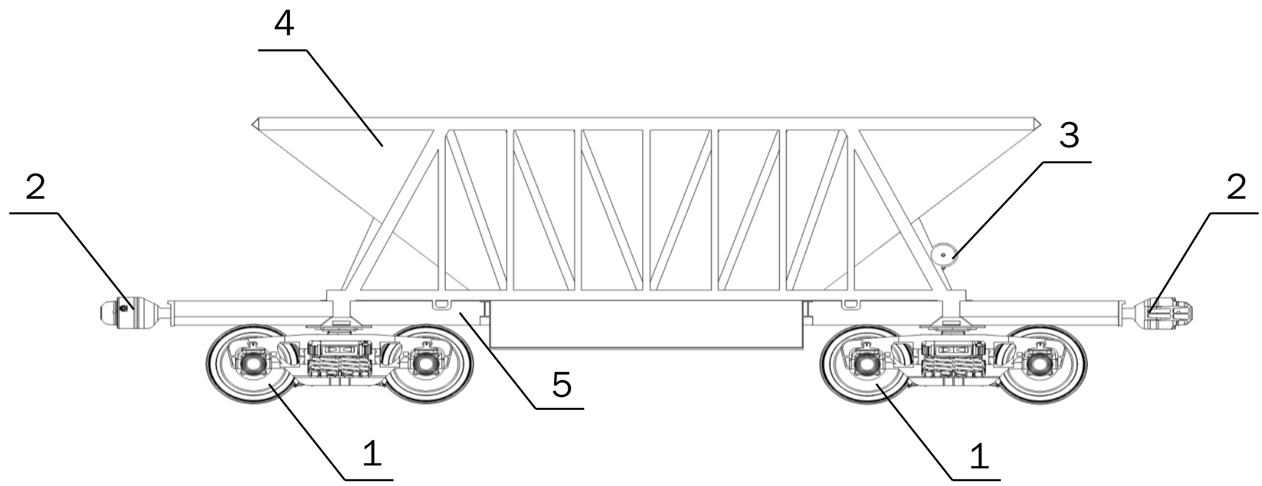

Fig. 1

Hopper car for transporting pellets and hot sinter

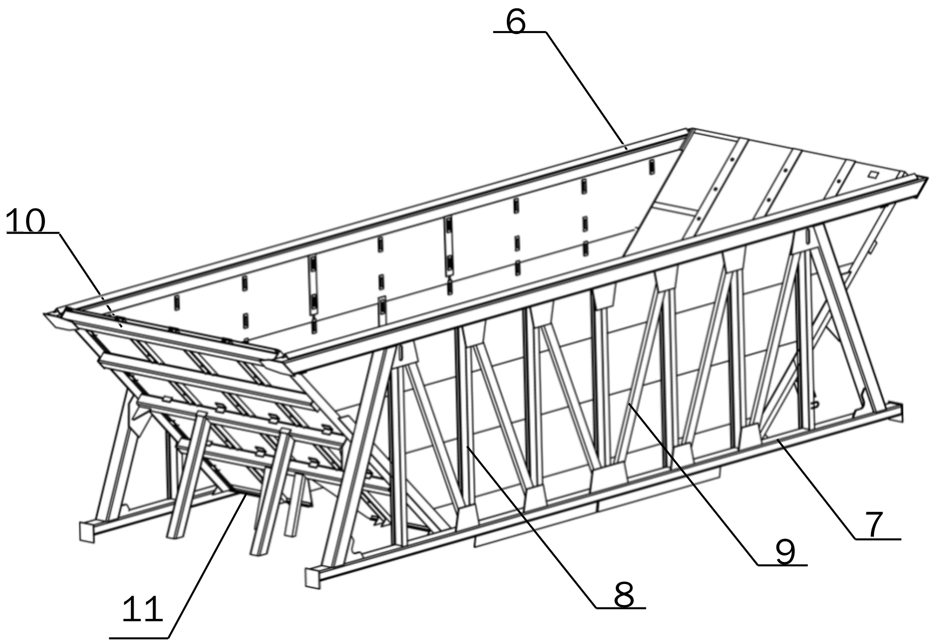

Fig. 2

Hopper car for transporting pellets and hot sinter

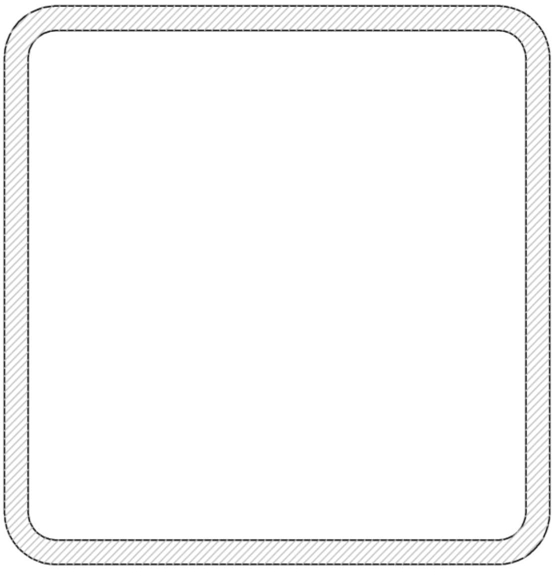

Fig. 3

Hopper car for transporting pellets and hot sinter

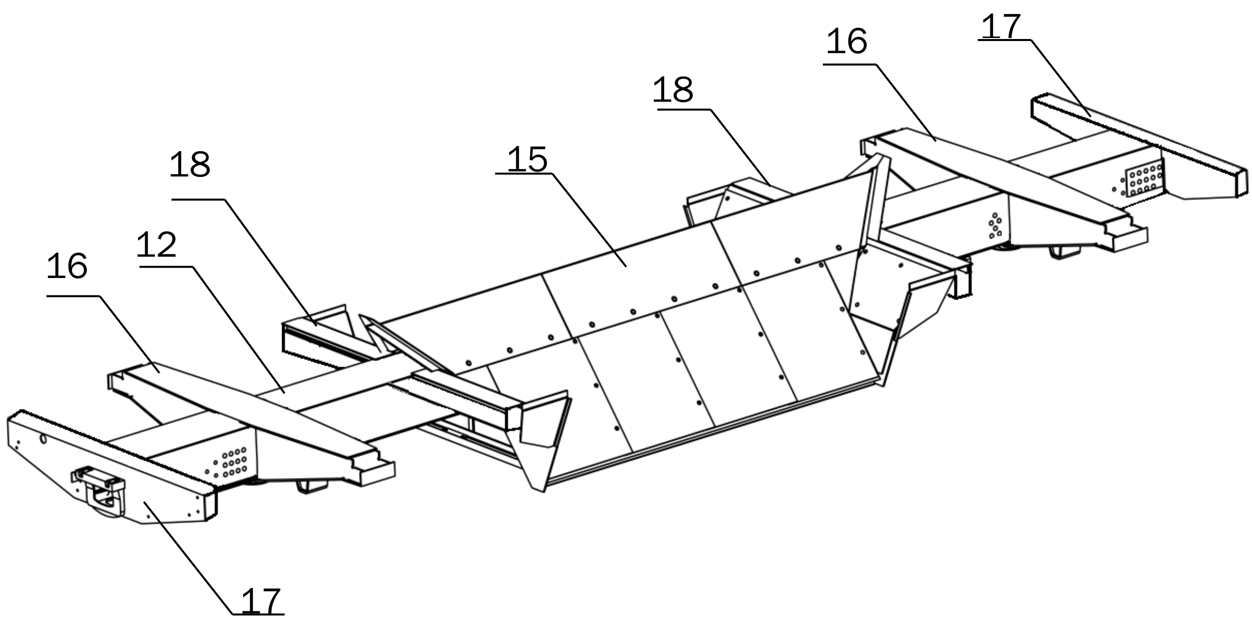

Fig. 4

Hopper car for transporting pellets and hot sinter

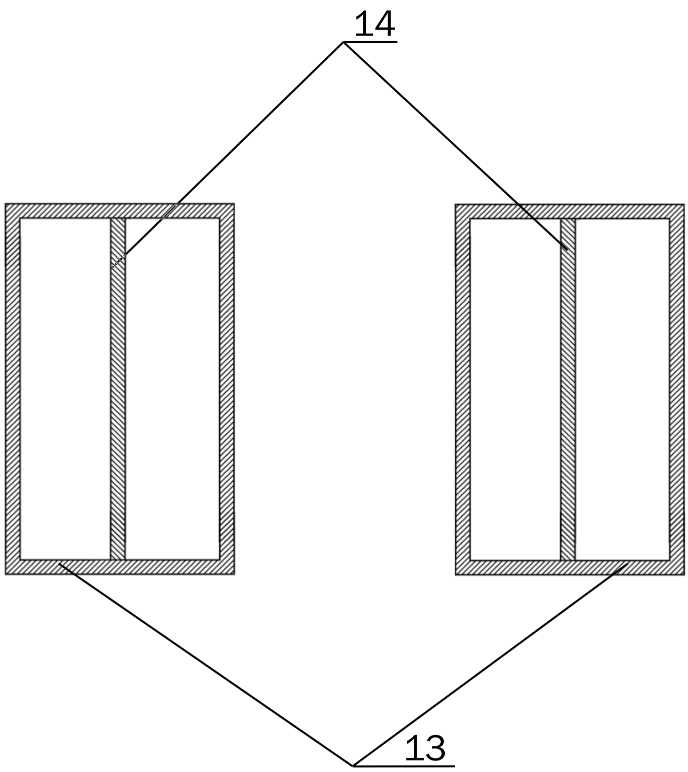

Fig. 5

Hopper car for transporting pellets and hot sinter

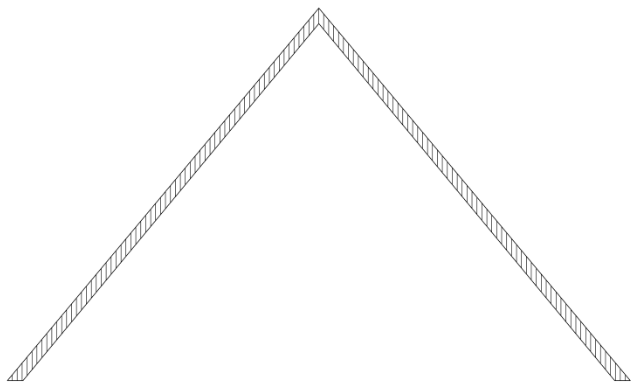

Fig. 6

IPC B61D

TANK CAR FOR TRANSPORTATION OF CARGOS WITH AN INCREASED TEMPERATURE

The utility model relates to wagon construction and can be used for railway transportation of bulk, heterogeneous bulk and liquid cargos with increased temperature.

Currently, hopper cars are used in railway transport for the transportation of bulk and heterogeneous bulk cargoes with increased temperature.

The design of a railway hopper gondola car for hot coils and sinter is known, which consists of a crew part module containing two double-axle bogies, an auto coupling module, a braking equipment module, a frame module with backbone and pivot beams, an unloading equipment module with an unloading shaft, a body module, which contains two vertical sidewalls having cladding and a frame consisting of top and bottom strapping, braces, connecting beams, which connect the bottom strapping and end beams of the frame module, and two inclined end walls, having a cladding and a frame consisting of upper and lower strapping, horizontal belts.

The backbone beam of the frame module is made of I-beams No 45, each of which has a welded construction. The upper sheet of the pivot beam is made of a steel sheet with a thickness of 10 mm. The unloading shaft of the unloading equipment module is made of a round pipe. The bearing units of the unloading equipment module are made with inserts of composite materials. The cladding of the side and end walls of the body module is made of 5 mm thick steel sheets. Upper and lower strappings, braces of the side walls, upper and lower strappings, horizontal belts of the end walls are made of profiles in the form of a square pipe. The connecting beams, which connect the lower strapping and the end beams of the frame module are made of the same longitudinal sleeper (UA 101213 C2, 11.03.2013).

The disadvantage of this design of the hopper car is the insufficient strength of the supporting structure under operational loads, and as a result, the appearance of cracks in it, as well as the impossibility of transporting liquid cargos in it.

Tank cars are mostly used for the transportation of liquid cargoes by railway.

A well-known tank car containing running parts, self-coupling, traction and braking equipment, a boiler connected with the frame, with a cross-sectional area in the middle part larger than in the cantilever parts. The boiler is made of at least five cylinder shells, which are bodies of rotation, and two bottoms. The middle cylinder shell is made in the form of two half-cylinders connected by flat inserts. The cantilever cylinder shells have cylindrical shape, and the intermediate cylinder shells, located between the middle and cantilever ones, are made of a cross-section with variable length, the contours connecting them with the middle and cantilever cylinder shells are congruent to the contours of the middle and cantilever cylinder shells, respectively. Rings are installed between two adjacent cylinder shells, in the lower parts of the middle and intermediate cylinder shells, in the area of their connection with rings, overlays are installed (UA 99142 U, dated 05.25.2015).

The disadvantage of this design of the tank car is the insufficient strength of the frame under the action of cyclic loads, and as a result, the appearance of cracks in it, as well as the impossibility of transporting goods with an elevated temperature in it.

The closest to the proposed object is a railway tank car (model 15-1443, TU 24.00.129-82), the design of which consists of a crew unit module containing two double-axle bogies, a self-coupling module, a braking equipment module, a module of the frame, which consists of the backbone, pivot, end beams and side girders, as well as the boiler module, which rests on the frame through the middle and end supports.

The reasons that prevent obtaining the required technical result are the insufficient strength of the load-bearing structure under the action of cyclic loads in operating conditions, as well as the impossibility of transporting goods with an increased temperature in it.

The basis of the utility model is the task of increasing the strength of the supporting structure of the tank car, and as a result, the resource of operation, as well as ensuring the possibility of transporting goods with an increased temperature in it.

The task is solved by the fact that in a tank car, the design of which consists of a crew unit module containing two double-axle carts, a self-coupling module, a brake equipment module, a frame module, which consists of backbone, pivot, end beams and side strappings, as well as the boiler module, which rests on the frame through the middle and end supports, the backbone beam consists of two pipes of rectangular section along the length of which the reinforcing diaphragm is placed, and the boiler is open and has a semi-cylindrical configuration and is made of composite heat-resistant material.

The introduction of new features in interaction with the known ones ensure an increase in the strength of the load-bearing structure of the tank car, and as a result, the resource of operation, as well as ensuring the possibility of transporting goods with an increased temperature in it.

The essence of the useful model is explained by the drawings, where

in fig. 1 shows the general view of the proposed tank car;

in fig. 2 – tank car frame module;

in fig. 3 – cross-section of the spinal beam.

The proposed tank car (fig. 1) consists of a crew part module 1, which contains two double-axle carts, a self-coupling module 2, a brake equipment module 3, a boiler module 4, which is open and has a semi-cylindrical configuration and is made of composite heat-resistant material, and as well as the frame module 5. The frame module (Fig. 2) includes a spinal beam 6, which consists of two pipes 7 of rectangular section along the length of which the reinforcing diaphragm 8 (Fig. 3) is placed. Also, the frame construction includes pivot beams 9 (Fig. 2), end beams 10 and side straps 11. The end parts of the boiler are freely mounted on wooden bars 12, which are attached with bolts to the metal grooves of the supports 13, installed on the pivot beams 9.

The proposed tank car works as follows. To form a freight railway train, the tank car is connected to the rear car and the front car (or locomotive) through the coupling device module 2 (Fig. 1), and to the train brake line through the brake equipment module 3. Vertical loads from the transported cargo, which placed in the tank car, are transmitted to the frame module (Fig. 2) and then to the axles of the wheel pairs of two double-axle carts (Fig. 1) of the crew unit module 1.

ABSTRACT

COVERED CAR FOR THE TRANSPORTATION OF CARGO WITH AN INCREASED TEMPERATURE

1. *Object of the invention*: a utility model.

2. *Field of application*: the utility model refers to railcar construction and can be used for rail transportation of single, container-unit loads, boxed cargoes, bulk cargoes, devices, various mechanisms, machine tools, machines and other cargoes that require protection from atmospheric precipitation.

3. *The essence of the invention* is that the ridge beam consists of two trough-like profiles covered above and below with horizontal sheets, the braces are made in the form of profiles of closed rectangular section, and the cladding of the side, end walls, doors and roof, as well as the floor covering is made of composite heat-resistant material.

4. *Technical result*: increasing the strength of the bearing structure of the covered car, and as a result, the resource of operation, as well as ensuring the possibility of transporting goods with an increased temperature in it.

Claims of the invention

A tank car, the structure of which consists of a crew part module containing two double-axle bogies, a coupling module, a brake equipment module, a frame module consisting of a backbone, pivots, end beams and side strappings, as well as a supported boiler module through the middle and end supports on the frame, **differs in** that the backbone beam consists of two pipes of rectangular section along the length of which the reinforcing diaphragm is placed, and the boiler is open and has a semi-cylindrical configuration and is made of composite heat-resistant material.

Tank car for transportation of cargoes with increased temperature

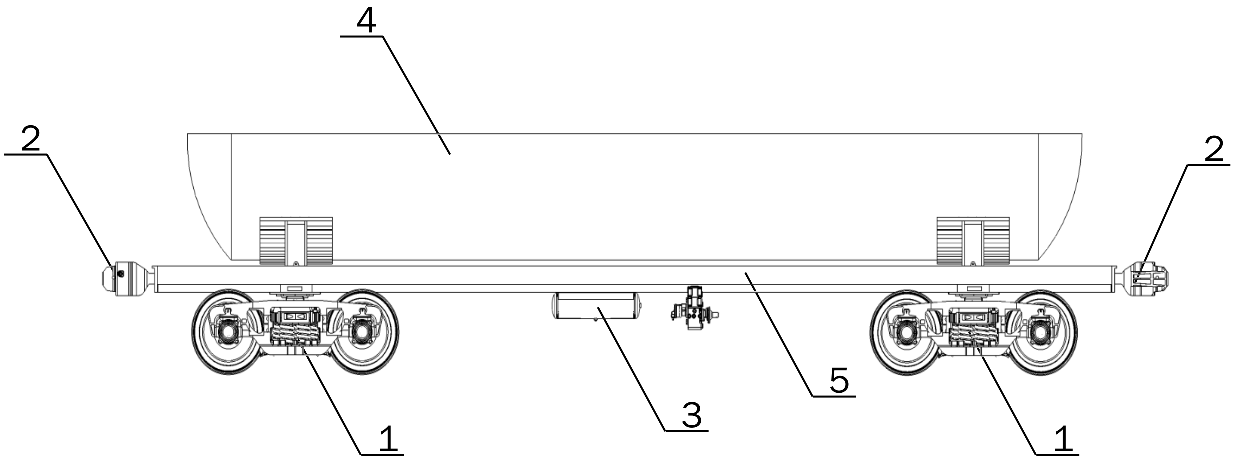

Fig. 1

Tank car for transportation of cargoes with increased temperature

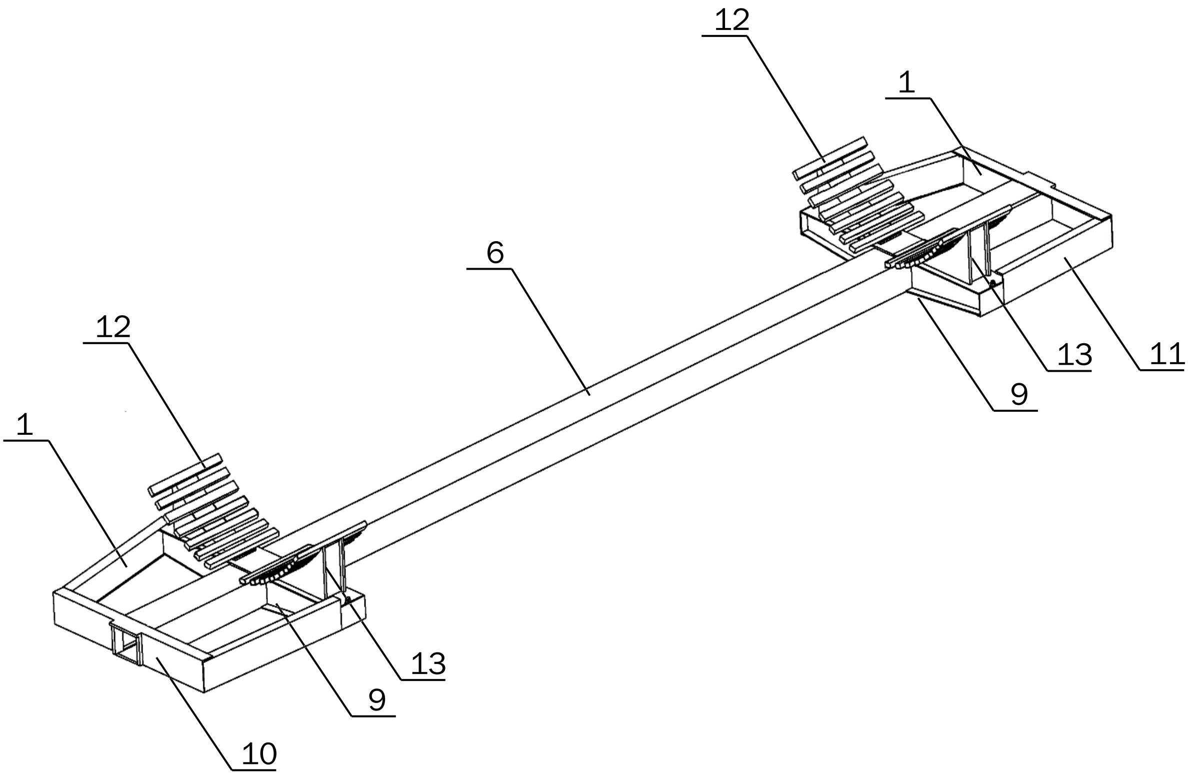

Fig. 2

Tank car for transportation of cargoes with increased temperature

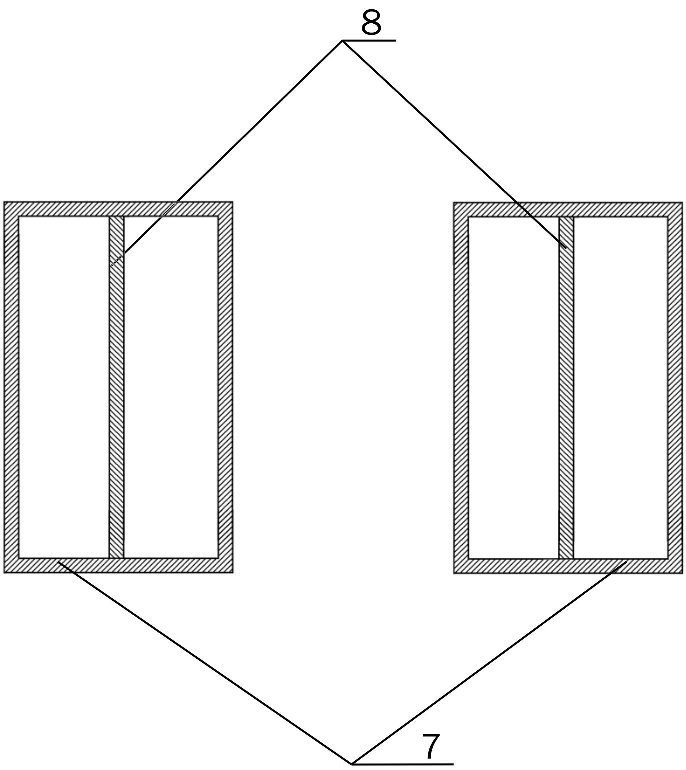

Fig. 3

IPC B61D 3/00

COVERED CAR FOR TRANSPORTATION OF CARGOS WITH INCREASED TEMPERATURE

The utility model is related to railcar construction and can be used for rail transportation of single, container-unit cargo, boxed cargos, bulk cargos, devices, various mechanisms, machine tools, machines and other cargos requiring protection from atmospheric precipitation, as well as cargos with increased temperature.

The well-known design of the covered car, which is mounted on carts, equipped with an autobrake and autocoupling, has a body. The body contains side and end walls with door openings, a floor, and a roof. In each side wall, two doorways are made, located at a certain distance from each other, each of which is closed by a door. The doorways are located symmetrically in relation to the middle of the car. The doors are sliding towards the car consoles (UA 105736 U, 11.04.2016).

The design of the covered car is also known, which includes a body installed on the running parts with sliding doors with a lower location of the mechanism for their movement and a roof that is immovably connected to its upper straps and is made in the form of a frame with evenly spaced transverse arches, closed from above by corrugated sheets with continuous corrugations located along the car, brake and auto-coupling equipment. The upper guides of the doors are immovably connected to the upper straps of the body, the roof is made of at least two parts connected to each other, its frame contains two longitudinal beams which the ends of the transverse arches are connected to, and two transverse beams installed in its ends and connected with longitudinal beams, and each end wall of the roof is equipped with a ventilation device (UA 29711 U, 25.01.2008).

The disadvantages of these car designs are the insufficient strength of the load-bearing structure under operating loads, and as a result, the appearance of cracks in it, as well as the impossibility of transporting goods with an elevated temperature in them.

The closest to the claimed object is a covered car model 11-217 (see M.I. Kharitonov, V.N. Pankin. (2004). Fright cars. Textbook: in 2 parts. Part 1:

Gondola cars and covered cars. Khabarovsk: Editorial Office of the Far Eastern State University of Communications, p. 52 – 53), the design of which consists of a crew part module containing two double-axle bogies, a self-coupling device module, a brake equipment module, a frame module with spinal, pivot, side, transverse, longitudinal, main transverse, end beams, braces, short and long beams of consoles and a body module containing two side walls having a skin and a frame consisting of an upper strapping, body struts, door struts, corner struts and two end walls having a skin and a frame consisting of a skin the upper frame, racks and roof, which has a sheathing and a frame consisting of arches.

The reasons preventing the achievement of the required technical result are the insufficient strength of the supporting structure of the car under the action of cyclic loads in operating conditions, as well as the impossibility of transporting goods with an elevated temperature in it.

The basis of the utility model is the task of increasing the strength of the load-bearing structure of the covered car, and as a result, the resource of operation, as well as ensuring the possibility of transporting goods with an increased temperature in it.

The task is solved by the fact that in a covered car, the structure of which consists of a module of the crew part containing two double-axle carts, a module of an autocoupling device, a module of braking equipment, a frame module with spinal, pivot, side, transverse, longitudinal, main transverse, end beams, braces, short and long beams of consoles and a body module containing two side walls having a sheathing and a frame, which consists of an upper strapping, body struts, door struts, corner struts and two end walls having a sheathing and a frame, which consists of the upper strapping, racks and roof, which has a sheathing and a frame that consists of arches, the ridge beam consists of two trough-like profiles covered from above and below with horizontal sheets, the braces are made in the form of profiles of a closed rectangular section, and the side sheathing , end walls, doors and roof, as well as the floor covering are made of composite heat-resistant material.

The introduction of new features in interaction with the known ones ensure an increase in the strength of the load-bearing structure of the covered car, and as a result, the resource of operation, as well as ensuring the possibility of transporting cargoes with an increased temperature in it.

The fig. 1 shows the general view of the proposed covered car; the fig. 2 – frame module of the covered car; the fig. 3 – cross-section of the spinal beam; the fig. 4 – section of brace; the fig. 5 – body module of a covered car.

The proposed railway covered car (Fig. 1) consists of a crew part module 1, which contains two double-axle bogies, an autocoupling device module 2, a brake equipment module 3, a body module 4 and a frame module 5 (Fig. 2), which includes a backbone beam 6, which consists of two trough-like profiles 7 covered from above and below by horizontal sheets 8 (Fig. 3). The frame also includes two pivot beams 9 (Fig. 2), lateral 10, transverse 11, longitudinal 12, main transverse 13, end 14 beams, braces 15, which are made in the form of profiles of closed rectangular section (Fig. 4), short and long beams of consoles 16 (Fig. 2). The body module (Fig. 5) contains two side walls having a sheathing and a frame, which consists of an upper strapping 17, body racks 18, door racks 19, corner racks 20 and two end walls having a sheathing and a frame, which consists of the strapping of the upper 21, racks 22 and the roof 23, which has a lining and a frame, which consists of arcs. At the same time, the lining of the side, end walls, doors and roof, as well as the floor covering, is made of composite heat-resistant material.

The proposed covered car works as follows. To form a freight railway train, the covered car is connected to the rear car and the front car (or locomotive) through the coupling device module 2 (Fig. 1), and to the train brake line through the brake equipment module 3. Vertical loads from the transported cargo placed in the covered car, are transmitted to the frame module (fig. 2) and then to the axles of the wheel pairs of two double-axle carts (fig. 1) of the crew unit module 1.

ABSTRACT

COVERED CAR FOR TRANSPORTATION OF CARGO WITH INCREASED TEMPERATURE

1. *Object of the invention*: a utility model.

2. *Field of application*: the utility model refers to railcar construction and can be used for rail transportation of single, container-unit cargoess, boxed cargoess, bulk cargoes, devices, various mechanisms, machine tools, machines and other cargoes that require protection from atmospheric precipitation, as well as cargo with increased temperature.

3. *The essence of the invention* is that the ridge beam consists of two trough-like profiles covered above and below with horizontal sheets, the braces are made in the form of profiles of closed rectangular section, and the cladding of the side, end walls, doors and roof, as well as the floor covering is made of composite heat-resistant material.

4. *Technical result*: increasing the strength of the bearing structure of the covered car, and as a result, the resource of operation, as well as ensuring the possibility of transporting cargoess with an increased temperature in it.

Claims of invention

A covered car, the structure of which consists of a crew section module containing two double-axle bogies, an autocoupling device module, a braking equipment module, a frame module with backbone, pivot, side, transverse, longitudinal, main transverse, end beams, braces, short and long beams consoles and a body module containing two side walls having a skin and a frame consisting of an upper strapping, body struts, door struts, corner struts and two end walls having a skin and a frame consisting of a strapping upper, racks and roof, which has a sheathing and a frame consisting of arches, **differs in** that the ridge beam consists of two trough-like profiles covered from above and below with horizontal sheets, the braces are made in the form of profiles of closed rectangular section, and the sheathing of the side, end walls, doors and roof, as well as the floor covering are made of composite heat-resistant material.

Covered car for transportation of cargoes with increased temperature

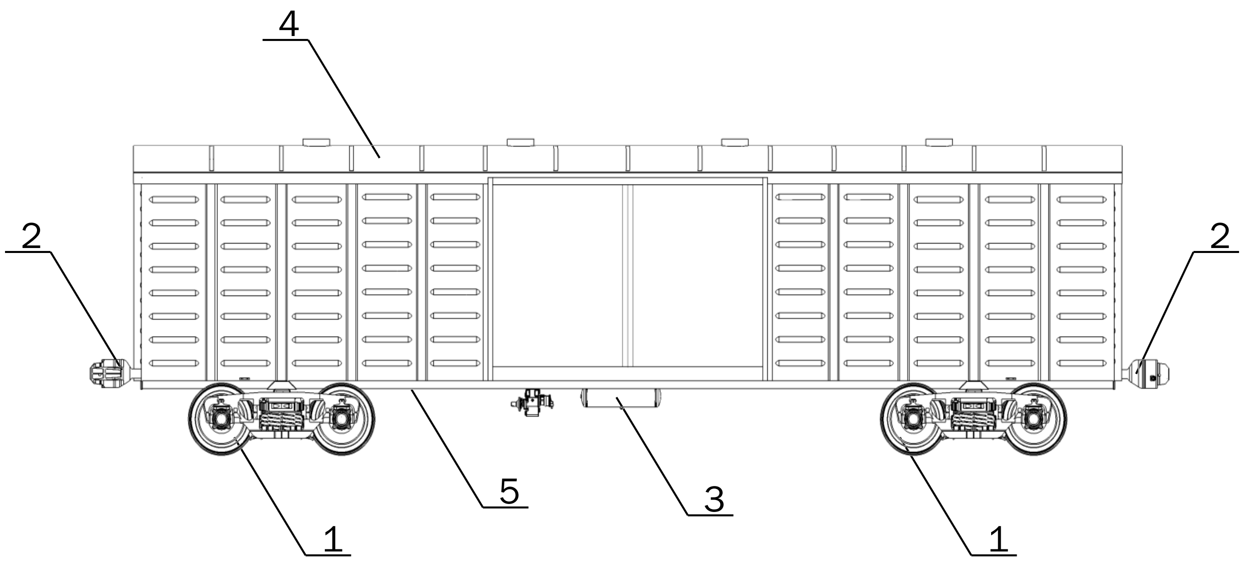

Fig. 1

Covered car for transportation of cargoes with increased temperature

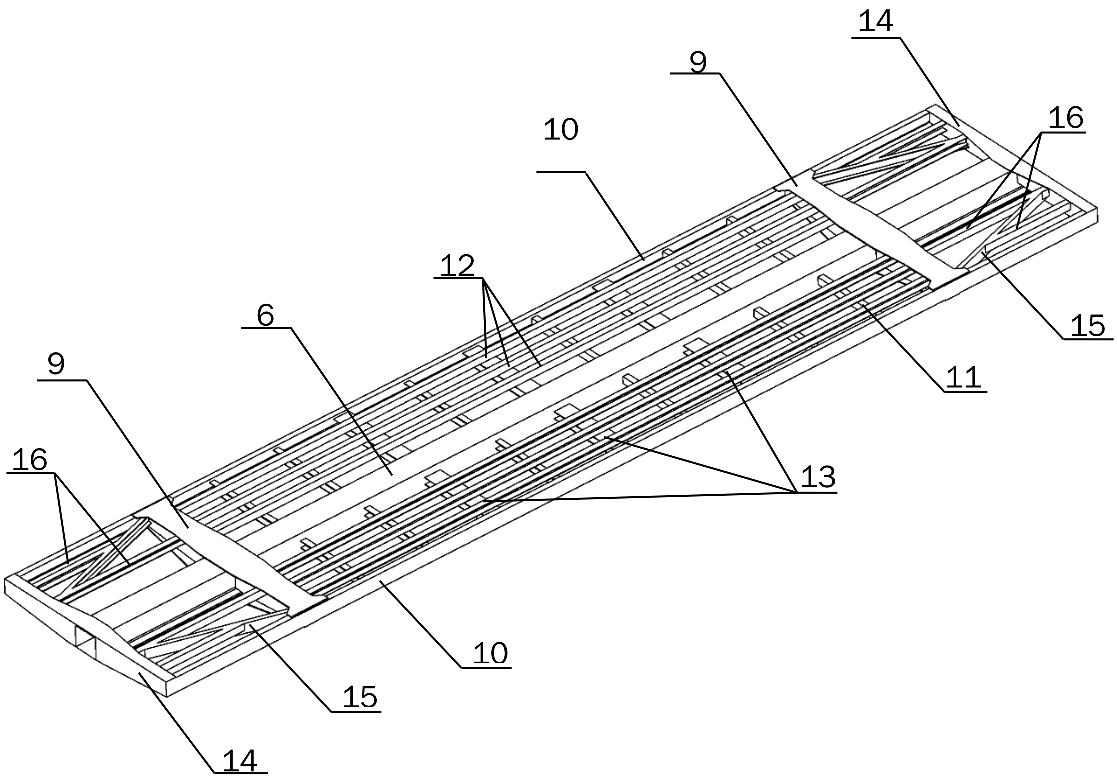

Fig. 2

Covered car for transportation of cargoes with increased temperature

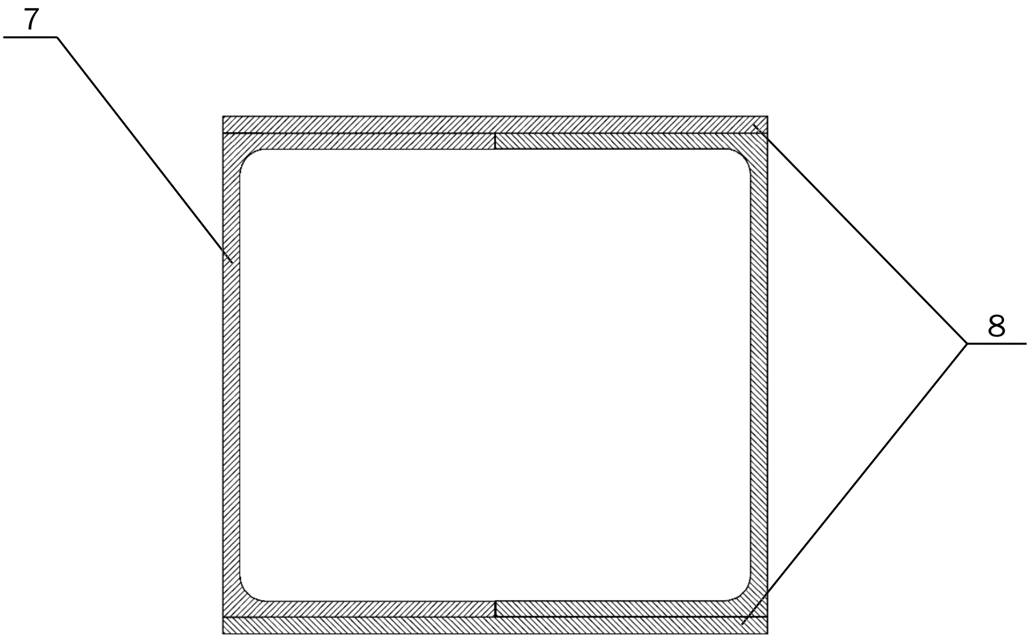

Fig. 3

Covered car for transportation of cargoes with increased temperature

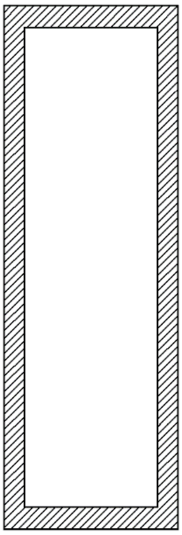

Fig. 4

Covered car for transportation of cargoes with increased temperature

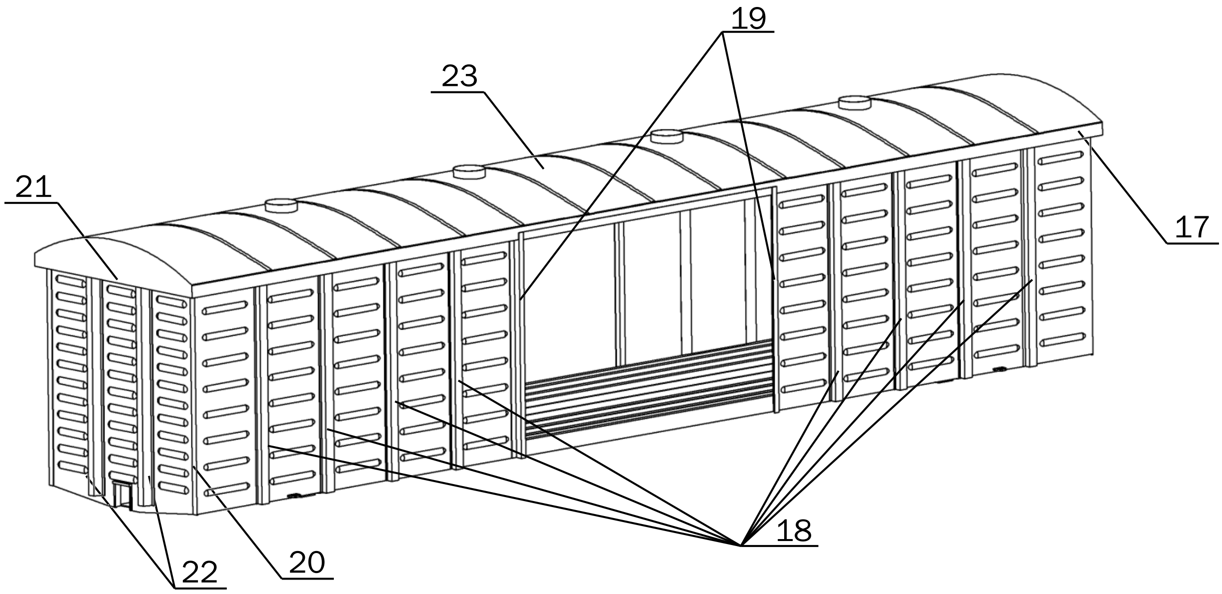

Fig. 5

S C I E N T I F I C   E D I T I O N

OLEKSIJ FOMIN
ALYONA LOVSKA

TEMPERATURE EFFECTS ON RAILWAY ROLLING STOCK COMPONENTS

MONOGRAPH

Part 1

Responsible for the layout: Bilous T.
Responsible designer: Bondarenko I.

Published (PDF): 10.10.2022. Signed for printing: 14.10.2022.
Format 60×84/16. Offset Paper. The headset is Franklin Gothic Book.
Digital printing. Conventionally printed sheets 8,37.
Circulation: 50 copies. Order № 344.

Printed from the finished original layout.

Publisher [ISBN]**:** Primedia E-launch LLC.
TX 75001, United States, Texas, Dallas.
E-mail: info@primediaelaunch.com | URL: www.primediaelaunch.com

Compiler and publisher: NGO European Scientific Platform
21037, Ukraine, Vinnytsia, Zodchykh str. 18/81
Tel.: +38 098 1948380; +38 098 1956755
E-mail: info@ukrlogos.in.ua | URL: www.ukrlogos.in.ua
Certificate of the subject of the publishing business: ДК No 7172 of 21.10.2020.

The purpose of the book is to highlight the features of temperature effects on the components of railway rolling stock and to create measures to improve the efficiency of its operation. Theoretical provisions, methodological bases and practical decisions on determination of temperature influence on components of rolling stock of railways at operational modes of loading are provided.

The monograph is intended for scientific and technical specialists whose activities are related to the design and study of mechanics of rolling stock structures, including scientists, designers, designers, researchers, doctoral students and graduate students.

The monograph can be used as a textbook for undergraduates and bachelors in relevant specialties.

Primedia eLaunch

9 798888 313183